AWARD NUMBER: W81XWH-19-1-0041

TITLE: A milk protein-hitchhiking strategy for the oral delivery of amphiphilic vaccines

PRINCIPAL INVESTIGATOR: Jiahe Li

CONTRACTING ORGANIZATION: Northeastern University, Boston MA

REPORT DATE: May 2021

TYPE OF REPORT: Annual

PREPARED FOR: U.S. Army Medical Research and Development Command
Fort Detrick, Maryland 21702-5012

DISTRIBUTION STATEMENT: Approved for Public Release;
Distribution Unlimited

The views, opinions and/or findings contained in this report are those of the author(s) and should not be construed as an official Department of the Army position, policy or decision unless so designated by other documentation.

REPORT DOCUMENTATION PAGE

Form Approved
OMB No. 0704-0188

Public reporting burden for this collection of information is estimated to average 1 hour per response, including the time for reviewing instructions, searching existing data sources, gathering and maintaining the data needed, and completing and reviewing this collection of information. Send comments regarding this burden estimate or any other aspect of this collection of information, including suggestions for reducing this burden to Department of Defense, Washington Headquarters Services, Directorate for Information Operations and Reports (0704-0188), 1215 Jefferson Davis Highway, Suite 1204, Arlington, VA 22202-4302. Respondents should be aware that notwithstanding any other provision of law, no person shall be subject to any penalty for failing to comply with a collection of information if it does not display a currently valid OMB control number. **PLEASE DO NOT RETURN YOUR FORM TO THE ABOVE ADDRESS.**

1. REPORT DATE:	2. REPORT TYPE:	3. DATES COVERED
MAY 2021	ANNUAL	15Apr2020-14Apr2021

4. TITLE AND SUBTITLE

A milk protein-hitchhiking strategy for the oral delivery of amphiphilic vaccines

5a. CONTRACT NUMBER
PR182271

5b. GRANT NUMBER
W81XWH-19-1-0041

5c. PROGRAM ELEMENT NUMBER

6. AUTHOR(S)
Jiahe Li

E-Mail: jiah.li@northeastern.edu

5d. PROJECT NUMBER

5e. TASK NUMBER

5f. WORK UNIT NUMBER

7. PERFORMING ORGANIZATION NAME(S) AND ADDRESS(ES)

Northeastern University
360 Huntington Avenue
Boston, MA, 02115

8. PERFORMING ORGANIZATION REPORT NUMBER

9. SPONSORING / MONITORING AGENCY NAME(S) AND ADDRESS(ES)

U.S. Army Medical Research and Development Command
Fort Detrick, Maryland 21702-5012

10. SPONSOR/MONITOR'S ACRONYM(S)
NEU

11. SPONSOR/MONITOR'S REPORT NUMBER(S)

12. DISTRIBUTION / AVAILABILITY STATEMENT

Approved for Public Release; Distribution Unlimited

13. SUPPLEMENTARY NOTES

14. ABSTRACT

We are grateful for this Discovery award to enable an oral vaccine delivery platform against infectious diseases. Following the last report, we have performed in vitro and in vivo experiments according to the original SOW. While we are encouraged by in vitro data we have obtained over the past year, to date our progress has been primarily hindered by the low efficacy in vivo. To address the lack of efficacy in vivo, we have made extensive efforts in two major directions: (1) development of an in vitro gut model to understand the transport properties of amphiphilic peptides; (2) identification of a more potent adjuvant system targeting the STING pathway to augment the in vivo performance. The latter effort has resulted in one manuscript recommended for publication pending a minor revision at Advanced Therapeutics. We are hopeful that with the new adjuvant system we would be able to induce immune responses following oral vaccination.

15. SUBJECT TERMS

None listed.

16. SECURITY CLASSIFICATION OF:			17. LIMITATION OF ABSTRACT	18. NUMBER OF PAGES	19a. NAME OF RESPONSIBLE PERSON
a. REPORT	b. ABSTRACT	c. THIS PAGE			19b. TELEPHONE NUMBER *(include area code)*
Unclassified	Unclassified	Unclassified	Unclassified	97	USAMRMC

TABLE OF CONTENTS

	Page
1. Introduction	4
2. Keywords	4
3. Accomplishments	5
4. Impact	9
5. Changes/Problems	9
6. Products	9
7. Participants & Other Collaborating Organizations	9
8. Special Reporting Requirements	10
9. Appendices	10

1. Introduction

Service members and civilian populations are potentially exposed to many emerging infectious diseases that are life-threatening. These include, but are not limited to, Zika virus (ZIKV), dengue, HIV, norovirus, hepatitis, and Middle East Respiratory Syndrome. However, many of these diseases remain among the leading causes of illness and death in the battlefield, and account for substantial spending on the related consequences of infection even after soldiers come back from the service. Many infectious diseases, however, can be prevented through vaccination. Developing a convenient and cost-effective vaccine delivery technology that can be deployed to service members and civilians remains highly desirable. Oral vaccination is a very powerful and effective approach for vaccination, because it can not only induce a broad immunity through the blood and lymphatics, but also help patrol a very thin lining in the respiratory, digestive, and reproductive systems for potential virus invasion. The latter is particularly important as many pathogens invade the body via sexual or respiratory transmission. However, the stomach presents a major barrier to successful delivery of protein-based vaccines to the intestines, in which immune cells would otherwise receive alarm signals. The stomach is highly acidic and also contains proteins that recognize vaccines as food sources to chop up. To address this challenge, we draw inspiration from two seemingly irrelevant disciplines − dairy science and bioconjugation chemistry − to develop a “plug and play” type of approach for oral delivery of vaccines. Our strategy is to repurpose a milk protein, α-lactalbumin, as a vehicle, which is known to be resistant to degradation by stomach. Since this protein naturally associates with many bioactive lipids such as Vitamin D, we propose to explore a range of lipid molecules derived from a common supplement (e.g. Vitamin D) and vegetable oil (e.g. oleic acid). As a proof of principle study, we link lipid molecules to a short strand of amino acids (an antigenic peptide) that instructs the host immune system to mount potent humoral and cellular immune responses against the pathogen of interest. We envision that co-administering these two components with α-lactalbumin will help them from being cleared by the stomach, and therefore a stronger signal will be sent to immune cells lying underneath the intestines.

2. Keywords

Oral vaccine, subunit vaccine, α-lactalbumin, immunization

3. Accomplishments (based on the SOW)

Major Task 1 (Aim 1): Chemical conjugation of lipids to peptide antigens and adjuvants

This task was completed and documented in the last annual report.

Major Task 2 (Aim 2): Complexation of lipid conjugates with α-lactalbumin

Subtask 1 Characterize physiochemical properties of different lipid conjugates complexed with α-lactalbumin: Year 2 marks the successful completion of this task. We used dynamic light scattering to measure the sizes and physical stabilities of amphiphilic antigen peptides and CpG ODN when incubated with α-lactalbumin at pH 8.0 to simulate the conditions in duodenal juices. As shown in Figure, the complexes remained relatively stable over 3-5 days.

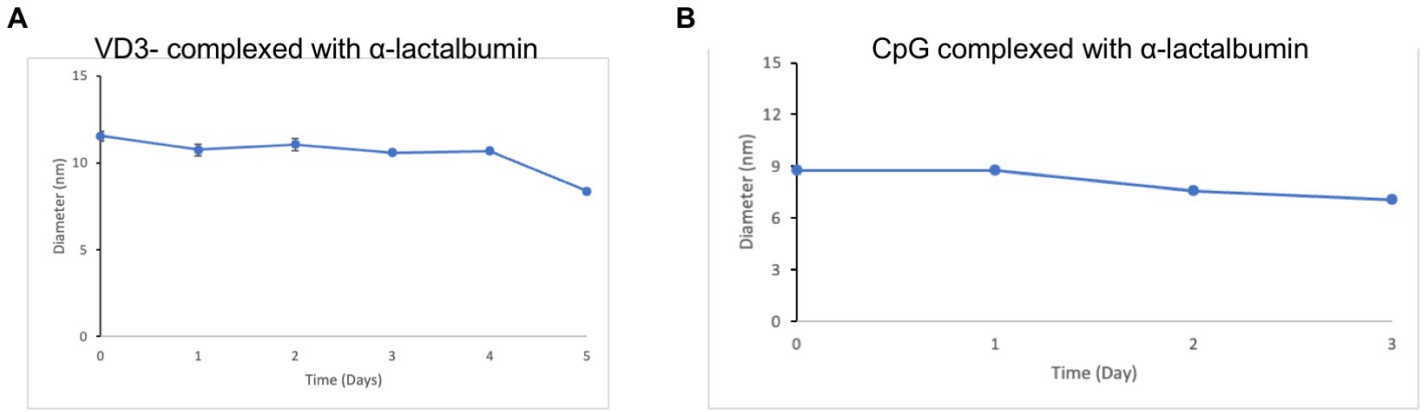


Figure 1. Dynamic light scattering (DLS) to measure the sizes of the complexes over 3-5 days under the pH 8.0 at room temperature. **(A)** Vitamin D conjugated peptides complexed with lactalbumin. **(B)** Vitamin D conjugated CpG complexed with lactalbumin.

Subtask 2 Evaluate the cytotoxicity of the complexes

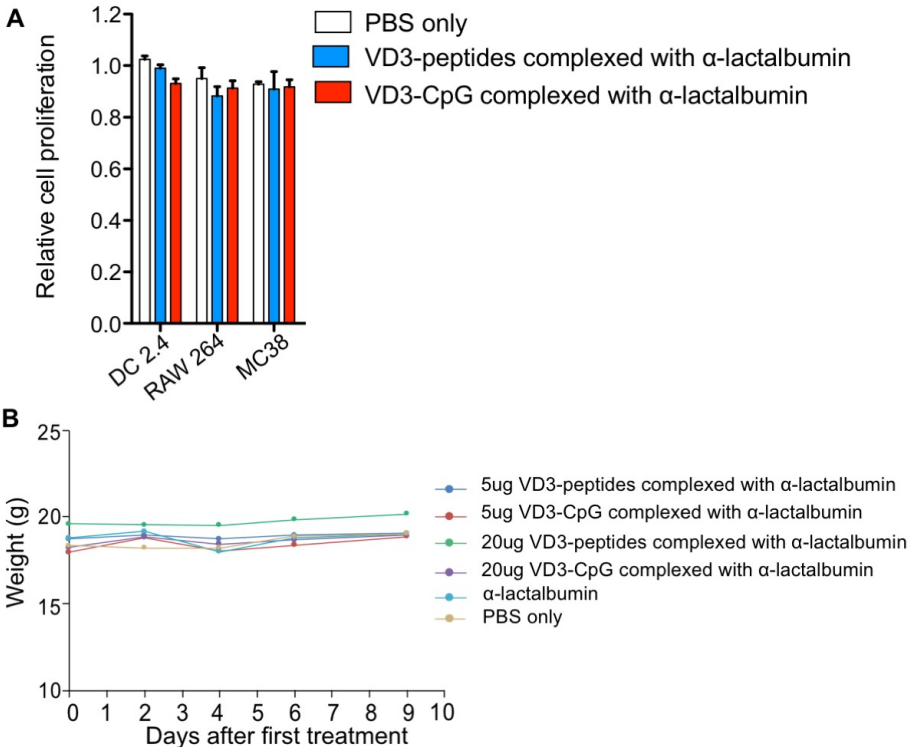


Figure 2. (A) MTT assays to measure the cytotoxcities of different complexes in three different cell lines, DC 2.4 (dendric cells), RAW 264.7 (macrophages) and MC38 (intestinal cells). Cells were treated the complexes for 48hr, and at the endpoint, MTT substrates were added into cells and incubated at 37C for 4 hours. Cells were lysed by DMSO and absorbance was measured at OD = 590 nm. Cell proliferation was calculated by normalizing to PBS treated cells. **(B)** Body weight measurement. ~7-week old C57BL/6 mice were orally administered with a single dose of indicated formulations. Body weights were measured every two days, and were compared to the vehicle treated group (PBS), indicating that no side effects were observed.

Next, we determined the cytotoxicity of the delivery systems using a standard MTT (3-4,5-dimethylthiazol-2-yl)-2,5-diphenyl tetrazolium bromide) assay using three mouse model cell lines: DC 2.4 (dendric cells), RAW264.7 (macrophage) and MC38 (colon cells). Compared to the vehicle control (PBS), 20ug VD3-peptide or VD3 CpG complexed with α-lactalbumin exhibited no reduction in cell proliferation at 24hr post incubation (**Figure 2A**). Afterwards, we evaluated the safety of our systems in wildtype C57BL/6 mice via oral gavage. Since the oral gavage technique was new to my new lab, we spent a month receiving the training from the animal facility at Northeastern University and then practiced on our own before we felt confident to perform the procedure. As show in **Figure 2B**, mouse body weights were measured every two days after one single oral administration of two different doses. Compared to the vehicle control PBS or lactalbumin, we did not observe detectable weight changes, suggesting that the compositions and doses were compatible and agreed with our in vitro cytotoxicity studies.

Major Task 3 (Aim 3): Evaluate the therapeutic efficacy in mice

Subtask 1 Investigate the pharmacokinetics and biodistribution of lipid conjugates/α-lactalbumin

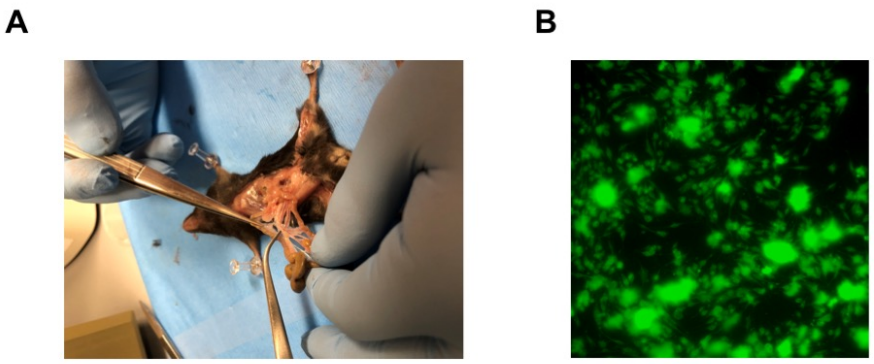


Figure 3. **(A)** Dissection of mesenteric lymph node from the C57BL/6 mouse. **(B)**. Confocal microscopy imaging showing the retention of FITC-labelled complexes in the lumen of the intestines.

We chose to fluorescently label α-lactalbumin rather than Vitamin-D peptide Vitamin D (CpG) because we previously found that fluorescent tagging of the small peptides or CpG severely affected the activities. α-lactalbumin is relatively large and therefore permitted extensive dye conjugation for *in vivo* trafficking. As show in **Figure 3A**, my PhD student, Mengdi Yang, was dissecting the mesenteric lymph nodes, which are the primary draining lymph nodes from oral delivery. Confocal microscopy showed that the retention of FTIC-labelled α-lactalbumin in intestines at 6hr post oral administration of α-lactalbumin complexed with 20ug VD3-peptide and VD3 CpG simultaneously (**Figure 3B**).

Subtask 2 Evaluate the oral vaccination efficacy of lipid conjugates/α-lactalbumin

According to the comments from the reviewers on our original proposal, we decided to focus on the humoral responses rather than the cellular immunity. To this end, we focused on $OVA_{323-339}$ (ISQAVHAAHAEINEAGR) with Vitamin D conjugation, and gavaged mice along with Vitamin D-conjugated CpG. As shown in **Figure 4**, one, two and four weeks after the second boost, we used ELISA to quantify the levels of $OVA_{323-339}$ –specific antibodies. Unfortunately, we did not observe noticeable detection of antibodies compared to the vehicle control.

A

#	Treatment Regimen
1	Vehicle control
2	α-lactalbumin
3	5ug VD3-peptide & VD3 CpG complexed with α-lactalbumin
4	20ug VD3-peptide & VD3 CpG complexed with α-lactalbumin
5	5ug VD3-peptide complexed with α-lactalbumin
6	20ug VD3-peptide complexed with α-lactalbumin
7	5ug VD3-CpG complexed with α-lactalbumin
8	20ug VD3-CpG complexed with α-lactalbumin

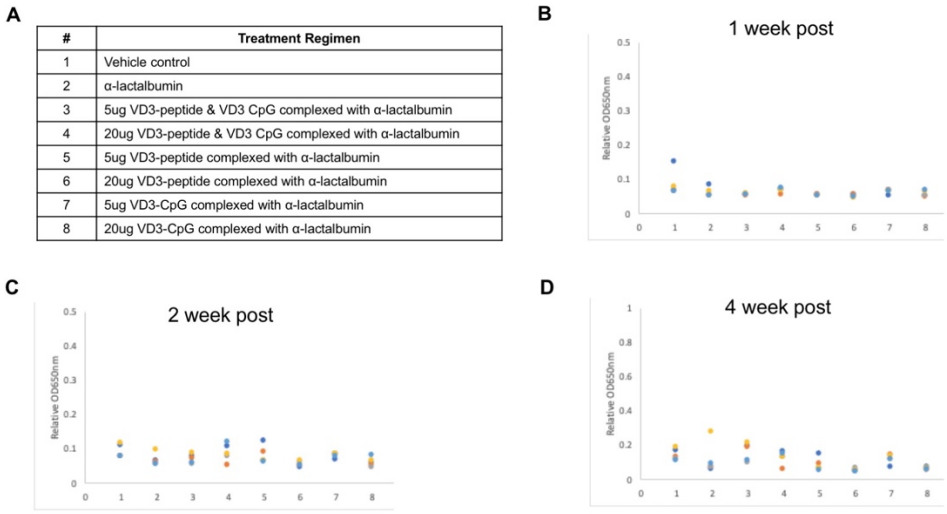


Figure 4. **(A)** Treatment regimens in C57BL/6 mice. Mice were gavaged with indicated formulations twice with a 2-week interval. **(B)** One, **(C)** two and **(D)** four weeks after the 2nd administration, mouse sera were collected for ELISA. The y axis indicated the absorbance of ELISA assays reflecting the relative levels of antigen-specific total antibodies.

We repeated the experiment one more time with another cohort of mice but remained unable to detect antibodies. After consulting with colleagues with expertise in mucosal delivery, we reasoned that the most likely reason is the lack of efficient delivery of the complexes across the intestinal barriers.

To test the above hypothesis, we established a gut-in-a-dish model to evaluate the transport of the amphiphilic peptides. To this end, an in vitro CACO-2 intestinal model was construed to mimic the intestinal epithelial cell monolayer (**Figure 5A**). The dextran 10 kDa fluorescein isothiocyanate (FITC) was used to monitor the CACO-2 cell layer permeability. Figure 3 shows that there is no FITC leakage at day 8 after plating cells, demonstrating that CACO-2 fully cover the permeable membrane. After confirming the integrity of the monolayer, free peptides or Vitamin D conjugated SIINFEKL peptides were added in the apical chamber (800 ng) while CFSE-labelled OT1 cells were added in basolateral chambers. As a positive control, we added vitamin D-peptides directly to CFSE-labelled OT1 cells. At 96hr post coculturing, we failed to detect any cell proliferation and activation in the groups separated by the monolayer of CACO-2, which simulated the intestinal barrier (**Figure 5B**). These experiments promoted us to think that the lack of immune stimulation in vivo is likely due to poor bioavailability of our conjugates to immune cells.

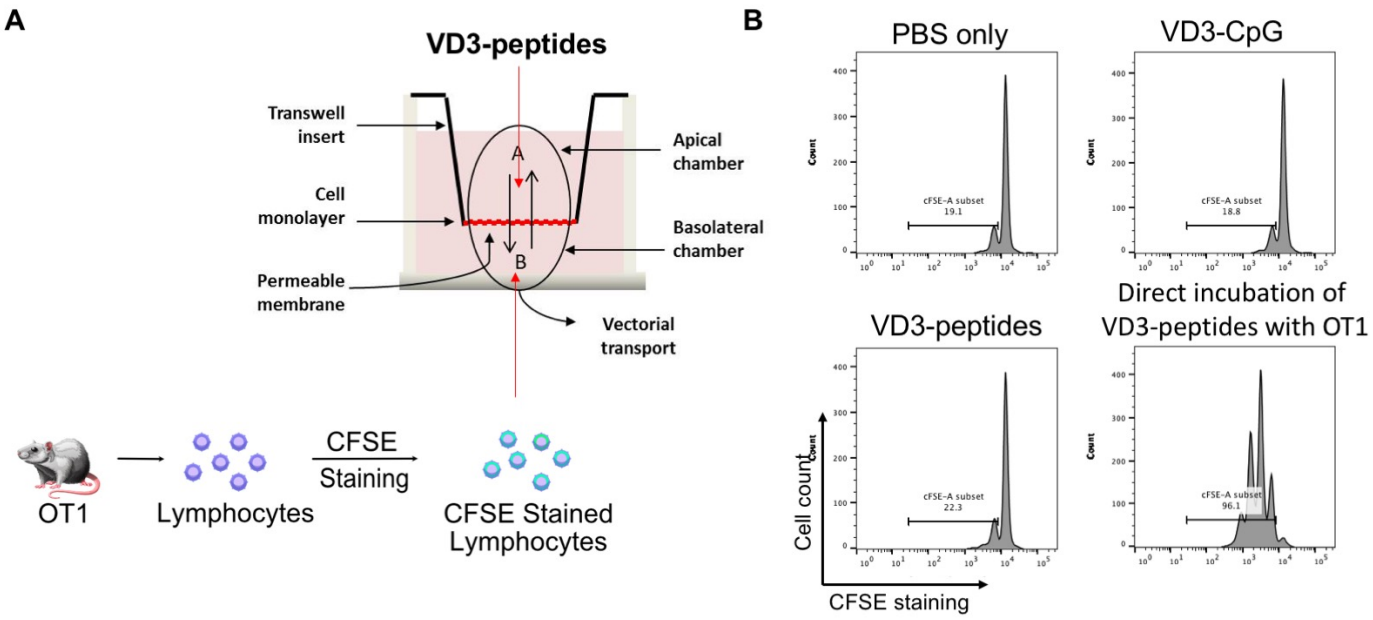


Figure 5. **(A)** Schematic of in vitro intestinal gut model and OT1 cells. **(B)** CFSE staining of OT1 T cell proliferation in response to peptide stimulation at 96hr post incubation. T cells were gated on viable dye and CD8 antibody.

Subtask 3 Explore alternative immune adjuvants to enhance the oral vaccination

Recent studies by others have shown that targeting the Stimulator of Interferon Genes (STING) pathway can enhance the mucosal immunity. In parallel, a separate effort in our lab has been focusing on activating the STING pathway via co-delivery of recombinant STING proteins and its agonist, cGAMP. In contrast to existing nano-formulations and synthetic depots to overcome the challenges in encapsulation and intracellular delivery of STING agonists (e.g., cGAMP), we recently repurposed the natural receptor STING as a highly modular and simple platform to efficiently bind and deliver cGAMP by a simple physical mixture prior to *in vitro* and *in vivo* applications (**Figure 6A and B**). Specifically, we took advantage of previous biochemical studies, in which the recombinant STING protein lacking the transmembrane domain (STINGΔTM) is known to bind cGAMP with high affinity (~5 nM of Kd). Furthermore, RNPs consisting of STINGΔTM and cGAMP could robustly activate the canonical Type I IFN signaling following delivery of the complexes via commercial transfection reagents in HEK293T that do not express endogenous STING (**Figure 6C**). On the contrary, recombinant STINGΔTM proteins with catalytically inactive mutations, including S366A and deletion of the last 9 amino acids (i.e., ΔC9), failed to activate the STING pathway in HEK293T. The “unconventional” function of STINGΔTM is unexpected since others have noted that the TM domain is essential for intracellular STING activation by mediating its oligomerization and translocation from the endoplasmic reticulum to the Golgi apparatus. Coincidentally, a previous study by James Chen’s group showed that the recombinant form of the C terminal tail corresponding to a shorter version of STINGΔTM can phosphorylate the STING targets TBK1 and IRF3 in cell-free extracts. To further explore the STINGΔTM as an immune adjuvant with the chicken ovalbumin, OVA as the model antigen

(**Figure 7A**). As shown in **Figure 7B and C**, following a prime-boost protocol, co-delivery of STINGΔTM and cGAMP markedly enhanced the total IgG levels compared to free cGAMP and other control groups.

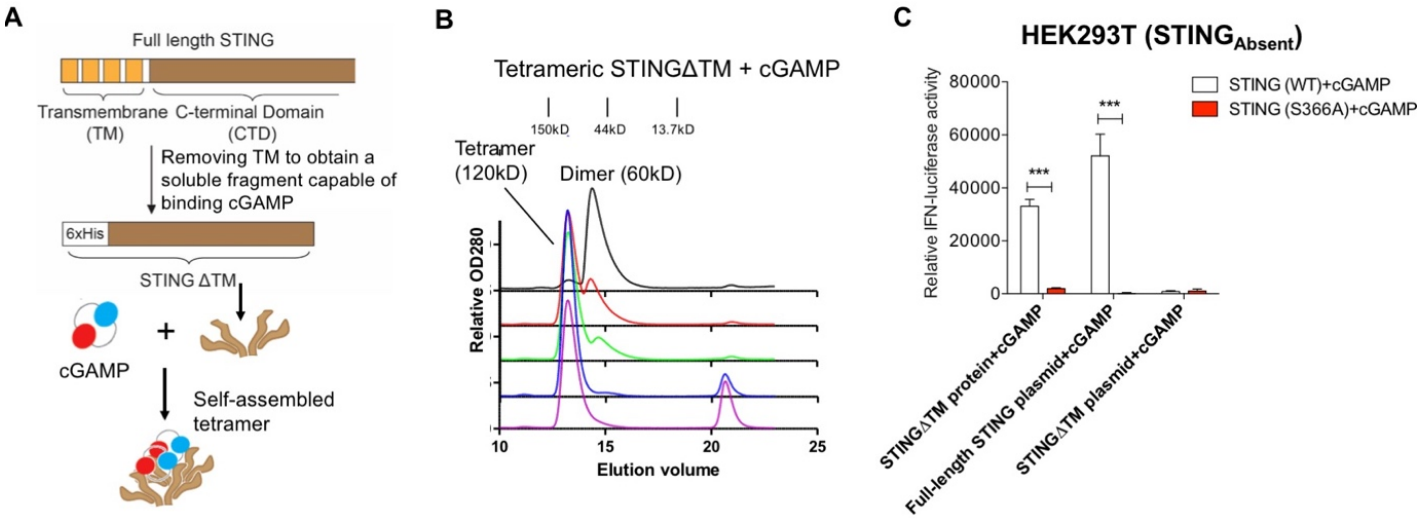


Figure 6. (A) Schematic of generating transmembrane-deficient STINGΔTM. **(B)** cGAMP binding induces tetramerization of STINGΔTM confirmed by the size exclusion chromatography. **(C)** Transfection of cGAMP+STINGΔTM protein or a plasmid encoding a full-length STING can activate type I IFN in HEK293T cells, while a plasmid encoding STINGΔTM does not.

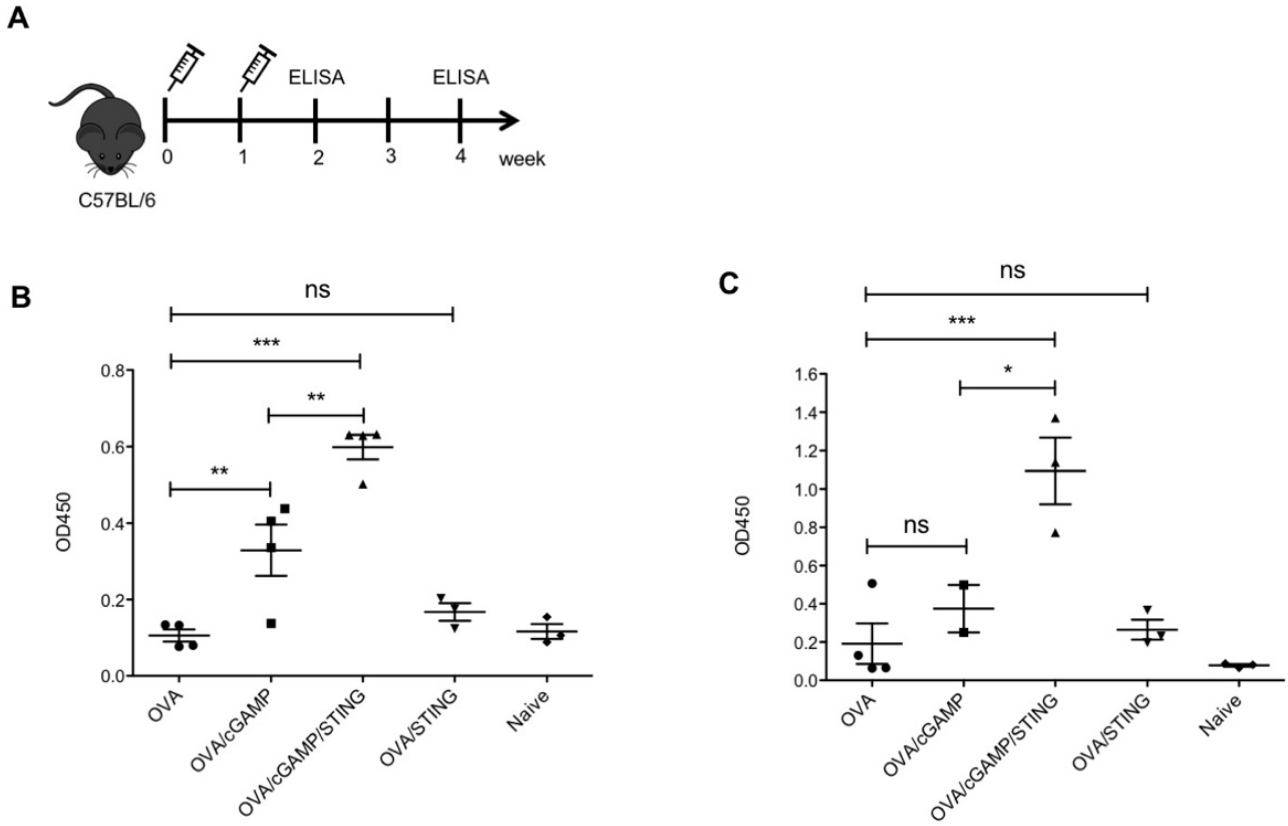


Figure 7. (A) Schematic of vaccination in mice. ELISA OVA-specific total IgG at **(B)** 1 week and **(C)** 3 weeks after boost.

4. Impact

In summary, in year 2 of this funding, we have confirmed the physiochemical stabilities of the complexes, characterize the safety in vitro and in vivo. Unfortunately, our first in vivo vaccination experiments did not result in efficacious induction of mucosal immune responses in mice. To debug the problems, first, we established an in vitro gut model to assess whether the lack of in vivo efficacy is due to poor bioavailability of the antigens/adjuvants. We used the transgenic mouse model OT1 that can recognize specific peptides. Indeed, we found that Vitamin D-conjugated peptides could barely cross the intact intestinal barrier using our in vitro gut model. In parallel, we asked whether alternative potent immune adjuvants such as the STING agonists could potentially enhance the oral vaccination. As of May 15th, we have published two relevant papers on exploring the STING pathway for vaccine adjuvants, and these two papers are partially funded by the Discovery award. At the moment, we are exploring the new STING formulation as an immune adjuvant for oral vaccination.

5. Changes/Problems

As discussed above, we identified the lack of in vivo immune responses from oral vaccination of our lactalbumin-based complexes despite encouraging data in vitro. Later on, we changed from in vivo to in vitro using the gut model to understand whether it was caused by poor bioavailability of the complexes. In parallel, in addition to the CpG adjuvant, we explored the STING pathway as a more potent immune adjuvant for oral vaccination. As a proof-of-concept, we showed that co-delivery of the recombinant STING protein with STING agonists such as cGAMP can enhance the efficacy of STING agonist delivery by ~100-fold. Encouraged by the preliminary data, our direction has slightly changed to focusing on the STING pathway to augment the efficacy of vaccination in mice.

6. Products

Journal articles:

Sun X, Hay I, Doran P, Basireddy S, Scott M, Wu Y, Al-Dossary AA, **Li J***. Delivery Strategies for STING Agonists, 2021, a Chapter for the book "Delivery Strategies in Immuno-Oncology" from ELSEVIER (In press)

Sun X, Ni Y, He Y, Yang M, Tani T, Kitajima S, Barbie DA, **Li J*.** Engineering the Immune Adaptor Protein STING as a Biologic, *Advanced Therapeutics*, 2021. (In press)

He Y, Hong C, Yan Z.E, Li Y, Zhu G, Yang M, Li Y, Sun X, Irvine DJ, Li J*, Hammond PT*. Self-Assembled cGAMP-STING ΔTM Signaling Complex as a Bioinspired Platform for cGAMP Delivery, *Science Advances*, 2020. (co-correspondence)

Provisional patent applications filed by Northeastern University:

DISC-2021/166	INV-21030	A Novel Adjuvant for Oral Vaccines Using Engineered Bacteria Targeting the STING Pathway	Deborah Bouchard, Ian Bricknell, Jiahe Li
DISC-2020/070	INV-20063	Recombinant Transmembrane Domain-Deficient STING as Biomimetic Protein Carrier for cGAMP Enhanced Cancer Immunotherapy	Jiahe Li

7. Participants & Other Collaborating Organizations

Name: Jiahe Li
Project Role: PI
Nearest Person-Month Worked: 1 month (summer) (Academic salary covered by NEU)

Name: Xin Sun
Project Role: Graduate student
Nearest Person-Month Worked: 12 months
Contribution to Project:

Name: Mengdi Yang
Project Role: Graduate Student
Nearest Person-Month Worked: 4 months (tuition is waived in the college of engineering at NEU)
Contribution to Project:

8. Special Reporting Requirements

9. **Appendices** Copies of papers published and in press are included in the Appendix

IMMUNOLOGY

Self-assembled cGAMP-STINGΔTM signaling complex as a bioinspired platform for cGAMP delivery

Yanpu He[1,2], Celestine Hong[1,2], Emily Z. Yan[1,2], Samantha J. Fletcher[1,2], Ge Zhu[3], Mengdi Yang[3], Yingzhong Li[1,4], Xin Sun[3], Darrell J. Irvine[1,4,5,6], Jiahe Li[3]*, Paula T. Hammond[1,2]*

Copyright © 2020 The Authors, some rights reserved; exclusive licensee American Association for the Advancement of Science. No claim to original U.S. Government Works. Distributed under a Creative Commons Attribution NonCommercial License 4.0 (CC BY-NC).

The stimulator of interferon (IFN) genes (STING) pathway constitutes a highly important part of immune responses against various cancers and infections. Consequently, administration of STING agonists such as cyclic GMP-AMP (cGAMP) has been identified as a promising approach to target these diseases. In cancer cells, STING signaling is frequently impaired by epigenetic silencing of STING; hence, conventional delivery of only its agonist cGAMP may be insufficient to trigger STING signaling. In this work, while expression of STING lacking the transmembrane (TM) domain is known to be unresponsive to STING agonists and is dominant negative when coexpressed with the full-length STING inside cells, we observed that the recombinant TM-deficient STING protein complexed with cGAMP could effectively trigger STING signaling when delivered in vitro and in vivo, including in STING-deficient cell lines. Thus, this bioinspired method using TM-deficient STING may present a universally applicable platform for cGAMP delivery.

INTRODUCTION

Cytosolic detection of pathogen- and cancer cell–derived DNA is a major mechanism for immune clearance by inducing type I interferons (IFNs), and the stimulator of IFN genes (STING) is a master regulator that connects DNA sensing via cyclic guanosine monophosphate (GMP)–adenosine monophosphate (AMP) synthase (cGAS) to IFN induction. As a transmembrane (TM) protein localized to the endoplasmic reticulum (ER), STING consists of an N-terminal TM domain and a C-terminal domain (CTD), the latter of which binds STING agonists [i.e., cyclic dinucleotides (CDNs) such as 2′3′ cyclic GMP-AMP (cGAMP)] and downstream signaling protein tank-binding kinase 1 (TBK1) (*1*). In addition to antibacterial and antiviral infections, recent evidence has shown an important role of STING in generating a spontaneous antitumor T cell response in the tumor microenvironment (TME) (*2*, *3*). Activation of the STING pathway in the TME can augment dendritic cell maturation and the production of type I IFNs and other cytokines, which elicit robust antitumor T cell responses and overcome resistance against immunosuppressive cells that inhibit antitumor immunity (*4*). These findings have motivated extensive investigations on the delivery of cGAMP as a strategy for cancer immunotherapy (*5*).

Several key challenges to cGAMP delivery stem from the molecular nature of cGAMP: As a negatively charged small molecule, it is difficult to deliver it to the cytoplasm where STING is located. Moreover, cGAMP is rapidly cleared in vivo, and thus, has limited access to tumors (*4*, *6*, *7*). Hence, existing efforts in delivering exogenous cGAMP have focused mostly on the development of novel biomaterials to improve cGAMP's bioavailability. However, one requirement for conventional cGAMP delivery to activate STING signaling is that the cell needs to have functional STING protein. Studies have shown that in cancer cells, STING signaling is frequently impaired because of epigenetic silencing of either STING or cGAS (*8*, *9*). In addition, it is still under debate whether all human populations are responsive to treatments of direct cGAMP administration. The human TMEM173 gene encoding for STING has high heterogeneity, approximately 19% of humans carry the HAQ STING variant (with three amino acid substitutions R71H-G230A-R293Q, hence the acronym HAQ). Recent literature has shown this mutation to be a null allele, resulting in substantial reduction in IFN-β expression (*10*–*14*), although some other studies argue that HAQ STING is actually functionally responsive (*15*, *16*).

Here, we developed a universal cGAMP delivery platform that can trigger STING signaling independent of endogenous STING functionality to fully address cells that are STING defective or deficient in humans due to either genetic heterogeneity or cancer. Previous studies have demonstrated that TM domain–deficient STING is capable of activating IFN regulatory factor 3 (IRF3) in cytosolic extracts (*17*), while others have noted that the TM domain is essential for intracellular STING activation by mediating its translocation from the ER to the Golgi apparatus, where it forms punctate structures indicative of oligomerization (*1*). This oligomerization—in particular, the formation of well-defined tetrameric or higher-order oligomeric structures—has been demonstrated to be essential to the STING signaling pathway by enabling TBK1 activation, which results in IRF3 binding and phosphorylation (*18*). While studies have observed a small fraction of cytosolic STING to aggregate upon the addition of cGAMP, the oligomerization of full-length STING is predicted to occur more favorably at high local concentrations on two-dimensional membranes (*19*, *20*). Unexpectedly, by titrating the amount of cGAMP to recombinant, TM domain–deficient STING (STINGΔTM) of ~30 kDa, we observed a near-complete shift in population toward a ~120 kDa–molecular weight ribonucleoprotein complex, suggesting a cGAMP-induced tetramerization. Furthermore, we assessed the functionality of this ribonucleoprotein and found it not only capable of augmenting type I IFN production in cells with endogenous STING expression but also fully activating

[1]Koch Institute for Integrative Cancer Research, Massachusetts Institute of Technology, Cambridge, MA 02139, USA. [2]Department of Chemical Engineering, Massachusetts Institute of Technology, Cambridge, MA 02139, USA. [3]Department of Biological Engineering, Northeastern University, Boston, MA 02115, USA. [4]Department of Biological Engineering, Massachusetts Institute of Technology, Cambridge, MA 02139, USA. [5]Department of Materials Science and Engineering, Massachusetts Institute of Technology, Cambridge, MA 02139, USA. [6]Howard Hughes Medical Institute, Chevy Chase, MD 20815, USA.
*Corresponding author. Email: jiah.li@northeastern.edu (J.L.); hammond@mit.edu (P.T.H.)

Downloaded from http://advances.sciencemag.org/ on May 13, 2021

type I IFN in STING-defective and even STING-deficient cell lines. Last, we exploited its application with in vivo vaccination studies and observed enhancement of both innate and adaptive immune responses, including the augmentation of type I IFN expression in vitro and of both tumor necrosis factor–α (TNF-α) and IFN-γ in vivo, robust antigen-specific T cell activation and antibody production, and significantly improved therapeutic efficiency in a prophylactic study with melanoma and a treatment study with colon cancer mouse models.

RESULTS

Overview of cGAMP delivery strategies

Most, if not all, existing strategies of STING agonist delivery involve directly encapsulating cGAMP into synthetic delivery vehicles, such as liposomes or polymersomes (Fig. 1A). The primary roles of the vehicles are to package the CDN, modulate cellular uptake, and facilitate endosomal escape (*4*, *6*, *21*). The vehicles themselves play no functional role in enabling STING signaling and, thus, can potentially result in decreased efficacy when treating cells with HAQ STING variants or cells deficient in endogenous STING. Consequently, we devised a bioinspired codelivery method that precludes the need for fully functional endogenous STING or cGAMP release from a vehicle, using a recombinant TM domain–deficient STING protein as a high-affinity, stable carrier [K_d ~73 nM (*22*)] for cGAMP. Furthermore, while preassembling STINGΔTM with cGAMP, we observed that this ribonucleoprotein complex is, in turn, able to tetramerize in response to cGAMP binding to STINGΔTM, forming the essential structure for TBK1 recruitment and downstream signaling (Fig. 1B).

cGAMP binding induces near-complete self-assembly of STINGΔTM into tetramers

To characterize the interaction between cGAMP and STINGΔTM protein, we performed fast protein liquid chromatography (FPLC) analyses in phosphate-buffered saline (PBS) and observed that STINGΔTM without cGAMP predominantly exist as dimers with an estimated molecular weight of 60 kDa (Fig. 2A). We titrated STINGΔTM protein with various molar ratios of cGAMP, incubated the mixture to reach equilibrium, and then injected the mixture through FPLC. While increasing the molar ratio of cGAMP: STINGΔTM, we observed the original STINGΔTM dimer population gradually shifting toward another well-defined population with an estimated molecular weight of 120 kDa, suggesting a transition to a tetrameric conformation. No free cGAMP was eluted from FPLC when STINGΔTM were mixed at less than 0.5 molar equivalence of cGAMP. It was only after cGAMP had tetramerized all STINGΔTM did it start to elute as free cGAMP (Fig. 2, A and C). We also observed with transmission electron microscopy (TEM) that STINGΔTM alone in PBS exists as particles ~14 nm in diameter, and when mixed with cGAMP, the particle diameters approximately doubled to ~29 nm, suggesting the formation of side-by-side tetrameric structures (fig. S1). To verify the role of cGAMP binding in inducing this tetramer self-assembly, we generated mutant STINGΔTM proteins R237A/Y239A for mouse STING and R238A/Y240A for human STING, known to abolish the cGAMP binding capability of STING protein (*20*). As shown in Fig. 2 (B and D), STINGΔTM R237A/Y239A showed a partially tetrameric structure independent of cGAMP but no further self-assembly with increasing amounts of cGAMP titrated. All cGAMP added eluted as free cGAMP.

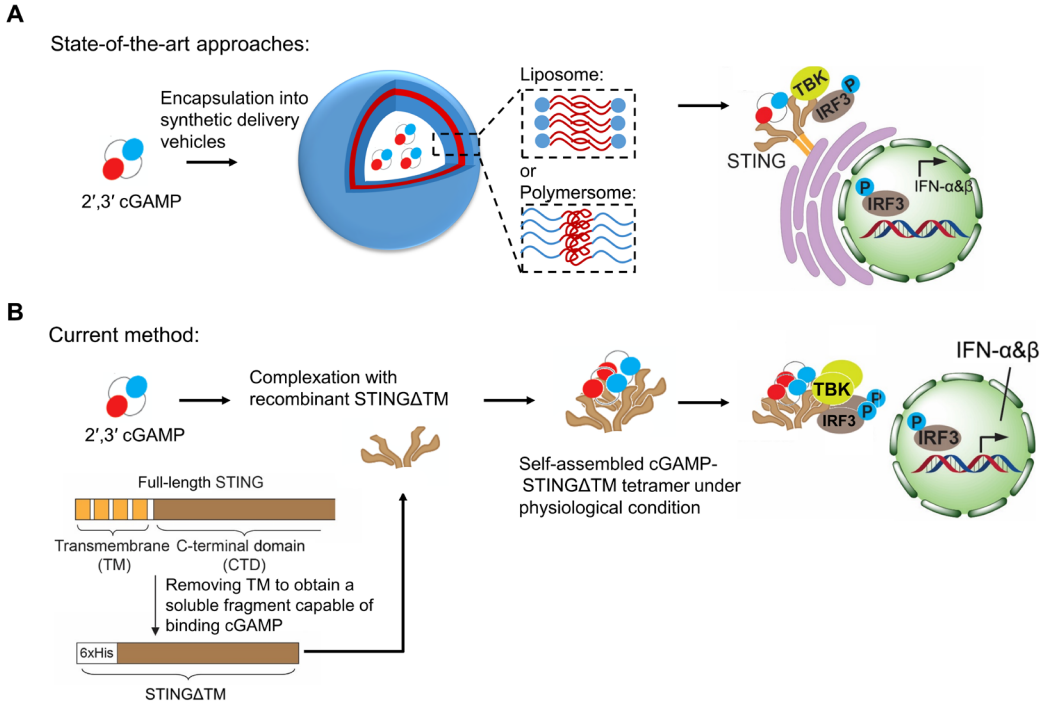


Fig. 1. Overview of state-of-the-art approaches of cGAMP delivery and schematics of recombinant STINGΔTM structure and therapeutic strategy. (**A**) State-of-the-art approaches through directly encapsulating cGAMP into liposomes or polymersomes for cell transfection. (**B**) Current strategy of delivering cGAMP with a recombinant, transmembrane-deficient STING as carrier in the form of a ribonucleoprotein complex.

Downloaded from http://advances.sciencemag.org/ on May 13, 2021

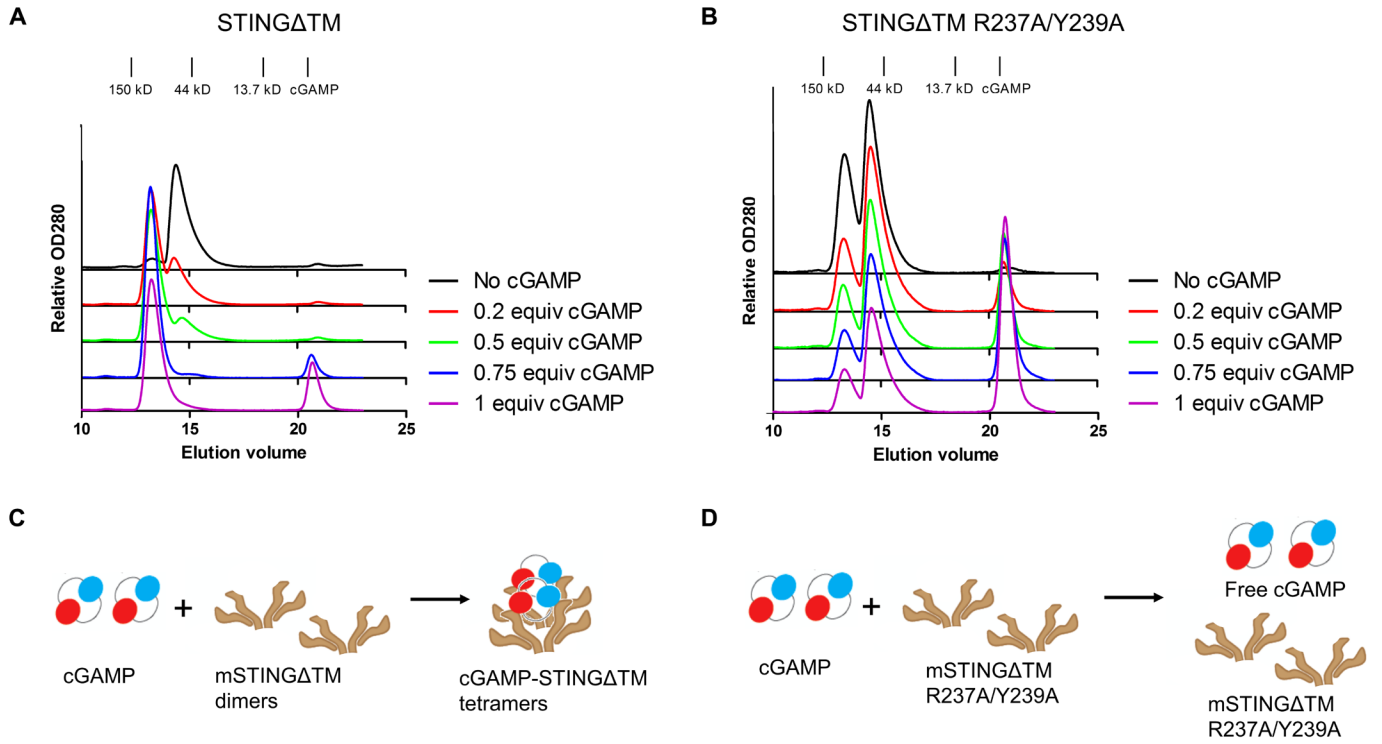


Fig. 2. cGAMP binding induces near-complete self-assembly of cGAMP-STINGΔTM tetramer. FPLC analyses of (**A**) mouse STINGΔTM and (**B**) R237A/Y239A mutant in PBS, titrated with various molar ratios of cGAMP and schematics of cGAMP-STINGΔTM tetramer self-assembly with (**C**) mouse STINGΔTM and (**D**) R237A/Y239A mutant, which is not capable of binding cGAMP.

Additional experiments were conducted with functional double mutants at the tetramer interface (Q272A/A276Q in mouse STINGΔTM) (fig. S2C). These mutants have been reported to disrupt the oligomerization of chicken STING, as well as abolish translocation and puncta formation induced by cGAMP (*20*). Unexpectedly, we observed the formation of tetrameric structures in the presence of these mutations. While beyond the scope of discussion in this work, these results may raise the possibility of a cGAMP-induced ΔTM tetrameric structure distinct from the wild-type (WT) STING oligomers studied in literature (*20*, *23*).

It has been reported that STING moves from the ER and aggregates via oligomerization of the cytosolic CTD following its activation by cGAMP. This aggregation is essential for the binding and phosphorylation of TBK1, which subsequently phosphorylates IRF3 and initiates the downstream pathway (*18*). Recent structural analyses of the STING-TBK1 protein complex revealed that because of geometric constraints, the S366 of STING cannot be phosphorylated by the same TBK1 dimer it is bound to; instead, it interacts with the kinase site of the neighboring TBK1. Hence, a minimum of two neighboring dimers—a tetrameric structure—is needed for successful signaling. It was also found that after full-length STING in cells binds cGAMP, they form side-by-side tetramers that could assemble into larger oligomers to facilitate this transphosphorylation (*20*). We observed that cells overexpressing STINGΔTM do not exhibit this clustering of STINGΔTM molecules upon addition of cGAMP; the protein is evenly distributed in the cytosol, as the N-terminal domain that modulates the translocation from the ER is missing. However, when we directly delivered the tetramerized STINGΔTM protein with cGAMP via a commercial transfection reagent into cells, we observed the clustering behavior of the STINGΔTM protein that is essential for IFN signaling (Fig. 3F). This was corroborated by in vitro activation tests of STING signaling, the details of which are discussed in the following section. We therefore hypothesize that the cGAMP-STINGΔTM tetrameric signaling complex created in the preassembly process was the pivotal factor for successful IFN signaling in cells.

cGAMP-STINGΔTM results in enhanced type I IFN signaling in vitro

Unless otherwise specified, we used human STINGΔTM for all human embryonic kidney (HEK) 293T cell in vitro IFN activation tests and mouse STINGΔTM for all remaining studies. In the figure legends, all proteins delivered in vitro and in vivo (denoted as ΔTM or mutants such as S365AΔTM) are referred to as STINGΔTM proteins, and all cGAMP codelivery groups comprise 1:1 molar equivalents of cGAMP:STINGΔTM. To verify the signaling efficacy of the cGAMP-STINGΔTM tetramer, we first delivered them to a mouse macrophage cell line RAW264.7 that has endogenous STING expression. Overall, we observed that the vehicle-free groups elicited higher IFN expression than the groups with commercial transfection reagent and that in both groups, cGAMP codelivery with STINGΔTM resulted in higher IFN expression than cGAMP delivered alone (Fig. 3B). In the presence of endogenous STING, mutant versions of cGAMP-STINGΔTM (S365A and R237A/Y239A) are as effective as the WT protein, suggesting that S365A and R237A/Y239A mutants may act as chaperones to shuttle cGAMP into cells while utilizing endogenous WT STING for activation of STING signaling.

We then tested the efficacy of cGAMP-STINGΔTM tetramer in an IFN-luciferase reporter cell line HEK293T, which was deficient in endogenous STING expression but expresses other essential proteins

Downloaded from http://advances.sciencemag.org/ on May 13, 2021

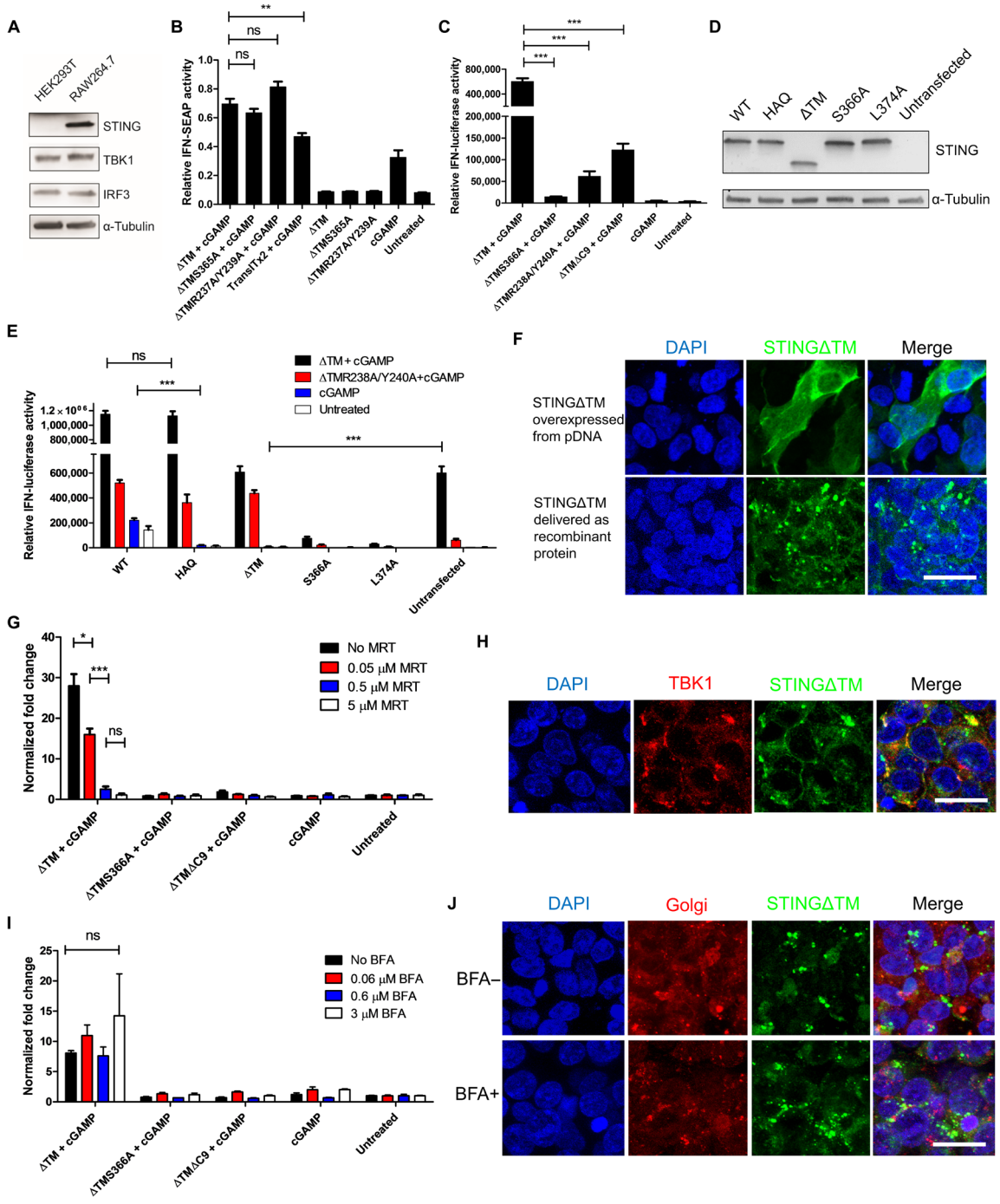


Fig. 3. cGAMP-STINGΔTM tetramer effectively triggers IFN expression in vitro, including in STING-deficient and STING-defective cell lines. (**A**) Immunoblotting of endogenous expression of STING, TBK1, and IRF3 in HEK293T and RAW264.7 cell line. (**B**) RAW264.7 cells ($n = 3$) and (**C**) HEK293T cells ($n = 4$) treated with different combinations/mutations of cGAMP-STINGΔTM tetramer (10 μg of STINGΔTM with 0.25 μg of cGAMP per milliliter). Luciferase and single enzyme activity–based protein profiling (SEAP) activity were determined 24 hours after treatment. (**D**) Immunoblotting of HEK293T cells transiently transfected with plasmid DNA overexpressing full-length human STING (WT, HAQ, S366A, and L374A) and hSTINGΔTM. (**E**) Transfected HEK293T cells ($n = 4$) in (D) treated with cGAMP-STINGΔTM tetramer (plus R238A/Y240A mutant), cGAMP only, and 10 μg of STINGΔTM with 0.25 μg of cGAMP per milliliter. Luciferase activity were determined 24 hours after treatment. (**F**) Confocal micrograph of HEK293T cells (upper) transfected with plasmid DNA encoding for STINGΔTM expression and then stimulated with cGAMP and (lower) with cGAMP-STINGΔTM tetramer delivered as ribonucleoprotein complex. (**G**) HEK293T cells ($n = 4$) pretreated with TBK1 inhibitor MRT67307 (MRT) and then treated with different combinations/mutations of cGAMP-STINGΔTM tetramer. (**H**) Confocal micrograph of HEK293T cells treated with cGAMP-STINGΔTM tetramer showing colocalization of STINGΔTM and TBK1. (**I**) HEK293T cells ($n = 4$) pretreated with BFA, which blocks ER-Golgi trafficking and then treated with different combinations/mutations of cGAMP-STINGΔTM tetramer. (**J**) Confocal micrograph of HEK293T cells ($n = 4$) treated with cGAMP-STINGΔTM tetramer showing no colocalization of STINGΔTM with Golgi apparatus, in the presence or absence of BFA. Values are reported as means ± SEM. ***$P < 0.001$, **$P < 0.01$, and *$P < 0.05$, as analyzed by one-way analysis of variance (ANOVA). Scale bars, 50 μm. ns, not significant.

Downloaded from http://advances.sciencemag.org/ on May 13, 2021

for the STING signaling pathway including TBK1 and IRF3 (Fig. 3A). We generated this cell line by integrating an IFN-stimulated response element (ISRE) that drives the expression of luciferase in HEK293T cells. In addition, we included three functional STINGΔTM mutants: S366A, R238A/Y240A, and ΔC9 (deleting nine amino acids from the C-terminal tail), which are known to abrogate STING phosphorylation, cGAMP binding, and TBK1 binding, respectively (*17*), and confirmed that the STINGΔTM protein is indeed functional in triggering the STING pathway independent of endogenous STING (Fig. 3C).

Although the axes of Fig. 3 (B and C) are not directly comparable due to the use of two different IFN reporters (raw ISG blue for the RAW264.7 cell line and luciferase for the HEK293T cell line), it is apparent that in both cases, IFN activity is increased via the codelivery of cGAMP with STINGΔTM. And while there visually appears to be a far larger difference in IFN activity between the cGAMP and STINGΔTM plus cGAMP group in the HEK293T system, this is due to the lack of endogenous STING in the HEK293T cell line, leading to a negligible amount of IFN activity. Conversely, this difference is less pronounced in the RAW264.7 system due to the presence of endogenous STING, which leads to measurable IFN–secreted embryonic alkaline phosphatase (SEAP) activity in the cGAMP-only group (as it is able to function with endogenous STING).

We also evaluated the IFN activity of additional small-molecule agonists using cdiGMP and $cGAM(PS)_2$, a synthetic, nondegradable cGAMP analog, as previously described in the HEK293T system (fig. S4A). The system exhibited behavior similar to that of the cGAMP plus STINGΔTM codelivery group, namely, that the codelivery of STINGΔTM with these agonists resulted in increased IFN activity relative to all functional mutants tested and agonist-only controls. These studies suggest that the recombinant protein STINGΔTM-mediated enhanced type I IFN signaling derives from the preassembly of agonist and STINGΔTM and is independent of cell type or CDN species.

Last, we used several chemical inhibitors including MRT67307 (MRT), brefeldin A (BFA), chloroquine (CQ), and bafilomycin A1 (BafA1) to comprehensively dissect the intracellular trafficking of the tetrameric complex through confocal microscopy and quantification of IFN activity: At 6 hours after transfection, we observed limited colocalization of STINGΔTM with early endosome antigen 1 (EEA1), an early endosome marker, suggesting the potential escape of the early endosome into the cytosol (fig. S3B). IFN activity was observed to decrease with increasing concentrations of MRT (TBK1 inhibitor), which indicates that the STING signaling does proceed via a TBK1-dependent pathway (Fig. 3G). In addition, confocal microscopy images (also taken 6 hours after transfection) confirmed the colocalization of TBK1 with STINGΔTM in punctate structures that resemble those formed by cGAMP-activated full-length STING (Fig. 3H) (*1*). Interactions with IRF3 have previously been shown by coimmunoprecipitation of STINGΔTM with phosphorylated IRF3 (*17*). The presence of BFA, an inhibitor of ER-Golgi protein trafficking previously shown to block the full-length STING-induced IRF pathway (*24*, *25*), appeared to have an insignificant effect on STINGΔTM-induced STING signaling (Fig. 3I). This was corroborated by no significant evidence of STINGΔTM colocalization with the Golgi apparatus with or without the addition of BFA (Fig. 3J), a markedly different phenomenon from literature reports of full-length STING localization with ERGIC (ER-Golgi intermediate compartment) disruptors (*24*, *26*).

Another departure from similar assays on full-length STING was observed upon treatment of the cells with BafA1, an autophagy inhibitor. IFN activity was found to be significantly dependent on the concentration of BafA1, with decreasing activity observed with increasing concentrations of BafA1 (fig. S3A), which could suggest the necessity of autophagosome-lysosome fusion in STINGΔTM-induced STING signaling. The eventual degradation of STINGΔTM via a lysosomal pathway was observed in its colocalization with lysosomal-associated membrane protein 1 (LAMP1) at 24 hours after transfection, which was not apparent at 6 hours after transfection (fig. S3D). This was consistent with the increased IFN activity observed upon incubation with increasing concentrations of CQ (an inhibitor of lysosomal enzymes) (fig. S3C), as had been reported in literature with full-length STING (*27*).

While in the literature there are mixed reports on HAQ sensitivity to STING agonists relative to WT STING (*10*–*15*, *18*), we set out to assess whether the codelivery of STINGΔTM and cGAMP can enhance IFN in HAQ-transfected cells in comparison to cGAMP-only treatment in HEK293T cells, which lack endogenous STING. HEK293T cells were transiently transfected with plasmid DNA encoding a full-length human STING (WT, 1 to 379 amino acids) or the HAQ allele, as a means to simulate cells with fully functioning STING and defective STING. Meanwhile, S366A (1 to 379 amino acids), L374A (1 to 379 amino acids), and STINGΔTM (139 to 379 amino acids) were also expressed separately in 293T as negative controls (Fig. 3D). Those cells with various defective STINGs were then treated with cGAMP-STINGΔTM tetramers, cGAMP mixed with STINGΔTM (R238A/Y240A), or cGAMP only. As shown in Fig. 3E, cells overexpressing HAQ STING were significantly less responsive to conventional cGAMP administration than cells expressing WT STING. Cells overexpressing STINGΔTM also did not result in significant IFN activity upon delivery of cGAMP only, a phenomenon previously reported in literature (*1*, *28*, *29*). However, when cGAMP was delivered in the form of cGAMP-STINGΔTM tetramers, both cells overexpressing HAQ STING and WT STING showed equally high levels of IFN expression. Increased IFN expression was also observed in cells overexpressing STINGΔTM. Untransfected cells likewise exhibited significantly higher IFN activity upon codelivery of the cGAMP-STINGΔTM tetramers when compared with cGAMP-only controls in untransfected cells and cells overexpressing WT STING. Therefore, we demonstrated that our method could potentially address the issue of STING heterogeneity in humans through the codelivery of cGAMP with a functional STINGΔTM carrier.

To conclude the in vitro characterization of our STINGΔTM-cGAMP tetrameric complex, we evaluated the expression of IFN-β, TBK1, and IRF3 in RAW264.7 and DC2.4 cell lines via quantitative polymerase chain reaction (qPCR), as a means of better understanding the effect of the delivery system on STING signaling intermediates (fig. S5). At 6 hours after treatment with cGAMP-STINGΔTM, we were able to observe a slight enhancement in TBK1, but not in IRF3 expression. Overall, delivery of cGAMP-STINGΔTM significantly increased the expression of IFN-β relative to cGAMP-only and STINGΔTM-only controls in both cell lines tested, demonstrating the capability of the system to achieve enhanced STING signaling in the presence of endogenous STING.

cGAMP-STINGΔTM induces dendritic cell maturation and strong humoral and cellular immune responses in vivo

To explore its application to boost the adjuvanticity potential of STING agonists (e.g., cGAMP), we first confirmed the influence of

Downloaded from http://advances.sciencemag.org/ on May 13, 2021

cGAMP-STINGΔTM on dendritic cell maturation in vitro and in vivo. In brief, we analyzed the expression of IFN-β in dendritic cells 6 hours after treatment with cGAMP-STINGΔTM and found a significant increase in expression levels relative to cGAMP only and STINGΔTM controls. We were, likewise, able to confirm the effect of the tetramers on dendritic cell maturation in vivo following the treatment of C57BL/6 mice, where we observed significant up-regulation of the dendritic cell maturation marker major histocompatibility complex (MHC)–II$^+$ in CD11c$^+$ cells in the cGAMP-STINGΔTM trial compared with STINGΔTM and naïve controls (Fig. 4, A and B).

We then evaluated the humoral immune response elicited against ovalbumin (OVA) antigens with or without the STING-cGAMP adjuvant. Five groups of C57BL/6 mice were immunized on day 0 and boosted on day 7 with 10 μg of OVA alone or OVA mixed with 2.5 μg of cGAMP and/or 100 μg of STINGΔTM via tail base injection, as illustrated in Fig. 4C. On days 14, 28, and 42, sera were collected for enzyme-linked immunosorbent assay (ELISA) to determine the anti-OVA total immunoglobulin G (IgG) level. The groups vaccinated with the combination of OVA, cGAMP, and STINGΔTM generated a significantly more robust and sustained total IgG-based antigen-specific immune response compared with other control groups (Fig. 4, D to F). Additional experiments also demonstrated that no systemic toxicity occurred from tetramer delivery (fig. S6), specifically that there was no significant increase in the level of inflammatory cytokines [interleukin-6 (IL-6) and TNF-α] when compared with the injection of PBS. Release of cGAMP-STINGΔTM from the tail base was also sustained for over a week, with trafficking to the draining (inguinal) lymph nodes (fig. S7) that was 20- to 50-fold higher than in either STINGΔTM-only or cGAMP-only controls.

We then quantified the antigen-specific T cell activation via tetramer and intracellular cytokine staining of peripheral blood mononuclear cells (PBMCs) (*30*). Groups of C57BL/6 mice were immunized on day 0 and boosted on day 7 via tail base injection with 50 μg of OVA alone or OVA mixed with 1 μg of cGAMP and/or 40 μg of STINGΔTM (or 40 μg of S365A STINGΔTM). On day 14, mice were bled and PBMCs were separated from the whole blood (Fig. 5A). For tetramer staining, PBMCs were stained with anti-CD8

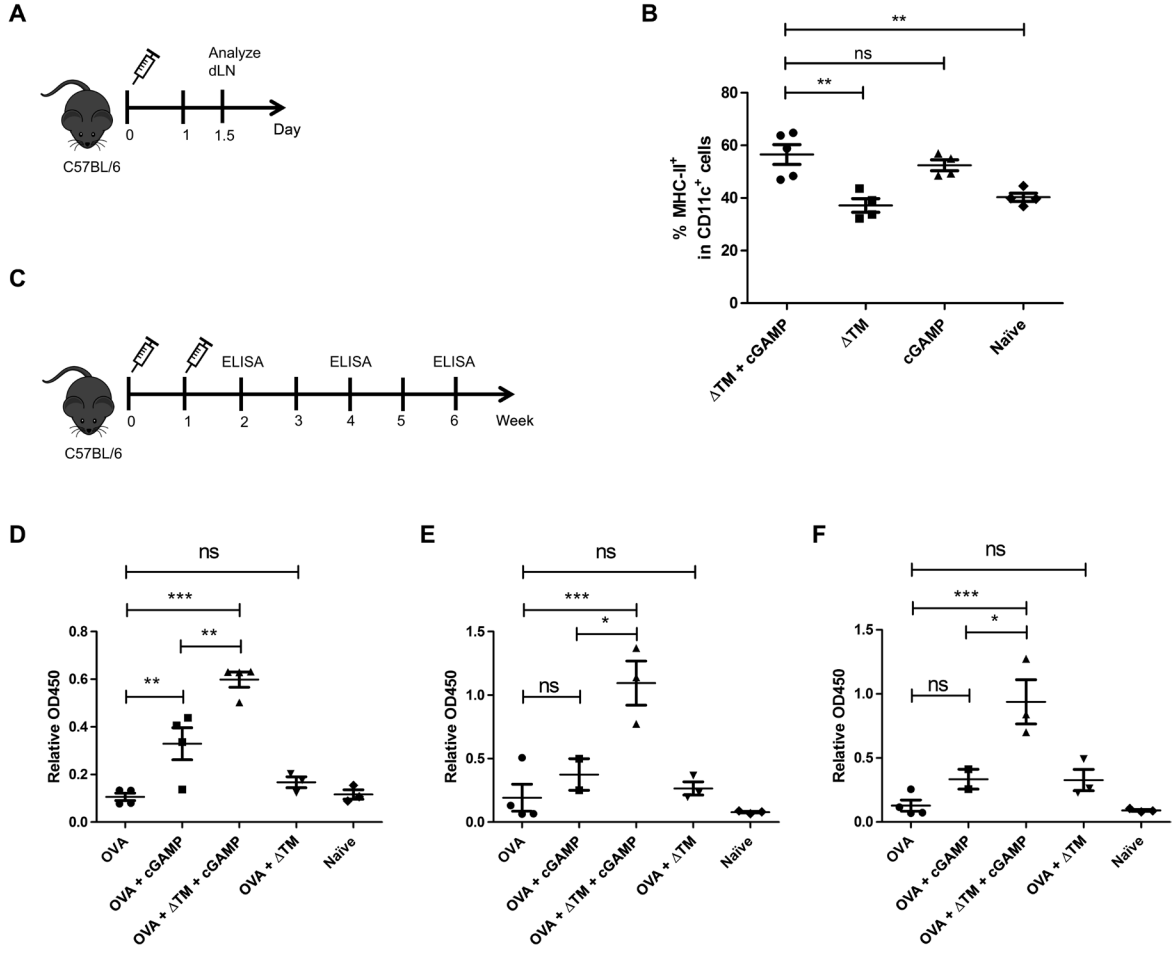


Fig. 4. cGAMP-STINGΔTM tetramer activates dendritic cells and promotes potent humoral response. (**A**) Groups of C57BL/6 mice ($n = 4$) were tail base injected with 40 μg of STINGΔTM, with or without 1 μg of cGAMP, or 1 μg of cGAMP alone on day 0, and then on day 1.5, draining (inguinal) lymph node lymphocytes were collected for analysis by flow cytometry. (**B**) Dendritic cell activation in draining (inguinal lymph node) gated by % MHC-II$^+$ cells in CD11c$^+$ cells. (**C**) C57BL/6 mice ($n = 4$) were immunized with 10 μg of ovalbumin (OVA) alone or OVA mixed with 2.5 μg of cGAMP or 100 μg of STINGΔTM or both via tail base injection on days 0 and 7. On days 14 (**D**), 28 (**E**), and 42 (**F**), OVA-specific total immunoglobulin G (IgG) antibody level in mouse serum was measured via enzyme-linked immunosorbent assay (ELISA). In (E) and (F), five mice were lost because of accidental cage flooding. Values are reported as means ± SEM. ***$P < 0.001$, **$P < 0.01$, and *$P < 0.05$, as analyzed by one-way ANOVA.

Downloaded from http://advances.sciencemag.org/ on May 13, 2021

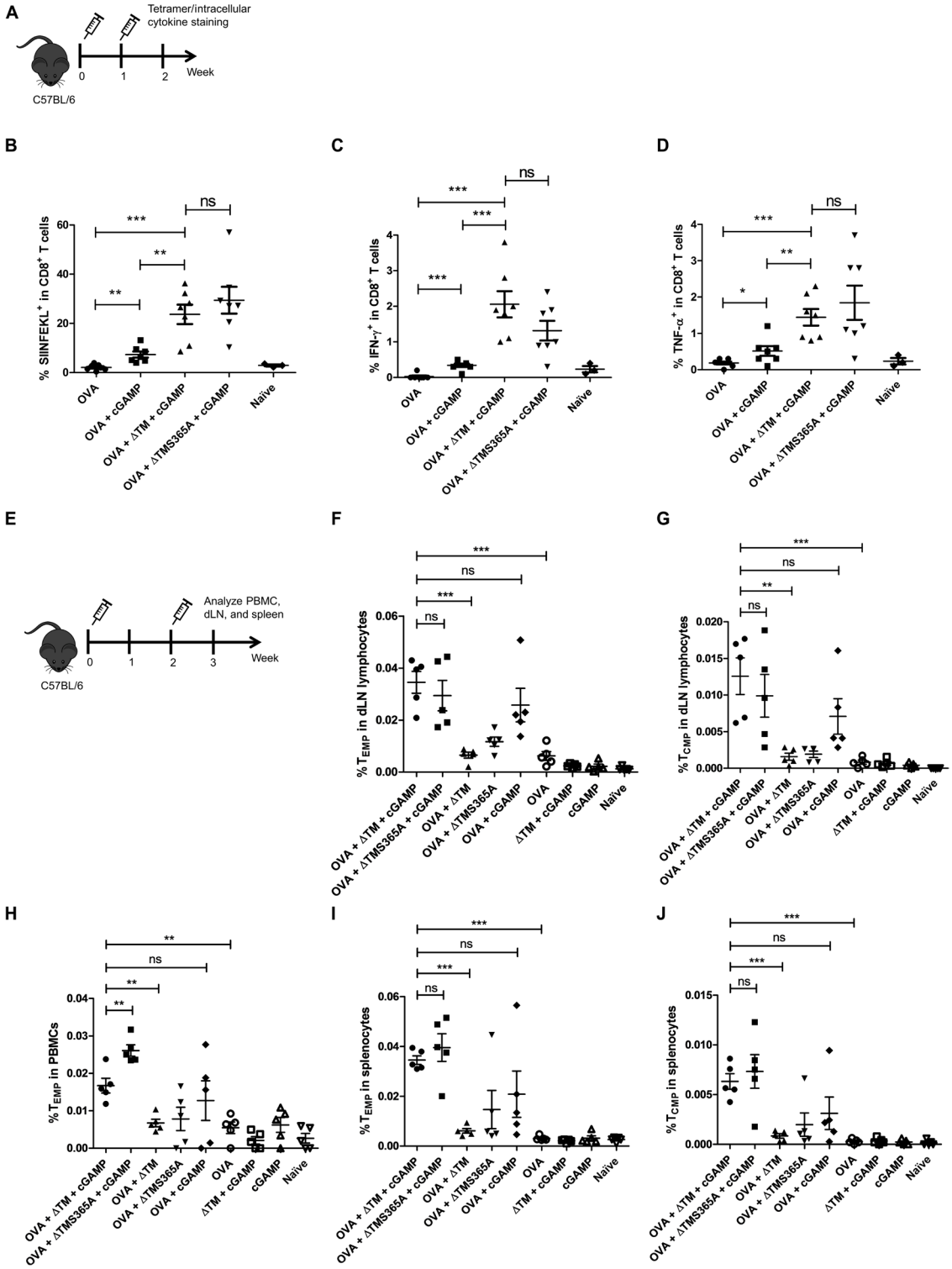


Fig. 5. cGAMP-STINGΔTM tetramer promotes robust antigen-specific T cell responses. (**A**) Groups of C57BL/6 mice ($n = 7$) were immunized with 50 μg of OVA alone or OVA mixed with 1 μg of cGAMP or 40 μg of STINGΔTM (or 40 μg of S365A STINGΔTM) on days 0 and 7. On day 14, PBMCs were collected and $CD8^+$ T cells were analyzed by CD8 OVA epitope SIINFEKL tetramer staining (**B**) or stimulated ex vivo with CD8 OVA epitope SIINFEKL and analyzed by intracellular cytokine staining of IFN-γ (**C**) and TNF-α (**D**). (**E**) Groups of C57BL/6 mice ($n = 5$) were immunized with 50 μg of OVA alone or OVA mixed with 1 μg of cGAMP or 40 μg of STINGΔTM (or 40 μg of S365A STINGΔTM) on days 0 and 14. On day 21, PBMCs and lymphocytes in dLN and splenocytes were collected and $CD8^+$ T cells were analyzed by CD8 OVA epitope SIINFEKL tetramer staining. Among $CD8^+$ SIINFEKL $tetramer^+$ T cells, effector memory precursors T_{EMP} were gated by $CD27^+$ $CD62L^-$ and $KLRG1^-$ [(**F**) in dLN lymphocytes, (**H**) in PBMCs, and (**I**) in splenocytes], and central memory precursors T_{CMP} were gated by $CD27^+$ $CD62L^+$ and $KLRG1^-$ [(**G**) in dLN lymphocytes and (**J**) in splenocytes, T_{CMP} was generally not found in PBMCs]. Values are reported as means ± SEM. $^{***}P < 0.001$, $^{**}P < 0.01$, and $^{*}P < 0.05$, as analyzed by one-way ANOVA.

Downloaded from http://advances.sciencemag.org/ on May 13, 2021

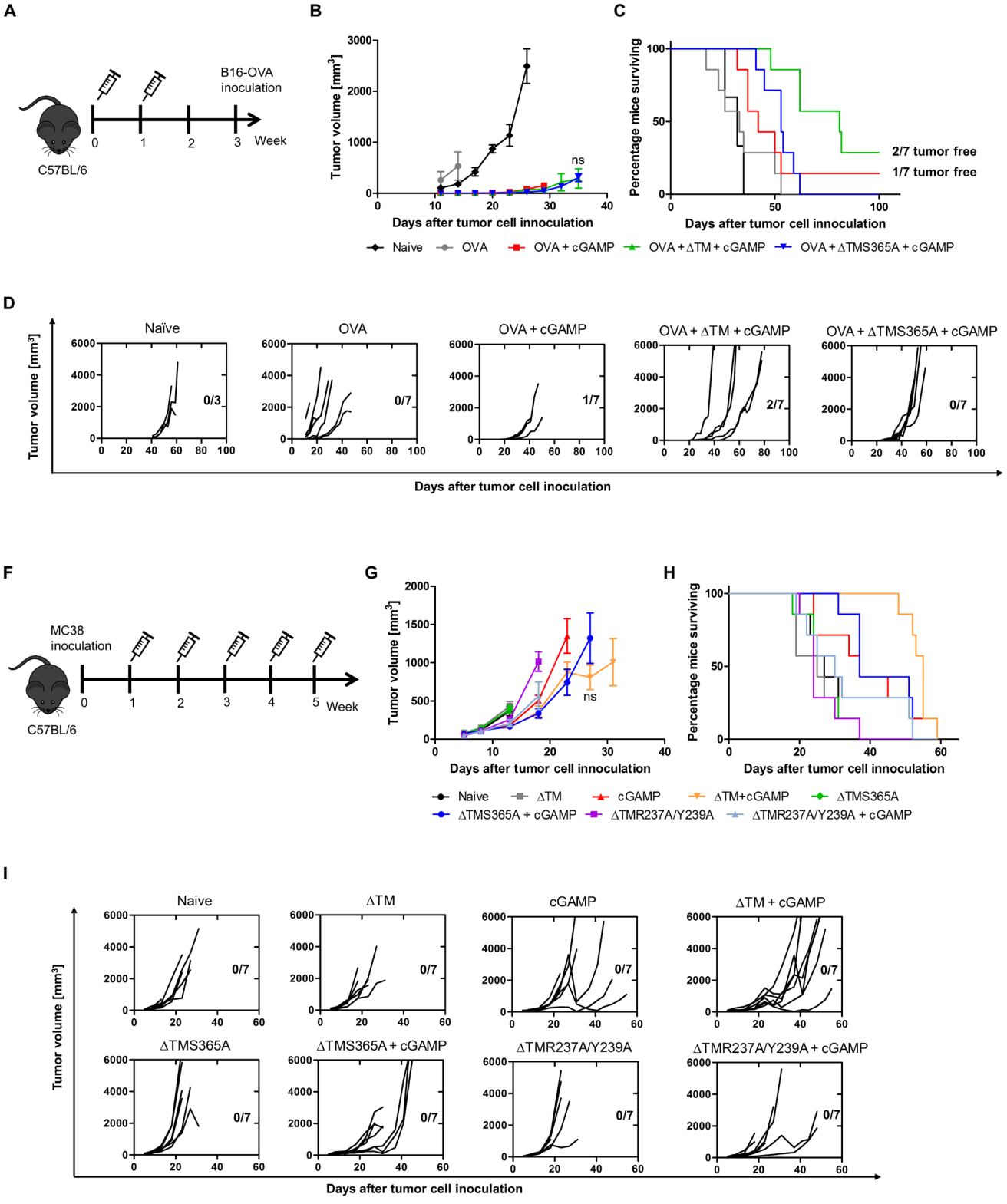


Fig. 6. cGAMP-STINGΔTM tetramer promotes potent antitumor immunity in B16 melanoma model. (**A**) Groups of C57BL/6 ($n = 7$) mice were immunized with 50 μg of OVA alone or OVA mixed with 1 μg of cGAMP or 40 μg of STINGΔTM (or 40 μg of S365ASTINGΔTM) on days 0 and 7. On day 21, mice were challenged with 1 million B16-OVA cells subcutaneously. Plots of overall (**B**) and individual (**D**) tumor growth curves, with numbers of surviving mice at the end of study (day 100) denoted. (**C**) Survival curves of mice. (**E**) Groups of C57BL/6 ($n = 7$) mice were first inoculated with 1 million MC38 cells and then treated with 100 μg of STINGΔTM (or 100 μg of S365A, R237A/Y239A STINGΔTM) mixed with 2.5 μg of cGAMP starting on day 7 for five times, 7 days apart via intratumoral injection. Plots of (**F**) overall and (**H**) individual tumor growth curves, with numbers of surviving mice at the end of study (day 60) denoted. (**G**) Survival curves of mice.

Downloaded from http://advances.sciencemag.org/ on May 13, 2021

antibody and H-2K^b/SIINFEKL tetramer. For intracellular cytokine staining, cells were first stimulated with SIINFEKL peptide. They were then stained with anti-CD8 antibody and permeabilized for intracellular cytokine staining of TNF-α and IFN-γ. Figure 5 (B to D) shows that antigen delivered with both STINGΔTM and S365AΔTM plus cGAMP significantly increased the percentage of SIINFEKL$^+$ and both TNF-α– and IFN-γ–secreting CD8$^+$ T cells, which indicates that the tetramers resulted in successful IFN induction in T cells and is consistent with our in vitro STING signaling activation tests with RAW264.7 cells. Representative flow plots with gating strategies are shown in fig. S8.

Last, we investigated the induction of memory T cell response through the use of model antigen OVA. Groups of C57Bl/6 mice were immunized on day 0 and boosted on day 14 via tail base injection with 50 μg of OVA alone or OVA mixed with 1 μg of cGAMP and/or 40 μg of STINGΔTM (or 40 μg of S365A STINGΔTM) (Fig. 5E). On day 21, mice were euthanized to harvest lymphocytes from the draining lymph nodes (dLN, inguinal) and splenocytes. As shown in Fig. 5 (F to J), the delivery of cGAMP-STINGΔTM resulted in the significant enhancement of SIINFEKL-specific central memory T cell precursors (CD8$^+$, SIINFEKL$^+$, CD27$^+$, CD62L$^+$, and KLRG1$^-$) and effector memory T cell precursors (CD8$^+$, SIINFEKL$^+$, CD27$^+$, CD62L$^-$, and KLRG1$^-$) (*31*).

cGAMP-STINGΔTM enhances the antitumor therapeutic efficacy

To explore the potential of cGAMP-STINGΔTM tetramer as a new mode of STING agonist–based cancer immunotherapy, we first evaluated the antitumor efficacy of cGAMP-STINGΔTM tetramers with a prophylactic study, using a melanoma cell line modified to express SIINFEKL peptide (B16-OVA) as an antigen epitope for vaccination. Groups of animals from the tetramer and intracellular cytokine staining study were challenged with 1 million B16-OVA cells at day 21 via subcutaneous injection (Fig. 6A). Tumor sizes were measured every 3 days to monitor the cancer progression and were recorded before the death of any mouse within a group. Hence, antitumor therapeutic efficacy was evaluated from both tumor volume (Fig. 6B) and mouse survival (Fig. 6, C and D). Groups vaccinated with cGAMP plus OVA, cGAMP plus S365AΔTM plus OVA, and cGAMP plus ΔTM plus OVA showed significantly enhanced protection against tumor challenge compared with the untreated and OVA-only control groups (Fig. 6B). Among these groups, cGAMP plus ΔTM plus OVA exhibited the slowest tumor progression and most prolonged survival, with two of seven mice achieving total protection and remaining tumor free (Fig. 6, C and D). The cGAMP plus S365AΔTM plus OVA group was also observed to result in improved survival when compared with the cGAMP plus OVA group. The vaccination efficacy is consistent with the IFN-γ and TNF-α expression level observed in the intracellular cytokine staining.

We then performed a therapeutic treatment study with an MC38 colon cancer model. C57BL/6 mice were inoculated with 1 million MC38 cells subcutaneously on day 0. After the primary tumor was established (between 50 and 80 mm^3), 100 μg of STINGΔTM (plus S365A, or R237A/Y239A) with or without 2.5 μg of cGAMP was injected intratumorally on days 7, 14, 21, 28, and 35 (Fig. 6E). The tumor size and survival were monitored on a schedule similar to that of the prophylactic study. Treatment with cGAMP, cGAMP plus S365AΔTM, and cGAMP plus ΔTM significantly reduced tumor burden, with the cGAMP plus ΔTM group having the overall best therapeutic effect and most prolonged survival (Fig. 6, F to H).

DISCUSSION

Numerous studies have suggested that the TM domain of STING protein is essential for intracellular STING signaling. Indeed, a STING-deficient cell line overexpressing TM-deficient STING will not undergo STING signaling upon free cGAMP delivery. However, we have found an interesting and well-defined self-assembled tetrameric structure of the TM-deficient STING protein with cGAMP under physiological conditions and found that when delivered to the cell, this ribonucleoprotein complex could effectively trigger the STING signaling pathway independent of the status of endogenous STING. While already confirmed through size exclusion chromatography, these tetramers could be further characterized via electrophoresis and ultracentrifugation in later studies. Ultimately, we developed this approach as a bioinspired method for cGAMP therapeutics to introduce a highly effective means of cGAMP delivery that potentially addresses the occurrence of defective STING in humans either due to cancer epigenetics or genetic heterogeneity. In the interest of translational relevance, we tested the therapeutic efficacy of the platform in vivo and found that the cGAMP-STINGΔTM tetramers can promote robust humoral response and antigen-specific T cell activation and elicit superior antitumoral immunity against a melanoma and a colon cancer model. In light of the role of activating STING signaling toward overcoming resistance against immune checkpoint blockade, future work can explore the delivery of cGAMP-STINGΔTM tetramers in combination with antiPD(L)1 and anti-CTLA4. Alternatively, genetic fusion of STINGΔTM tetramers with tumor-specific antigen peptides may enable simultaneous delivery of STING agonist–based adjuvant and antigens into dendritic cells to maximize the immune response. In summary, this work may open a new paradigm toward engineering immune adaptors to address vaccinology and immunotherapy.

MATERIALS AND METHODS

STINGΔTM protein purification

The STINGΔTM protein of mouse (138 to 378 amino acids) and human (139 to 379 amino acids) were synthesized by gBlock (IDT) and cloned into pSH200 plasmid (a gift from X. Shen at Duke University) via Nco I and Not I. Mutants were created by site-specific mutagenesis based on the plasmids encoding for STINGΔTM (primers listed in table S1). His-tagged STINGΔTM protein was expressed in DE3 *Escherichia coli* (mSTING ΔTM in BL21 DE3, hSTINGΔTM in Rosetta DE3), cultured at 37°C until OD600 reaches 0.4, and then induced with 0.5 mM isopropyl-β-D-thiogalactopyranoside (IPTG) at 18°C overnight. After induction, cells were centrifuged and lysed at room temperature for 20 min in protein binding buffer (50 mM sodium phosphate, 0.5 M NaCl, and 10 mM imidazole) with 1% Triton X-100 and lysozyme (1 mg/ml) and sonicated at 18 W (with 3-s on and 5-s off intervals) for a total of 5 min on ice. Cell lysate was then centrifuged at 14,000*g*, 4°C for 30 min and incubated with cobalt beads (HisPur Cobalt Resin; Thermo Fisher Scientific, 89964) followed by washing (50 mM sodium phosphate, 0.5 M NaCl, 10 mM imidazole, and 0.1% Triton X-114), elution (50 mM sodium phosphate, 0.5 M NaCl, and 150 mM imidazole), and desalting (buffer exchange to 20 mM Hepes, 150 mM NaCl, 10% glycerol, and 1 mM

Downloaded from http://advances.sciencemag.org/ on May 13, 2021

DTT). Protein concentration was determined by bicinchoninic acid (BCA) assay, and protein purity was verified by SDS–polyacrylamide gel electrophoresis (SDS-PAGE) and FPLC.

FPLC characterization of cGAMP-STINGΔTM complex

The ribonucleoprotein complexes of cGAMP-STINGΔTM (and R237A/Y239A, Q272A/A276Q mutants) were analyzed using an AKTA pure FPLC. Three hundred micrograms of protein in 0.5 ml of PBS with various molar ratios of cGAMP was first mixed and incubated at room temperature for 30 min. The sample was injected into 10 ml of superloop and then loaded onto a Superdex 200 Increase 10/300 GL column (column volume of 23.56 ml) followed by isocratic elution of 1.25 column volume with PBS at 1 ml/min flow rate. The protein concentration was monitored with OD280. A fraction collector was used to collect 0.5 ml of fractions for SDS-PAGE analyses (fig. S2, A and B).

Cell culture

HEK293T cells were obtained from the American Type Culture Collection (ATCC; Rockville, MD, USA) and cultured in Dulbecco's modified Eagle's medium (DMEM) (Invitrogen) with 10% fetal bovine serum (FBS) and 1% penicillin/streptomycin. Nuclear factor κB (NF-κB) Reporter RAW264.7 (RAW-Blue cells) were obtained from InvivoGen and cultured in DMEM with 10% heat-inactivated FBS and 1% penicillin/streptomycin. All cell lines were used at low passage number and tested negative for *Mycoplasma* contamination.

In vitro STING signaling activation assays

RAW-Blue cells were seeded in 96-well plates at 3×10^5 cells/ml in 100 μl of DMEM with 10% heat-inactivated FBS and 1% penicillin/streptomycin per well. After 24 hours of incubation, 5 μg of mSTING ΔTM protein (or mutants) with 0.125 μg of cGAMP premixed and equilibrated in 20 μl of Opti-MEM media was added to each well and incubated overnight. After incubation, 20 μl of the induced RAW-Blue cell supernatant was added to 180 μl of QUANTI-Blue solution per well of a 96-well plate. The plate was incubated in 37°C for 6 to 10 hours until a visible color difference was observed. IFN-SEAP activity was then determined by the absorbance at 635 nm with a spectrophotometer.

For the HEK293T cells, we first generated a reporter derivative from this cell line by transfecting pGL4.45[luc2P/ISRE/Hygro] (Promega) and stably selected in hygromycin (200 μg/ml). The pGL4.45[luc2P/ISRE/Hygro] vector contains five copies of an ISRE that drives transcription of the luciferase reporter gene luc2P (*Photinus pyralis*). luc2p is a synthetically derived luciferase sequence with humanized codon optimization that is designed for high expression and reduced anomalous transcription. The luc2P gene contains hPEST, a protein destabilization sequence, which allows luc2P protein levels to respond more quickly than those of luc2p to induction of transcription. The cells were seeded in six-well plates at 3×10^5 cells/ml in 2.5 ml of DMEM with 10% FBS and 1% penicillin/streptomycin. After an overnight incubation, the cells were transiently transfected with plasmids (a gift from L. Jin, University of Florida) encoding for expression of full-length hSTING (1 to 379 amino acids) WT, HAQ, S366A, and L374A, plus the TM domain–deficient hSTING (139 to 379 amino acids). Commercial transfection reagent TransIT-X2 was used to help transfection (2 μg of plasmid DNA mixed with 4 μl of TransIT-X2 in 250 μl of Opti-MEM media for each six well). The following day, cells were redistributed into 96-well plates at a seeding density of 3×10^5 cells/ml in 100 μl of media per well to be treated with cGAMP-STINGΔTM after 24 hours of incubation [2 μg of protein with or without 0.05 μg of CDNs cGAMP, $cGAM(PS)_2$, or cdi-GMP per well, with the help of 4 μl of TransIT-X2]. For assays with chemical inhibitors, HEK293T cells were treated with TBK1 inhibitor MRT67307 (InvivoGen, catalog no. inh-mrt; 6 hours before cGAMP-STINGΔTM treatment), CQ (Enzo, catalog no. 51005-CLQ; 2 hours before cGAMP-STINGΔTM treatment), BafA1 (InvivoGen, catalog no. tlrl-baf1; 2 hours before cGAMP-STINGΔTM treatment), and BFA (InvivoGen, catalog no. inh-bfa; 2 hours before cGAMP-STINGΔTM treatment). Transfected cells were also harvested for Western blotting.

Western blotting

Cells were washed with PBS and collected in T-PER tissue protein extraction reagent (30 μl per million cells) with Halt protease and phosphatase inhibitor cocktail (Thermo Fisher Scientific, no. 78442). The cells were lysed at 4°C for 30 min and centrifuged at 14,000*g* for 10 min. The protein concentration in the supernatant was determined via BCA assay, and SDS-PAGE samples were prepared as 50 μg of total protein in 30 μl of SDS-PAGE loading buffer. Anti-TBK1 (Cell Signaling, no. 3504), anti-STING (Novus Biologicals, NBP2-24683), anti–β-actin (Cell Signaling), and anti-tubulin (Cell Signaling).

Quantification of STING signaling–associated protein expression by qPCR

Total RNA was extracted using RNeasy micro kit (Qiagen, 74004) and reverse transcribed to cDNA with reverse transcription kit (Thermo Fisher Scientific, 4374966). cDNA was amplified and quantified by a Roche LightCycler 480 real-time PCR system. qPCR primers used for detection are mTBK1-F:GACATGCCTCTCTCCTGTAGTC, mTBK1-R:GGTGAAGCACATCACTGGTCTC, mIRF3-F:CGGAAAGAAGTGTTGCGGTTAGC, mIRF3-R:CAGGCTGCTTTTGCCATTGGTG, mIFN-β-F:GCCTTTGCCATCCAAGAGATGC, and mIFN-β-R:ACACTGTCTGCTGGTGGAGTTC.

Immunocytochemistry

Transfection and immune staining were performed in Millicell EZ chamber slides (Millipore Sigma, Temecula, CA, USA). Cells were fixed by 4% formaldehyde in PBS for 15 min, permeabilized by 0.4% Triton X-100 on ice for 10 min, and stained with rabbit anti-STING antibody (1:400; Novus bio, NBP2-24683) overnight at 4°C, or in the case of cells transfected with FLAG-STINGΔTM, stained with Cy3-conjugated anti-FLAG antibody (Sigma, A9594). For recombinant STING, proteins were conjugated with NHS–Alexa Fluor 488 (Thermo Fisher Scientific). Other primary antibodies used are anti-TBK1 (Abcam, ab235253), anti-LAMP1 (Cell Signaling, 9091S), and anti-EEA1 (Cell Signaling, 3288S). After washing with PBS containing 0.05% Tween 20, cells were stained with secondary antibodies including Alexa Fluor 568–conjugated goat anti-rabbit IgG antibody (Thermo Fisher Scientific, no. A-11011) and Alexa Fluor 488–conjugated donkey anti-rabbit IgG antibody (Thermo Fisher Scientific, no. A-32790). Nuclei were counterstained with 4′,6-diamidino-2-phenylindole (DAPI) and Golgi apparatus was stained with Golgi-ID green detection kit (Enzo Life Sciences, 51028-GG). Cells were imaged with an inverted Olympus IX83 microscope

Downloaded from http://advances.sciencemag.org/ on May 13, 2021

equipped with a Hamamatsu ImagEM high-sensitivity camera at the Swanson Biotechnology Center (MIT).

Mice and immunizations

C56BL/6 (B6), C57BL/6-Tg(TcraTcrb)1100Mjb/J (OT-1) mice were purchased from the Jackson laboratory and housed in the MIT Animal Facility. All mouse studies were performed according to the protocols approved by the MIT Division of Comparative Medicine. Experiments were conducted using female mice 8 to 12 weeks old. For immunizations performed with tail base injections, 50 μl was injected per side of the tail, 100 μl dosage total in PBS. Blood was collected via cheek bleeding, 100 to 150 μl of blood each time collected in 5 μl of 0.5 M EDTA at pH 8. For the humoral response experiments, B6 mice were immunized with 10 μg of OVA alone or OVA mixed with 2.5 μg of cGAMP and/or 100 μg of mSTING ΔTM or both on days 0 and 7. Sera were collected on a biweekly basis starting from day 14 for ELISA analyses of anti-OVA total IgG level. For the tetramer, intracellular cytokine staining, and B16 prophylactic study, groups of B6 mice received 50 μg of OVA or OVA mixed with 1 μg of cGAMP or plus 40 μg of mSTING (or S365A) ΔTM protein on days 0 and 7. On day 14, PBMCs were collected for tetramer and intracellular cytokine staining. For the memory T cell precursor study, B6 mice were immunized with the same dosage at day 0 as prime and day 14 as boost. On day 21, blood was collected via cheek bleeding, and dLN inguinal lymph nodes and spleens were harvested. Blood was processed in the same way to obtain PBMCs. For the in vivo dendritic cell activation study, B6 mice were immunized with the same dosage at day 0 and euthanized at day 1.5 to harvest for inguinal lymph nodes. For the systemic toxicity study, groups of B6 mice were bled before and 2 hours after tail base injections of 1 μg of cGAMP mixed with 2 μl of TransIT-X2 or 40 μg of mSTING dissolved in 100 μl of PBS or PBS only as control. ΔTM protein PBMCs of OT-1 mice were collected as a positive control for SIINFEKL-specific T cell activation. On day 21, mice were inoculated with 1 million B16-OVA cells subcutaneously in the right hind flank. For the MC38 treatment study, groups of B6 mice were inoculated with 1 million MC38 cells subcutaneously in the right hind flank on day 0 and then treated weekly with 100 μg of mSTING ΔTM protein (or S365A, R237A/Y239A) with or without 2.5 μg of cGAMP starting on day 7 for five times.

ELISA, intracellular cytokine staining, and tetramer staining

Blood collected were centrifuged at 500*g* for 3 min. Sera were removed for ELISA detection of IL-6 (R&D, catalog no. DY406), TNF-α (R&D, catalog no. DY410), and OVA-specific antibody levels. ELISA assays were made in-house by coating high-binding ELISA plate (Corning) with protein (OVA) (10 μg/ml) or capture antibody for mouse IL-6 and TNF-α in 50 mM sodium bicarbonate buffer (pH 9.6) overnight. On the next day, wells were washed with PBS followed by blocking with 1% BSA in PBS at room temperature (RT) for an hour. Diluted sera were added into wells and incubated at RT for 2 hours. Detection antibodies for IL-6 and TNF-α, or anti-mouse IgG, horseradish peroxidase–linked antibody (Cell Signaling, catalog no. 7076) was diluted in 1% BSA in PBS at 1:5000. Samples were washed extensively with 1x PBS containing 0.05% Tween 20 in between. TMB (BioLegend) was used as the substrate, and reaction was quenched by HCl. Plates were measured at optical density (OD) of 450 nm.

The blood cell pellet was lysed with red blood cell lysing buffer Hybri-Max (Sigma-Aldrich, R7757) and washed with PBS to obtain PBMCs. Inguinal lymph nodes and spleens were first homogenized with frosted microscope slides and filtered through cell strainers in fluorescence-activated cell sorting buffer. Lymphocytes were then ready for staining. Splenocytes were processed with red blood cell lysis buffer before staining. For intracellular cytokine staining, the PBMCs were first stimulated by resuspending in 400 μl of RPMI media with 10% FBS, 0.1 mM nonessential amino acids, 50 μM β-mercaptoethanol, 1% penicillin/streptomycin, SIINFEKL peptide (1 μg/ml) (Anaspec Inc., AS-60193-1), and BD GolgiStop (4 μl of BD GolgiStop for every 6 ml) and incubated at 37°C for 4 hours. The PBMCs were then treated with Fc blocker (anti-mouse CD16/CD32 monoclonal antibodies) followed by viability staining (LIVE/DEAD fixable aqua stain; Thermo Fisher Scientific, L34965) and surface staining with anti-CD8 antibodies (BioLegend, 100707; clone 53-6.7). After the surface staining, the PBMCs were then fixed, permeabilized, and stained with anti-mouse IFN-γ (BioLegend, 505825; clone XMG1.2) and anti-mouse TNF-α (BioLegend, 506107; clone TN3-19.12) antibodies, and then analyzed on a BD FACSCanto flow cytometer. For tetramer staining, the PBMCs obtained from blood were, likewise, directly treated with Fc blocker, viability staining, and surface staining with anti-CD8 and H-2Kb/SIINFEKL tetramer, and then fixed with formaldehyde. For the memory T cell precursor study, PBMCs, lymphocytes, and splenocytes were treated with Fc blocker, viability staining, and surface staining with anti-CD8, H-2Kb/SIINFEKL tetramer, anti-mouse CD27 (BioLegend, 124212, clone LG.3A10), anti-mouse KLRG1 (BioLegend, 138416, clone 2F1/KLRG1), and anti-mouse CD62L (BioLegend, 104436, clone MEL-14). For the dendritic cell maturation study, lymphocytes were treated with Fc blocker, viability staining, and surface staining with anti-mouse CD11c (BioLegend, 117310, clone N418) and anti-mouse MHC class II (BioLegend, 107606, clone M5/114.15.2). Stained cells were then washed and analyzed on a BD FACSCelesta and LSRFortessa flow cytometer.

In vivo imaging

Balb/c mice tail base injected (on both sides of the tail) with Cy7-NHS ester–labeled STINGΔTM-cGAMP complex, Cy7-labeled STINGΔTM, and Cy7-labeled cGAMP were imaged under isoflurane anesthesia with Xenogen IVIS system. Acquisition and analysis of images were performed with Living Image software (Xenogen).

Statistical analysis

All statistical analyses were performed using GraphPad Prism 5.03 (San Diego, CA, USA). Data were analyzed with one-way analysis of variance (ANOVA) followed by Student's *t* test for statistical significance.

SUPPLEMENTARY MATERIALS

Supplementary material for this article is available at http://advances.sciencemag.org/cgi/content/full/6/24/eaba7589/DC1

View/request a protocol for this paper from *Bio-protocol*.

REFERENCES AND NOTES

1. B. Zhao, F. du, P. Xu, C. Shu, B. Sankaran, S. L. Bell, M. Liu, Y. Lei, X. Gao, X. Fu, F. Zhu, Y. Liu, A. Laganowsky, X. Zheng, J.-Y. Ji, A. P. West, R. O. Watson, P. Li, A conserved PLPLRT/SD motif of STING mediates the recruitment and activation of TBK1. *Nature* **569**, 718–722 (2019).
2. S.-R. Woo, M. B. Fuertes, L. Corrales, S. Spranger, M. J. Furdyna, M. Y. K. Leung, R. Duggan, Y. Wang, G. N. Barber, K. A. Fitzgerald, M.-L. Alegre, T. F. Gajewski, STING-dependent cytosolic DNA sensing mediates innate immune recognition of immunogenic tumors. *Immunity* **41**, 830–842 (2014).

Downloaded from http://advances.sciencemag.org/ on May 13, 2021

3. L. Corrales, S. M. McWhirter, T. W. Dubensky Jr., T. F. Gajewski, The host STING pathway at the interface of cancer and immunity. *J. Clin. Invest.* **126**, 2404–2411 (2016).
4. S. T. Koshy, A. S. Cheung, L. Gu, A. R. Graveline, D. J. Mooney, Liposomal delivery enhances immune activation by STING agonists for cancer immunotherapy. *Adv. Biosyst.* **1**, 1600013 (2017).
5. T. Ohkuri, A. Kosaka, K. Ishibashi, T. Kumai, Y. Hirata, K. Ohara, T. Nagato, K. Oikawa, N. Aoki, Y. Harabuchi, E. Celis, H. Kobayashi, Intratumoral administration of cGAMP transiently accumulates potent macrophages for anti-tumor immunity at a mouse tumor site. *Cancer Immunol. Immunother.* **66**, 705–716 (2017).
6. D. Shae, K. W. Becker, P. Christov, D. S. Yun, A. K. R. Lytton-Jean, S. Sevimli, M. Ascano, M. Kelley, D. B. Johnson, J. M. Balko, J. T. Wilson, Endosomolytic polymersomes increase the activity of cyclic dinucleotide STING agonists to enhance cancer immunotherapy. *Nat. Nanotechnol.* **14**, 269–278 (2019).
7. T. W. Dubensky Jr., D. B. Kanne, M. L. Leong, Rationale, progress and development of vaccines utilizing STING-activating cyclic dinucleotide adjuvants. *Ther. Adv. Vaccines* **1**, 131–143 (2013).
8. J. Ahn, H. Konno, G. N. Barber, Diverse roles of STING-dependent signaling on the development of cancer. *Oncogene* **34**, 5302–5308 (2015).
9. T. Xia, H. Konno, G. N. Barber, Recurrent loss of STING signaling in melanoma correlates with susceptibility to viral oncolysis. *Cancer Res.* **76**, 6747–6759 (2016).
10. L. Jin, L. G. Xu, I. V. Yang, E. J. Davidson, D. A. Schwartz, M. M. Wurfel, J. C. Cambier, Identification and characterization of a loss-of-function human MPYS variant. *Genes Immun.* **12**, 263–269 (2011).
11. S. Patel, S. M. Blaauboer, H. R. Tucker, S. Mansouri, J. S. Ruiz-Moreno, L. Hamann, R. R. Schumann, B. Opitz, L. Jin, The common R71H-G230A-R293Q human TMEM173 is a null allele. *J. Immunol.* **198**, 776–787 (2017).
12. S. Patel, L. Jin, TMEM173 variants and potential importance to human biology and disease. *Genes Immun.* **20**, 82–89 (2019).
13. J. S. Ruiz-Moreno, L. Hamann, J. A. Shah, A. Verbon, F. P. Mockenhaupt, M. Puzianowska-Kuznicka, J. Naujoks, L. E. Sander, M. Witzenrath, J. C. Cambier, N. Suttorp, R. R. Schumann, L. Jin, T. R. Hawn, B. Opitz; CAPNETZ Study Group, The common HAQ STING variant impairs cGAS-dependent antibacterial responses and is associated with susceptibility to Legionnaires' disease in humans. *PLOS Pathog.* **14**, e1006829 (2018).
14. S. Patel, S. M. Blaauboer, H. R. Tucker, S. Mansouri, J. S. Ruiz-Moreno, L. Hamann, R. R. Schumann, B. Opitz, L. Jin, Response to comment on "The common R71H-G230A-R293Q human TMEM173 is a null allele". *J. Immunol.* **198**, 4185–4188 (2017).
15. K. E. Sivick, N. H. Surh, A. L. Desbien, E. P. Grewal, G. E. Katibah, S. M. McWhirter, T. W. Dubensky Jr., Comment on "The Common R71H-G230A-R293Q Human TMEM173 Is a Null Allele". *J. Immunol.* **198**, 4183–4185 (2017).
16. J. Fu, D. B. Kanne, M. Leong, L. H. Glickman, S. M. McWhirter, E. Lemmens, K. Mechette, J. J. Leong, P. Lauer, W. Liu, K. E. Sivick, Q. Zeng, K. C. Soares, L. Zheng, D. A. Portnoy, J. J. Woodward, D. M. Pardoll, T. W. Dubensky Jr., Y. Kim, STING agonist formulated cancer vaccines can cure established tumors resistant to PD-1 blockade. *Sci. Transl. Med.* **7**, 283ra52 (2015).
17. Y. Tanaka, Z. J. Chen, STING specifies IRF3 phosphorylation by TBK1 in the cytosolic DNA signaling pathway. *Sci. Signal.* **5**, ra20 (2012).
18. G. Surpris, J. Chan, M. Thompson, V. Ilyukha, B. C. Liu, M. Atianand, S. Sharma, T. Volkova, I. Smirnova, K. A. Fitzgerald, A. Poltorak, Cutting edge: Novel Tmem173 allele reveals importance of STING N terminus in trafficking and type I IFN production. *J. Immunol.* **196**, 547–552 (2016).
19. C. Zhang, G. Shang, X. Gui, X. Zhang, X.-c. Bai, Z. J. Chen, Structural basis of STING binding with and phosphorylation by TBK1. *Nature* **567**, 394–398 (2019).
20. G. Shang, C. Zhang, Z. J. Chen, X.-c. Bai, X. Zhang, Cryo-EM structures of STING reveal its mechanism of activation by cyclic GMP–AMP. *Nature* **567**, 389–393 (2019).
21. M. C. Hanson, M. P. Crespo, W. Abraham, K. D. Moynihan, G. L. Szeto, S. H. Chen, M. B. Melo, S. Mueller, D. J. Irvine, Nanoparticulate STING agonists are potent lymph node–targeted vaccine adjuvants. *J. Clin. Invest.* **125**, 2532–2546 (2015).
22. X. Zhang, H. Shi, J. Wu, X. Zhang, L. Sun, C. Chen, Z. J. Chen, Cyclic GMP-AMP containing mixed phosphodiester linkages is an endogenous high-affinity ligand for STING. *Mol. Cell* **51**, 226–235 (2013).
23. S. Ouyang, X. Song, Y. Wang, H. Ru, N. Shaw, Y. Jiang, F. Niu, Y. Zhu, W. Qiu, K. Parvatiyar, Y. Li, R. Zhang, G. Cheng, Z.-J. Liu, Structural analysis of the STING adaptor protein reveals a hydrophobic dimer interface and mode of cyclic di-GMP binding. *Immunity* **36**, 1073–1086 (2012).
24. N. Dobbs, N. Burnaevskiy, D. Chen, V. K. Gonugunta, N. M. Alto, N. Yan, STING activation by translocation from the ER is associated with infection and autoinflammatory disease. *Cell Host Microbe* **18**, 157–168 (2015).
25. H. Ishikawa, Z. Ma, G. N. Barber, STING regulates intracellular DNA-mediated, type I interferon-dependent innate immunity. *Nature* **461**, 788–792 (2009).
26. B. Hiller, V. Hornung, STING Signaling the enERGIC Way. *Cell Host Microbe* **18**, 137–139 (2015).
27. D. Liu, H. Wu, C. Wang, Y. Li, H. Tian, S. Siraj, S. A. Sehgal, X. Wang, J. Wang, Y. Shang, Z. Jiang, L. Liu, Q. Chen, STING directly activates autophagy to tune the innate immune response. *Cell Death Differ.* **26**, 1735–1749 (2019).
28. D. L. Burdette, K. M. Monroe, K. Sotelo-Troha, J. S. Iwig, B. Eckert, M. Hyodo, Y. Hayakawa, R. E. Vance, STING is a direct innate immune sensor of cyclic di-GMP. *Nature* **478**, 515–518 (2011).
29. P.-H. Wang, S.-Y. Fung, W.-W. Gao, J.-J. Deng, Y. Cheng, V. Chaudhary, K.-S. Yuen, T.-H. Ho, C.-P. Chan, Y. Zhang, K.-H. Kok, W. Yang, C.-P. Chan, D.-Y. Jin, A novel transcript isoform of STING that sequesters cGAMP and dominantly inhibits innate nucleic acid sensing. *Nucleic Acids Res.* **46**, 4054–4071 (2018).
30. P. Giannetti, A. Facciabene, N. La Monica, L. Aurisicchio, Individual mouse analysis of the cellular immune response to tumor antigens in peripheral blood by intracellular staining for cytokines. *J. Immunol. Methods* **316**, 84–96 (2006).
31. Y. Li, C. Shen, B. Zhu, F. Shi, H. N. Eisen, J. Chen, Persistent antigen and prolonged AKT–mTORC1 activation underlie memory CD8 T cell impairment in the absence of CD4 T cells. *J. Immunol.* **195**, 1591–1598 (2015).

Acknowledgments: We acknowledge B. Zhao and P. Li at the Department of Biochemistry and Biophysics at Texas A&M University for supplying cGAMP, G. Paradis at the MIT Koch Institute Flow Cytometry Core for providing help in setting up the flow cytometer, and D. S. Yun at the MIT Koch Institute Nanotechnology Materials core for providing assistance in TEM imaging. **Funding:** This work was supported by the Department of Defense Congressionally Directed Medical Research Program's (CDMRP) Ovarian Cancer Research Program, Cancer Center Support Grant (CCSG) Pilot Awards at David H. Koch Institute for Integrative Cancer Research at MIT, and the Institute for Soldier Nanotechnologies (ISN) at MIT, Northeastern University Faculty start-up funding, and Peer Reviewed Medical Research Program from the Department of Defense's Congressionally Directed Medical Research Programs (W81XWH18PRMRPDA). **Author contributions:** J.L. and Y.H. designed the experiments. Y.H., J.L., C.H., E.Z.Y., S.J.F., G.Z., M.Y., Y.L., and X.S. performed the experiments. P.T.H., J.L., and D.J.I. supervised the study. Y.H., C.H., J.L., and P.T.H. wrote the manuscript. **Competing interests:** The authors declare that they have no competing interests. **Data and materials availability:** All data needed to evaluate the conclusions in the paper are present in the paper and/or the Supplementary Materials. Additional data related to this paper may be requested from the authors.

Submitted 2 January 2020
Accepted 28 April 2020
Published 12 June 2020
10.1126/sciadv.aba7589

Citation: Y. He, C. Hong, E. Z. Yan, S. J. Fletcher, G. Zhu, M. Yang, Y. Li, X. Sun, D. J. Irvine, J. Li, P. T. Hammond, Self-assembled cGAMP-STINGΔTM signaling complex as a bioinspired platform for cGAMP delivery. *Sci. Adv.* **6**, eaba7589 (2020).

Downloaded from http://advances.sciencemag.org/ on May 13, 2021

Engineering the Immune Adaptor Protein STING as a Biologic

Xin Sun[1], Yun Ni[1], Yanpu He[1], Mengdi Yang[1], Tetsuo Tani[2], Shunsuke Kitajima[2,4], David A. Barbie[2,3], Jiahe Li[1, *]

[1]Department of Bioengineering, Northeastern University, Boston, MA, 02115, United States.

[2]Department of Medical Oncology, Dana–Farber Cancer Institute, Boston, MA, United States

[3]Belfer Center for Applied Cancer Science, Dana-Farber Cancer Institute, Boston, MA, United States

[4]Department of Cell Biology, Cancer Institute, Japanese Foundation for Cancer Research, Tokyo, Japan

[*]Correspondence:

Department of Bioengineering, Northeastern University, Boston, MA, 02115, United States. Email: jiah.li@northeastern.edu. Phone: 1-617-373-3233

KEY WORDS: STING, cyclic dinucleotides, vaccine and immunotherapy.

ABSTRACT

Activation of the stimulator of interferon genes (STING) pathway through cyclic dinucleotides (CDNs) has been explored extensively as potent vaccine adjuvants against infectious diseases as well as to increase tumor immunogenicity towards cancer immunotherapy in solid tumors. Over the last decade, a myriad of synthetic vehicles, including liposomes, polymers, and other nanoparticle platforms, have been developed to improve the bioavailability and therapeutic efficacy of STING agonists in preclinical mouse models. In comparison to synthetic materials, protein-based carriers represent an attractive delivery platform owing to their biocompatibility, amenability to genetic engineering, and intrinsic capacity to form well-defined structures. In the present work, we have engineered the immune adaptor STING as a protein-based delivery system for efficient encapsulation and intracellular delivery of CDNs. Through genetic fusion with a protein transduction domain, the recombinant STING can spontaneously penetrate cells

to markedly enhance the delivery of CDNs in a mouse vaccination model and a syngeneic mouse melanoma model. Moreover, motivated by recent findings that certain tumor cells can evade immune surveillance via loss of STING expression, we further unveiled that our STING platform can serve as a functional vehicle to restore the STING signaling in a panel of lung and melanoma cell lines with impaired STING expression. Taken together, our STING-based protein delivery platform may offer a unique direction towards targeting STING-silenced tumors as well as augmenting the efficacy of STING-based vaccine adjuvants.

INTRODUCTION

The cytosolic DNA sensing pathway involving cyclic GMP-AMP synthase (cGAS) and the stimulator of interferon genes (STING) represents an essential innate immune mechanism in response to foreign pathogens(1). Upon detection of cytosolic DNA, the intracellular nucleic acid sensor cGAS catalyzes the productions of cyclic dinucleotides (CDNs) such as 2'3'-cyclic GMP-AMP (cGAMP), which functions as a second messenger to bind the adaptor protein STING to initiate type I interferon (IFN) production and boost dendritic cell (DC) maturation and T cell infiltration(2). Meanwhile, the cGAS-STING signaling pathway is profound at sensing neoplastic progression by promoting type I IFN production and initiating cytotoxic T cell-mediated anti-tumor immune response(3). These fundamental studies have accelerated the development of utilizing synthetic STING agonists to activate the innate and adaptive immune responses as a monotherapy or in combination with immune checkpoint blockade (ICB) for cancer immunotherapy(4,5).

Despite the promise of CDNs such as cGAMP as immune adjuvants, they suffer from several limitations: **(1)** CDNs exhibit fast clearance from the injection site, which may induce systemic toxicity, **(2)** naturally derived CDNs are susceptible to enzymatic degradation, which can lower the efficacy of adjuvanticity potential, and **(3)** CDNs have inefficient intracellular transport properties due to limited endosomal escape or reliance on the expression of a specific transporter protein(6–8). To address these challenges, existing efforts are largely focused on two main directions: **(1)** generation of novel biomaterial-based delivery systems to improve the *in vivo* delivery of CDNs to activate

innate immune cells, and **(2)** discovery of new STING agonist analogs via medicinal chemistry and drug screening to confer greater chemical stability and improved pharmacokinetics(7–11).

Here, we sought to develop a new delivery system that can offer structural simplicity and modularity from the perspective of delivery vehicle design, while becoming an add-on technology by incorporating newly discovered synthetic STING agonist compounds. To this end, we previously uncovered an unnatural function of a recombinant STING protein that lacks the hydrophobic transmembrane (TM) domain (hereinafter referred to as STINGΔTM)(12). Notably, following delivery via commercial transfection reagents, the STINGΔTM/cGAMP complexes can activate the STING signaling pathway even in cells without endogenous STING expression. In our present work, to bypass the need for any synthetic delivery material, we sought to engineer a protein-based carrier for STING agonists by generating a cell-penetrating STINGΔTM (CP-STINGΔTM) through genetic fusion with a cell-penetrating domain, named Omomyc. As a dominant-negative form of the human *MYC* oncogene, Omomyc was originally identified to target *KRAS*-driven tumor cells in several NSCLC xenograft mouse models(13). Intriguingly, in a synthetic vehicle-free mode, CP-STINGΔTM markedly enhanced delivery of cGAMP in cells, which differ in the levels of endogenous STING expression or cell type. To prove its utility *in vivo*, we first explored CP-STINGΔTM to enhance the delivery of cGAMP as an adjuvant in a mouse model vaccinated with chicken ovalbumin(14). Furthermore, in a syngeneic mouse model of melanoma, we explored a combination immunotherapy regimen consisting of an ICB inhibitor, anti-PD-1, and STING agonism(15,16). Collectively, our work demonstrated the potential of repurposing the immune sensing receptor as a vehicle to encapsulate and deliver immune adjuvants towards vaccine and cancer immunotherapy development.

RESULTS

Overall Scheme of cGAMP delivery by CP-STINGΔTM

In contrast to existing delivery strategies such as nanoformulations or synthetic depots to overcome the challenges in encapsulation and intracellular delivery of STING agonist

(e.g., cGAMP), we have repurposed the natural receptor STING as a highly modular and simple platform to efficiently bind and deliver cGAMP *in vitro* and *in vivo*(7). Specifically, we took advantage of previous biochemical studies, in which the recombinant C-terminal domain of STING protein (STINGΔTM, 139-379aa for human and 138-378aa for mouse) is known to bind cGAMP with high affinity and stability(17,18). Additionally, in our previous work, we serendipitously uncovered that the recombinant STINGΔTM could form complexes with cGAMP, and activate the downstream STING signaling following delivery of the complexes by commercial transfection reagents in HEK293T that do not express endogenous STING. On the contrary, recombinant STINGΔTM proteins with catalytically inactive mutations, including S366A and deletion of the last 9 amino acids (i.e., ΔC9), failed to activate the STING pathway in HEK293T(19,20). Building on this serendipitous discovery, to bypass the need for transfection reagents, here we developed a cell-penetrating (CP)-STINGΔTM to deliver cGAMP into different cell types via genetic fusion of a cell-penetrating protein (**Figure 1a** and **b**). Notably, in contrast to cell-penetrating peptides such as trans-activating transcriptional activator (TAT), we have chosen the Omomyc mini-protein as our cell-penetrating moiety for three reasons: (1) Omomyc (91 amino acids) is derived from a dominant-negative form of the human *MYC* oncogene and has recently shown specific targeting and potent tumor cell penetration capabilities in human cancer cell lines and xenograft mouse models; (2) The natural dimer conformation of Omomyc coincides with STINGΔTM, which also exists as a dimer in the absence of cGAMP; (3) Omomyc may not cause an immunogenicity issue owing to its human origin(13).

Since the C terminal amino acids of STING directly interact with downstream effector proteins, including TBK1 and IRF3, we genetically fused the cell-penetrating protein Omomyc to the N terminus of STINGΔTM to prevent any steric hindrance posed by Omomyc (**Figure 1c**). In addition, we generated two essential CP-STINGΔTM mutants to help dissect the mechanisms underlying enhanced delivery of cGAMP: one lacks the effector function to engage with the downstream STING signaling pathway and the other fails to bind cGAMP (Table 1)(21–23). After recombinant protein expression in *E. coli*, we purified 6x Histidine (His) tagged proteins via the metal affinity purification and size

exclusion chromatography. As shown in **Figure S1**, both size exclusion chromatography studies and SDS-PAGE confirm that the fusion protein can be purified with high yield and homogeneity from *E. coli*. Additionally, the denatured proteins exhibited predicted molecular weights in SDS-PAGE, while the SEC graphs show that CP-STINGΔTM likely forms a tetramer under a native condition in agreement with our previous study(12).

STING variants*	Description
STINGΔTM	STING lacking the N terminal transmembrane domain
STINGΔTMΔC9	9-amino acid deletion at the C terminus that abolishes type 1 IFN induction
STINGΔTM(R238A/Y240A)	Deficient for cGAMP binding
CP-STINGΔTM	Inclusion of cell-penetrating domain -- Omomyc to bypass transfection reagent
CP-STINGΔTMΔC9	
CP-STINGΔTM(R238A/Y240A)	
CP-STINGΔTM-dsred	

Table 1: STING variants used in this study. * Amino acid positions represent the human STING (1-379aa), which are conserved in the mouse STING (1-378aa)**.**

CP-STINGΔTM can effectively internalize cells

While Omomyc protein itself has been shown to internalize different lung cancer cell lines *in vitro* as well as in mouse lung xenografts, it remains to be investigated whether genetic fusion of Omomyc with STINGΔTM can indeed penetrate cells spontaneously. To assess the cell-penetrating potential of CP-STINGΔTM, we treated two human non-small cell lung cancer (NSCLC) cell lines with low or absent STING, H1944 and A549(24), for 24 hours followed by immunostaining against an 8-amino acid FLAG epitope (DYKDDDDK) encoded in between Omomyc and STINGΔTM. Because the FLAG epitope is not known to be expressed by mammalian cells, we could make use of anti-FLAG staining to distinguish exogenously delivered STING protein variants from endogenous STING proteins. Moreover, in contrast to covalently conjugating proteins with fluorescent dyes, which typically modify the surface amine or cysteine groups of proteins, our approach can

prevent altering the pharmacokinetics of intracellular protein accumulation. As shown in **Figure 2a** and **c**, CP-STINGΔTM exhibited efficient intracellular uptake in H1944 and A549, while STINGΔTM alone failed to internalize cells owing to the lack of Omomyc to promote cell penetration. In addition, we also genetically fused Omomyc to the catalytically inactive mutant STINGΔTMΔC9, which is known to abolish STING function due to the deletion of 9 amino acids at the very C terminus. As shown in **Figure S2a, c,** and **e**, CP-STINGΔTMΔC9 showed comparable degrees of internalization, which confirmed that the intracellular uptake is mediated by Omomyc instead of STING. To further corroborate our findings beyond fluorescence microscopy, we performed flow cytometry to confirm the uptake profiles of different STING variants after intracellular staining against the same synthetic epitope FLAG (**Figure 2b** and **d**). In addition to the NSCLC cell lines, we validated the uptake of CP-STINGΔTM and CP-STINGΔTMΔC9 in human melanoma and ovarian cancer cell lines by fluorescence microscopy and flow cytometry (**Figure S2b, d,** and **e**). Finally, to dissect the mechanism by which the cell-penetrating STINGΔTM enters cells, we tested a range of small molecule inhibitors targeting different endocytic pathways including: 5-(N-Ethyl-N-isopropyl) amiloride (EIPA), chlorpromazine, Dynasore, cyclodextrin, and Filipin. Among the small molecule inhibitors we have tested, a macropinocytosis inhibitor, EIPA and an endocytosis inhibitor, Dynasore exhibited a dose-dependent inhibition of CP-STINGΔTM in H1944 (**Figure 2e-g** and **Figure S2f,g**)(13,25). In contrast, inhibitors targeting other uptake pathways failed to inhibit the uptake of CP-STINGΔTM (**Figure S2h,** and **i**). Of note, our findings agree with the previous work, in which the Omomyc protein itself was taken up by cancer cells primarily through the macropinocytosis and endocytosis pathways(13). Therefore, we conclude that the cell-penetrating capability of the fusion protein is mediated by Omomyc in a macropinocytosis and endocytosis-dependent manner.

CP-STINGΔTM enhances cGAMP delivery and STING activation in a panel of lung and melanoma cell lines with impaired STING expression

In contrast to innate immune cells, which are highly sensitive to cGAMP-mediated STING activation, previous work by others have shown that downregulation of STING in tumor cells greatly reduced the sensitivity of cancer cells to STING agonists, which can promote

immune suppression and exclusion of cytotoxic T cells in the tumor microenvironment (TME)(24,26). Therefore, we sought to ask whether the fusion protein could promote intracellular delivery of the STING agonist cGAMP in a panel of cell lines with reduced sensitivity to STING agonists. We first focused on two $STING_{low}$ NSCLC cell lines, H1944 and H2122**,** in which the expression of endogenous STING is downregulated due to histone methylation at the native STING promoter(24). As shown in **Figure 3a** and **S3c**, we compared "CP-STINGΔTM + cGAMP", "CP-STINGΔTMΔC9 + cGAMP", free cGAMP, and lipofectamine-transfected cGAMP to vehicle control-treated cells. Of note, a 1:1 molar ratio of one STING dimer to one cGAMP was prepared for different STING/cGAMP complexes. Impressively, the codelivery systems comprising "CP-STINGΔTM + cGAMP" or "CP-STINGΔTMΔC9 + cGAMP" required ~100-fold lower concentration of cGAMP than free cGAMP or lipofectamine-transfected cGAMP to induce comparable levels of CXCL10, one of the chemokines that can be induced by the STING pathway(27,28). In addition, since the STING activation in tumor cells can upregulate major histocompatibility complex I (MHC-I) to promote cytotoxic T cell recognition, we measured the surface expression of MHC-I in the same cancer cells(29). Consistent with measurement of CXCL10 by ELISA, "CP-STINGΔTM + cGAMP" and "CP-STINGΔTMΔC9 + cGAMP" similarly enhanced surface expression of MHC class I in H1944 and melanoma cells (**Figure S3d** and **e**).

To explain our findings, we first ruled out the possibility of endotoxin contamination resulting from protein purification from *E. coli*, as CP-STINGΔTM or CP-STINGΔTMΔC9 protein alone of equivalent concentrations did not induce CXCL10 (**Figure 3a**). It is intriguing, however, delivery of cGAMP by the catalytically inactive CP-STINGΔTMΔC9, in which the interaction of STING with TBK1 and IRF3 is disabled, enhanced the STING activation to a degree similar to that of the wildtype (i.e., CP-STINGΔTM) (**Figure 3a**). We hypothesized that in the $STING_{low}$ cell lines H1944 and H2122, the CP-STINGΔTM primarily may serve as a chaperon by promoting delivery of cGAMP into tumor cells. To test this hypothesis, we generated two additional fusion proteins: CP-dsRed and CP-STINGΔTM (R238A/R240A). Importantly mutations of the 238th arginine (R238) and 240th tyrosine (Y240) to alanine (A) are known to abolish the ability of STING to bind

cGAMP(23). As shown in **Figure 3a, S3d,** and **e**, these two protein variants failed to enhance CXCL10 production to the same extent as "CP-STINGΔTM + cGAMP" and "CP-STINGΔTMΔC9 + cGAMP". Therefore, through genetic mutations that inactivate two separate functions of STING, including the effector and cGAMP-binding capabilities, we have found that in $STING_{low}$ cells, CP-STINGΔTM primarily act as a chaperon to efficiently deliver cGAMP intracellularly and therefore greatly enhancing the STING activation.

Motivated by the ability of CP-STINGΔTM to markedly enhance cGAMP delivery and STING activation in $STING_{low}$ cells, we further extended our observations to A549 (human NSCLC) and SK-MEL-5 (human melanoma), which do not express endogenous STING ($STING_{absent}$)(24,30). Interestingly, we found that only "CP-STINGΔTM + cGAMP" induced CXCL10, while the catalytically inactive CP-STINGΔTMΔC9 along with cGAMP did not (**Figure 3b**). Additionally, "STINGΔTM + cGAMP" failed to induce CXCL10, which can be explained by the absence of Omomyc to facilitate cell penetration (**Figure 3a)**. These observations imply that codelivery of CP-STINGΔTM and cGAMP functionally restored the deficient STING signaling in $STING_{absent}$ cells. To further confirm this hypothesis, we utilized Clustered Regularly Interspaced Short Palindromic Repeats (CRISPR) to genetically knock out endogenous cGAS and STING, respectively in H1944. Notably, the cGAS knockout is known to inhibit the production of endogenous cGAMP(31). Consistent with data in $STING_{low}$ cell lines, in H1944 with cGAS knockout but intact STING, both "CP-STINGΔTM + cGAMP" and "CP-STINGΔTMΔC9 + cGAMP" could comparably induce CXCL10 expression, suggesting that endogenous cGAMP is not required for the activation of STING signaling (**Figure S3f**). In H1944 with only STING knockout, however, CXCL10 expression was induced by "CP-STINGΔTM + cGAMP" but not the catalytically inactive "CP-STINGΔTMΔC9 + cGAMP" (**Figure 3c**), which is consistent with findings in A549 and SK-MEL-5 cells, in which endogenous STING expression is completely absent (**Figure 3b** and **S3f**). In addition, concurrent treatment with a TBK1 inhibitor, MRT, repressed the production of CXCL10 in the cells treated with "CP-STINGΔTM + cGAMP" and "CP-STINGΔTMΔC9 + cGAMP" (**Figure 3d**)(12). Therefore, through both genetic and pharmacological inhibition of key proteins in the STING pathway, we have shown that "CP-STINGΔTM + cGAMP" acts as a functional

complex to induce STING signaling in the cells lacking endogenous STING expression. Finally, since cGAMP can be degraded by Ectonucleotide pyrophosphatase/phosphodiesterase 1 (ENPP1), which is abundant in extracellular and intracellular environments, another possibility for enhanced cGAMP delivery is that CP-STINGΔTM may protect cGAMP from ENPP1-mediated hydrolysis(8). To test this possibility, we explored cGAM$(PS)_2$(Rp/Sp), a synthetic non-degradable cGAMP analog, in H1944, and observed that "CP-STINGΔTM + cGAM$(PS)_2$(Rp/Sp)" and "CP-STINGΔTMΔC9 + cGAM$(PS)_2$(Rp/Sp)", markedly enhanced CXCL10 production in comparison to cGAM$(PS)_2$(Rp/Sp) alone of equivalent concentration or at a 10x concentration transfected by a commercial transfection reagent. Moreover, CP-STINGΔTM (R238A/R240A), in which the two mutations R238A and R240A abolish the cGAMP binding, failed to enhance CXCL10 production in the codelivery with cGAM$(PS)_2$(Rp/Sp) (**Figure 3e)**.

CP-STINGΔTM improves the efficacy of cGAMP as an immune adjuvant

cGAMP has been explored as a potent vaccine adjuvant that promotes both humoral and cellular immune responses in different mouse vaccination models(32). However, free cGAMP is prone to fast clearance and degradation owing to low molecular weight (~600 Da) and the presence of hydrolyzable phosphoester bonds, respectively. To address these limitations, a myriad of synthetic biomaterials have been developed to enhance the delivery efficacy of cGAMP. In our own work, motivated by enhanced activation of the STING pathway by CP-STINGΔTM in different cell types, we ask whether it could serve as a protein-based delivery platform to efficiently deliver cGAMP as an immune adjuvant. To this end, we made use of the murine dendritic cell line DC 2.4 as a model of antigen-presenting cells (APCs)(7). Similar to our findings in cancer cells, it was shown that CP-STINGΔTM + cGAMP greatly induced expression of CXCL10 and surface expression of MHC-I compared to free cGAMP (**Figure 4a** and **b**).

Next, we tested our hypothesis in wild-type C57BL/6 mice by vaccinating them with a model antigen, chicken ovalbumin (OVA), along with free cGAMP or cGAMP + CP-STINGΔTM serving as an immune adjuvant(12). Following a priming-boost protocol with

a two-week interval, we quantified the levels of OVA-specific total IgG as well as type I IFN-associated IgG2c from mouse serum, of which the latter IgG subtype can be induced through activation of the STING pathway. As shown by the OVA-specific ELISA, the "OVA + cGAMP + CP-STINGΔTM" treatment group increased the levels of OVA-specific IgG and IgG2c by nearly ten-fold compared to "OVA + cGAMP + CP-STINGΔTM (R237A/Y239A)", "OVA + cGAMP + STINGΔTM", and "OVA + cGAMP" (**Figure 4b and c, S4a-d**). To examine the cellular responses, we measured the percentage of CD8 T cells carrying the MHC-I-SIINFEKL epitope ($OVA_{257-264aa}$) via tetramer staining (**Figure S4b**). In agreement with studies in humoral responses, "OVA + cGAMP + CP-STINGΔTM" exhibited the highest induction of SIINFEKL-specific CD8 T cells among different treatment groups. Furthermore, when comparing CP-STINGΔTM to STINGΔTM, the latter of which does not have the cell-penetrating protein domain, CP-STINGΔTM markedly enhanced OVA-specific IgG and IgG2c as well as SIINFEKL-restricted CD8 T cells (**Figure 4b, c,** and **S4a-d**)(33). We reasoned that it is due to increased retention and intracellular uptake mediated by the cell-penetrating protein Omomyc. Indeed, in a later experiment, we found that CP-STINGΔTM exhibited greater retention in tumors than STINGΔTM at 96 hours post injection (**Figure 6a** and **b**). Next, we made use of the same cohort of vaccinated C57BL/6 mice to examine whether the increased induction in antigen-specific IgG and CD8 levels could confer greater protection in a prophylactic syngeneic mouse melanoma model. Specifically, one week after the boost, we challenged the mice with B16 melanoma cells engineered to express the SIINFEKL epitope. As shown in **Figure 4d** and **e**, the cohort vaccinated with "OVA + cGAMP + CP-STINGΔTM" combination displayed the slowest tumor growth rates and longest survival rates.

Codelivery of CP-STINGΔTM and cGAMP augments tumor cell killing by antigen-specific T cells *ex vivo*

In addition to promoting maturation and cross-presentation of dendritic cells for T cell priming, which serves as the very first step of immune clearance of tumor cells, activation of the STING pathway in tumor cells has been shown to augment cytotoxic T cell-mediated cancer cell killing by upregulating MHC-I on the surface of tumor cells(29). Motivated by the aforementioned vaccination and prophylactic mouse model studies, we

next explored whether CP-STINGΔTM and cGAMP can enhance tumor cell killing. To this end, in an *ex vivo* model, we generated two isogenic B16 melanoma cell lines expressing either SIINFEKL-GFP fusion or GFP alone, and treated them with free cGAMP, "cGAMP + CP-STINGΔTM", "cGAMP + CP-STINGΔTMΔC9" and "cGAMP + CP-STINGΔTM (R237Y239A)" for 48 hours(34). After the supernatant was removed from the tumor cells, CFSE-stained SIINFEKL-specific CD8 T cells, which were harvested from lymph nodes of OT-1 mice, were cocultured with tumor cells (**Figure 5a**). It is noteworthy that by pretreating tumor cells with cGAMP and different STING protein variants followed by washing and coculturing with antigen-specific T cells, we specifically tested the effects of STING activation in tumor cells. As shown in **Figure 5b** and **c**, following a 120-hour coculture, cGAMP complexed with CP-STINGΔTM and CP-STINGΔTMΔC9 induced the highest T cell proliferation as evidenced by T cell division-mediated CFSE dilution in flow cytometry. Moreover, the highest efficacy of tumor killing was detected in the same treatment groups by staining viable tumor cells with MTT after washing away nonadherent T cells (**Figure 5d**). Of note, the tumor killing was only detectable in B16 cells bearing the SIINFEKL epitope but not in the GFP-expressing B16 cells in the coculture with OT-1 cells, indicating that the increased T cell proliferation and tumor cell killing were antigen-specific (**Figure S5a** and **b**). To confirm that the increased T cell proliferation and killing resulted from enhanced tumor cell recognition by OT-1 T cells, after treating SIINFEKL-expressing B16 with cGAMP and different STING variants for 48 hours, we quantified the expression levels of MHC-I and SIINFEKL-restricted MHC-I on the surface of tumor cells by flow cytometry. As shown in **Figure 5e** and **S5c**, only "CP-STINGΔTM + cGAMP" and "CP-STINGΔTMΔC9 + cGAMP" markedly upregulated the expression of MHC-I and SIINFEKL-restricted MHC-I in comparison to free cGAMP and other control treatment groups. We reason that since B16 cells express endogenous STING (**Figure S3a**), CP-STINGΔTM acted as a chaperon to enhance cGAMP delivery into tumor cells in this setting.

Codelivery of CP-STINGΔTM and cGAMP enhances the therapeutic efficacy of ICB

Having validated the enhanced tumor cell killing by OT-1 cells via codelivery of CP-STINGΔTM and cGAMP *ex vivo*, we further examined whether this approach could

augment the efficacy of the combination immunotherapy involving STING agonism and ICB. Here, we made use of an immunogenic mouse melanoma cancer model bearing YUMMER1.7 tumor cells for three reasons: First, YUMMER1.7 cells carry *Braf* mutation and *Pten* loss that mimic the most frequent mutations happening in melanoma patients(35). Second, tumors with increased immunogenicities are generally responsive to ICB, such as anti-PD-(L)1, among which lung cancer and melanoma are of high mutation burden(36). Third, STING activation in the TME has been shown to improve the therapeutic efficacy of ICB in different syngeneic mouse cancer models(37).

Before the treatment study, we first confirmed that CP-STINGΔTM can internalize tumor cells and other cell types in the TME. Specifically, when YUMMER1.7 tumors reached ~150 mm^3 in C57BL/6 mice, a single dose of CP-STINGΔTM was administered intratumorally. Mice were sacrificed at 96 hours, and tumors were harvested for cryo-sectioning and immunostaining using the anti-FLAG antibody specific for recombinant STING protein variants. As shown in **Figure 6a**, CP-STINGΔTM but not STINGΔTM was readily detectable across different tumor slices in a homogeneous pattern at 96 hours after a single intratumoral administration, and CP-STINGΔTM was primarily localized in the cytoplasm, suggesting that the presence of the cell-penetrating domain Omomyc domain facilitated the retention of recombinant STING in the TME. To corroborate this finding, in a separate cohort of mice, single cells were prepared for intracellular staining against the same FLAG epitope. Similar to our *in vitro* cellular uptake studies, CP-STINGΔTM efficiently internalized tumor cells in comparison to STINGΔTM that lacks the cell-penetrating capability (**Figure 6b**).

Next, we investigated the therapeutic efficacy of CP-STINGΔTM and cGAMP in combination with anti-PD1 in the Yummer1.7 syngeneic mouse model (**Figure 6c**). Of note, we initiated treatment in mice with relatively large subcutaneous tumors, which are more challenging to treat with immunotherapy than smaller tumors(7). After tumors reached ~150 mm^3, CP-STINGΔTM, CP-STINGΔTMΔC9, CP-STINGΔTM(R237A/Y239A) and STINGΔTM were intratumorally administered with cGAMP, while anti-PD1 was given intraperitoneally at optimized doses every two days

for a total of four treatments (**Figure 6c**). Over the duration of treatment, no significant weight loss was detected among different treatment groups in comparison to the vehicle control group (**Figure S6a**). Importantly, both CP-STINGΔTM and CP-STINGΔTMΔC9 showed marked reduction in the tumor progression compared to CP-STINGΔTM(R237A/Y239A) and STINGΔTM treatment groups (**Figure 6d** and **e**). These findings agree with our studies *in vitro*: (1) The mutations R237A/Y239A in STING abolish the binding of cGAMP, and therefore CP-STINGΔTM(R237A/Y239A) cannot effectively deliver cGAMP into target cells. (2) STINGΔTM alone cannot efficiently penetrate target cells due to the absence of the Omomyc protein. (3) because cancer cells and hematopoietic cells in tumors express endogenous STING, CP-STINGΔTM plays a chaperon role in enhancing the intracellular delivery of cGAMP such that there was no detectable difference between CP-STINGΔTM and CP-STINGΔTMΔC9, the latter of which cannot activate the STING signaling. In addition to tumor volume therapeutic efficacy, we further measured proinflammatory cytokines in a separate cohort of mice bearing the same tumor cells(38). The treatment group of "CP-STINGΔTM + cGAMP" displayed increased expression of TNFα, IFNγ, and CXCL10 in comparison to "STINGΔTM + cGAMP" and the untreated group (**Figure 6f, g** and **Figure S6b**).

DISCUSSION

In this study, we have successfully developed a protein carrier (CP-STINGΔTM) for efficient cytosolic delivery of STING agonists by merging the inherent capacity of the transmembrane deleted STING (STINGΔTM) in binding cGAMP and activating the downstream STING signaling with the cell-penetrating (CP) miniprotein Omomyc, the latter of which was recently validated in several preclinical NSCLC mouse xenograft model as an anti-cancer therapy. Importantly, while the N terminus of Omomyc is responsible for cell targeting, the C terminus of STINGΔTM is involved in intracellular STING functions(19). Additionally, the two protein domains exist as a dimer on their own. Therefore, the fusion protein consisting of CP and STINGΔTM can in theory function properly with the natural configuration and stoichiometry. To confirm the functionality and versatility of the fusion protein CP-STINGΔTM, we tested a panel of NSCLC and melanoma cancer cell lines since these two cancer types can benefit from existing

immunotherapy owing to high tumor mutational burden. Intriguingly, we found that CP-STINGΔTM plays distinct roles in these cell lines depending on the levels of endogenous STING expression. Specifically, codelivery of CP-STINGΔTM and cGAMP restores the STING signaling in cancer cells either naturally deficient for STING expression or genetically knocked out by CRISPR, indicating that CP-STINGΔTM and cGAMP forms a functional complex in this setting. On the contrary, CP-STINGΔTM serves as a chaperon to markedly promote the delivery of cGAMP in cells with down-regulated STING expression, requiring a 100-fold lower concentration of cGAMP than free cGAMP in STING activation and subsequent type I IFN induction. To explore the potential translation of the platform, we further confirmed potent T cell proliferation and anti-tumor immune responses *ex vivo* and extended the observation in vivo using a mouse model of vaccination. Finally, we investigated the translational potential of our platform in combination with the ICB using a syngeneic mouse melanoma model. Collectively, our CP-STINGΔTM system may provide a new paradigm of delivering STING agonists towards vaccines and cancer immunotherapy.

The most important finding of our study is that CP-STINGΔTM in complex with cGAMP can form a functional complex to activate the endogenous STING signaling in cancer cells deficient for STING. This attribute may have critical clinical implications in melanoma and lung cancers. Notably, existing STING agonism strategies have centered around developing DNA-damaging reagents to activate tumor cells to produce endogenous cGAMP, reversing the epigenetic inhibition of STING/cGAS expression, and exogenously administering STING agonists. These approaches, however, can be hampered by the fact that endogenous STING and/or cGAS are frequently silenced in tumor cells as a mechanism to evade anti-tumor immune responses(39). Specifically, the loss of tumor-intrinsic STING expression has been shown to impair tumor cell antigenicity and susceptibility to lysis by tumor-infiltrating lymphocytes through the downregulation of MHC class I expression on the surface of cancer cells. In addition to NSCLC and melanoma, decreased expression of STING in tumor cells has been correlated with poor prognosis in patients with gastric and colon cancers(26,40). Conversely, activation of tumor-intrinsic

STING signaling has been found to dictate chemotherapy-induced anti-tumor cytotoxic T cell responses (e.g., olaparib) in triple-negative breast cancer(41,42).

In comparison to many existing synthetic delivery systems, our CP-STING protein as a delivery vehicle is unique in several aspects: (1) Instead of electrostatic complexation, which is particularly challenging to dinucleotides owing to low charge densities, we have made use of the inherent strong affinity between the C-terminus of STING and its agonist to efficiently encapsulate STING agonists. (2) The CP-STINGΔTM itself is in essence a single long polymer with a fixed degree of "polymerization", and therefore is structurally well defined as evidenced by size exclusion chromatography and SDS-PAGE. This feature may minimize batch-to-batch variations, commonly occurring in synthetic delivery vehicles. (3) The fusion protein can be produced and purified from the standard *E. coli* based recombinant protein expression system in a high yield in conjunction with the low-cost metal affinity purification, which is easily accessible to many laboratories.

Future studies can involve comprehensive pharmacological characterization of the CP-STINGΔTM in the setting of systemic delivery to optimize the dose and frequency of the fusion protein. Additionally, by employing transgenic mouse models with STING deficiency in different cell types (e.g., tumor cells versus different immune cell subtypes), we can further elucidate exact targets of CP-STINGΔTM, and therefore assess the contribution of tumor-intrinsic STING in developing anti-tumor immune responses. Finally, given the modularity of the fusion protein, we can potentially substitute the cell-penetrating domain with a more specific protein domain such as nanobody to target particular cell type or TME such that our fusion platform can be extended to targeted delivery of STING agonists in a manner similar to antibody drug conjugates(43). Alternatively, direction fusion of a nanobody such as anti-PD (L)1 with STINGΔTM may simultaneously leverage ICB and STING in a single protein format. Therefore, our approach may offer a unique direction towards the STING-based therapeutics.

MATERIALS AND METHODS

Chemicals and antibodies

2’3’-cyclic-GMP-AMP (cGAMP) is a generous gift from Dr. Pingwei Li at Texas A&M University. Tween-20, Triton X-100, Triton X-114 were all purchased from Sigma-Aldrich (St Louis, MO). Carboxyfluorescein succinimidyl ester (CFSE) was purchased from Tonbo Biosciences (San Diego, CA). All other chemicals were purchased from ThermoFisher (Waltham, MA) and used as received. Human CXCL10/IP-10 and mouse CXCL10/IP-10 ELISA Kit, Murine TNF-alpha, and Murine IFN-gamma were respectively purchased from R&D system (Minneapolis, MN) and Peprotech (Rocky Hill, NJ). Zombie Dyes, Alexa647 anti-DYKDDDDK Tag Antibody (Clone L5), APC anti-mouse CD8a (Clone 53-6.7), FITC anti-mouse CD3 (clone 145-2C11), PerCP-Cy5.5 anti-mouse CD4 (Clone 129.29) , PE anti-mouse CD8a (clone 53-6.7), PerCP-Cy5.5 cd11b (Clone M1/70), FITC anti-mouse cd11c (Clone N418), PE anti-mouse CD45 (clone 30-F11), Alexa 488 anti-mouse CD45 (clone 30-F11), FITC anti-human HLA-A,B,C Antibody (clone W6/32), FITC anti-mouse H-2Kb/H-2Db Antibody (Clone 26-8-6) were from Biolegend (San Diego, CA). Primary antibodies of STING/TM173 (D2P2F), alpha-Tubulin (DM1A), TBK1/NAK (D1B4) were from Cell signaling technology (CST, Danvers, MA). Secondary antibodies of goat anti-rabbit IgG-HRP and goat anti-mouse IgG-HRP are from Santa Cruz Biotech (Santa Cruz, CA). InVivoMAb anti-mouse PD-1 (CD279) was purchased from BioXCell (Lebanon, NH).

Expression and purification of STING∆TM protein variants

The human STING∆TM protein (139-379aa) and mouse STING∆TM (138-378aa) variants were synthesized by gblock (IDT, Coralville, IA), and cloned into pSH200 vector (a generous gift from Prof. Xiling Shen at Duke University) containing a 6xhistidine tag (His-tag), between *NcoI* and *NotI* sites. Mutants were generated with site-specific mutagenesis based on the human STING∆TM plasmids. All plasmids were confirmed by sequencing. STINGΔTM variants were expressed as His-tag proteins from BL21 (DE3) Escherichia coli (*E. coli*). All proteins were expressed as cultures grown in Luria-Bertani broth (LB) (5g sodium chloride, 5g tryptone, 2.5g yeast extract, and 500 mL of distilled water), supplemented with 100 µg/ml Ampicillin. After outgrowth at 37°C with 225 rpm in a shaker, and until optical density (OD600) reached 0.6, 1 mM IPTG was added to induce the protein expression for 16 to 18 hours at 20°C and 225 rpm. Cells were then collected

by centrifugation at 5000x g for 20 minutes at room temperature. The bacterial pellets were resuspended in a 10 mL protein binding buffer (50 mM sodium phosphate, 0.5 M sodium chloride, 10 mM imidazole) and stored at -80°C until purification. The frozen cultures were thawed and lysed with 1% Triton-100, 1 mg/mL lysozyme, 1mM PMSF, and one EDTA-free protease inhibitor cocktail tablet at room temperature for 20 min. The lysate was disrupted by ultrasonication at 5-second intervals for a total of 5 min each at 18 W on ice. Insoluble debris was removed by centrifugation at 12000x g for 60 min, at 4 °C. Protein purification was carried out by affinity chromatography using Cobalt agarose beads. 10 mL of raw protein extracts were applied to the protein binding buffer-equilibrated beads, followed by three washes with protein binding buffer plus 0.1% Triton-114 for endotoxin removal. After elution (50 mM sodium phosphate, 0.5 M Sodium chloride, 150 mM imidazole), protein extracts were loaded to fast protein liquid chromatography (FPLC, NGC Quest 10 Chromatography System, Biorad) for 3X PBS buffer exchange and purification. Protein fractions detected at λ = 280 nm were collected. Purified STINGΔTM variants concentrations were determined by DC protein assay and purities were verified by SDS-PAGE. Protein aliquots were kept at -80˚C at all times until further use.

Animal work

All work with C57BL/6J mice (females, 7-10 weeks old) and OT-1 transgenic mice (The Jackson Laboratory, Bar Harbour, ME) was performed in accordance with institutional guidelines under protocols of NU-20-0312R (C57BL/6J) and NU-19-0106R (OT-1) approved by Northeastern University-Institutional Animal Care and Use Committee (NU-IACUC). All mice were maintained in a pathogen-free facility following the National Research Council of the National Academies.

Cell lines and cell culture

Non-small cell lung cancer cell lines A549, H1944, and H2122 harboring KRAS/LKB1 co-mutations and H1944 Knockouts (H1944 STING-knockout, H1944 cGAS-knockout, H1944 scramble-knockout) were generous gifts from Dr. David Barbie's lab. Human and murine cell lines of B16F10, HeLa, HEK293T, SK-MEL-3, and SK-MEL-5, were obtained

from the American Type Culture Collection (ATCC, Rockville, MD). Yummer1.7 was requested from the Koch Institute (Cambridge, MA). B16-OVA(257-264aa) and Yummer1.7-OVA(257-264aa) were generated through transfection with plasmids encoding full lengths of OVA and EGFP, and sorted by FACS for GFP expression. A549, SK-MEL-3, SK-MEL-5, Yummer1.7, HeLa, and HEK293T were cultured in Dulbecco's modified Eagle's medium (DMEM) supplemented with 10% fetal bovine serum (FBS), 100 U/mL penicillin-streptomycin, and 100x Non-Essential Amino Acid (NEAA). H1944, H2122, HCC44, and H23 were cultured in RPMI-1640 supplemented with 10% FBS, 100 U/mL penicillin-streptomycin, and 100x NEAA. H1944 STING-knockout, H1944 cGAS-knockout, and H1944 scramble-knockout were cultured in RPMI-1640, with 10% FBS, 100 U/mL penicillin-streptomycin, 100x NEAA with 1μg/mL puromycin selection. Cells were kept in a humidified incubator with 5% carbon dioxide (CO_2) at 37˚C and routinely tested mycoplasma negative by PCR. All the cell experiments were performed between passages 2 and 10.

Lentivirus production and cell line generation

Lentiviral vector plasmids of *pFUW Ubc OVA (252-271aa) EGFP, EGFP Luciferase puro (663)* were used to generate lentiviral particles. 7.5 μg of packaging plasmid psPAX2, 2.5 μg of envelope plasmid pMD2.G, 10μg of Lentiviral vector plasmids, and 10 μL TransIT-X2 were mixed in 1 mL Opti-MEM. After 30 minutes of incubation at room temperature, the plasmid mixture was added to 70% confluency HEK293T cells. Supernatants were collected at 48 hours and 72 hours after transfection and centrifuged at 1000 g for 10 minutes to remove the debris. Harvested Lenti-viral supernatants were kept at –80 C until further cell line generation. After targeted cell lines of B16F10 and Yummer 1.7 reached 70% confluency, lentiviral supernatants were added to the cells with 8 μg/mL polybrene. Transfected cells were selected with 1 μg/mL puromycin.

Enzyme-linked immunosorbent assay (ELISA)

For human CXCL10 and mouse CXCL10, cells (1 to $2x10^4$) were cultured with premixed complexes of 40 μg/mL, or 10 μg/mL STINGΔTM variants with or without 1 μg/mL or 0.25 μg/mL cGAMP for 72 hours. Conditioned supernatants were collected for ELISA

quantification according to the manufacturer's instructions. Values represent the average of four to six replicates from at least two independent experiments. For analysis of anti-OVA IgG level, we conducted the ELISA as previously described(44). For cytokine quantification in the treatment study, tumors were harvested and grounded in tissue protein extraction reagent (T-PER^{TM}) with 1% proteinase inhibitors. The lysates were incubated at 4 °C for 30 min with rotation. The supernatant from each lysate was collected after removing debris through centrifugation. The quantifications of CXCL10, TNF-α, and IFN-γ were performed according to the manufacturer's instructions.

Immunofluorescence staining

A549, H1944, and HeLa were seeded in chamber slides at a density of ~5x10^4 24 hours before incubation with 40 μg/mL STINGΔTM variants and 1 μg/mL cGAMP complexes. After another 24 hours, cells were washed with PBS once, and fixed with 70% ethanol. After permeabilization with PBS containing 0.1% Triton X-100 for 15 minutes, cells were washed and incubated with the anti-DYKDDDDK Tag antibody at 1:500 dilution in 1xPBS with 1% BSA and 0.05% TWEEN 20 (PBST) at 4˚C overnight. Cells were then washed for 30 minutes in PBST, and incubated with Alexa488-Phalloidin (CST) in 1:100 dilution for 1 hour. After washing cells with PBST for three times for 10 minutes each, cells were counter-stained with DAPI in mounting media at room temperature. Images of the cells were visualized and captured by Nikon Eclipse Ti2 microscope (Tokyo, Japan) and analyzed by ImageJ (NIH).

Fluorescence imaging analysis

Three days after injection with complexes, tumors were harvested and placed in OCT in tissue cassettes and frozen on ice for cutting into 8-10μm sections in slides. The slides were washed with PBS for 10 min at room temperature, dried on a paper towel and incubated with anti-CD45 diluted in the antibody buffer (10% FBS in PBS) for 1 hour at room temperature in the dark. After three washes with PBS, the slides were fixed in 4% paraformaldehyde in PBS. Slides were incubated with 0.025% saponin in PBS for permeabilization. Anti-DYKDDDDK were added on the sections for overnight incubation at 4 ˚C in the dark. Slides were washed in PBS with 0.0025% saponin for 10 min twice.

After incubating with secondary antibody for 1 hour in the dark, slides were rinsed with PBS with 0.0025% saponin and counterstained with DAPI. The stained tumor slides were imaged using a Nikon microscope.

Flow cytometry

For uptake study, $1x10^5$ cells were seeded in 12-well plates in their corresponding complete culture medium and incubated for 24 hours. After treatment with 40 μg/mL STINGΔTM variants with or without 1 μg/mL cGAMP for 24 hours, cells were washed with PBS and treated with trypsin for at least 15 minutes to remove STING proteins nonspecifically bound to the cell surface. Cells were transferred to 96-well v-bottom plates and collected through 300xg centrifugation for 3 minutes. After twice washes with 200 μl PBS, cells were fixed with 70% ethanol for 20 minutes. The fixed cells were washed with PBS for 10 minutes three times. Cells were resuspended in anti-DYKDDDDK Tag Antibody at 1:1000 dilution in antibody dilution buffer (1xPBS containing 1% BSA and 0.05% Tween 20) and incubated for 2 hours at room temperature in the dark. Antibodies were removed by rinsing cells with PBST three times. The cell suspension in PBS was loaded to Attune flow cytometry (Thermofisher, Waltham, MA). Doublets and dead cells were excluded before analysis.

For *in vitro* MHC-I analysis, 10000 cells were incubated with 40 μg/mL STINGΔTM variants and 1 μg/mL cGAMP in a complete culture medium for 48 hours before staining. Cells were rinsed by PBS, detached by 100μl 5mM EDTA in PBS with a fixable live/dead dye, NIR Zombie Dye (Biolegend), at 1:1000 dilution for dead cell exclusion. After staining was quenched by FACS buffer (5% FBS, 2mM EDTA, 0.1% sodium azide in PBS), cells were resuspended by FACS buffer containing 0.4μg/ml anti-human HLA-A,B,C antibody or FITC anti-mouse H-2Kb/H-2Db antibody, and incubated on ice for 30 min in the dark. Stained cells were washed twice and resuspended in the FACS buffer for flow cytometric analysis in FlowJo (Franklin Lakes, NJ). After excluding doublets and debris of dead cells, gating strategies determined through control staining were applied for analysis while compared with FITC Mouse IgG2a, κ Isotype control antibody stained cells.

For OT-1 CD8+ T cells stimulation, CFSE stained lymphocytes were collected through 500x g centrifuge for 3 min and washed with 200µl PBS. 100µl Zombie dye in PBS at 1:1000 dilution was added to the lymphocyte and incubated for 30 min at room temperature avoiding light. Zombie dye staining was quenched by 100µl FACS buffer. After 3 min centrifuge at 500x g, OT-1 $CD8^+$ T cells were selected by 100µl APC anti-mouse CD8a Antibody in FACS buffer at 1:1000 dilution after 30 min incubation on ice. Co-stained cells were resuspended in the FACS buffer and quantified under the flow cytometer.

For *in vivo* tumor profiling, dissected tumors were digested in 1 mg/mL collagenase D for 1 hour at 37 ˚C. Single-cell suspensions were obtained from mincing the tumor through a 70 µm cell strainer. After staining with NIR zombie dye for dead cell exclusion, cells were neutralized and blocked with anti-CD16/CD32 for 5 minutes on ice and stained with antibodies against surface markers CD45, CD3, CD4, CD8, CD11b, CD11c on ice for 30 minutes in FACS buffer. For intracellular staining, cells were fixed, permeabilized, and stained with anti-DYKDDDDK tag antibody. All samples were analyzed by FlowJo after loading to the flow cytometer.

Cell viability assay

The effects of STINGΔTM variants and cGAMP complexes on cell viability were determined by 3-(4,5-dimethylthiazol-2-yl)-2,5-diphenyltetrazolium bromide (MTT) assay. 1000 cells were seeded in 96-well plates and treated with 40µg/mL STINGΔTM variants and 1µg/mL cGAMP for 120 hours in 5% CO2 at 37˚C in a humidified incubator. Cells were further incubated with 0.5 mg/mL MTT dissolved in sterilized 1x PBS at 37°C for 2 hours before DMSO was added into each well to dissolve formazan crystals. The absorbance of each well was determined at 570 nm on an automated Bio-Rad microplate reader (Bio-Rad Laboratories, Hercules, CA). Untreated cells as control were considered to be 100% viable.

Lymphocyte preparation from lymph nodes in OT-1 mice

The mesenteric, inguinal, axillary, and brachial lymph nodes dissected from OT-1 mouse were homogenized to generate a single cell suspension, and the released cells in lymphocyte growth medium (RPMI1640 complete media and 50μM 2-mercaptoethanol) were pelleted and resuspended in 10ml PBS. The lymphocyte was washed and stained with 1μM CFSE in 1x PBS for 20 min until the staining was terminated by 10% FBS. The stained lymphocyte was resuspended and cultured in lymphocyte growth medium in a humidified incubator to release excessive CFSE. After 2 hours incubation, lymphocyte was collected and resuspended in lymphocyte growth medium with 20U/ml interleukin (IL)-2.

Coculture of OT1 lymphocytes with B16-OVA or YUMMER 1.7-OVA

100μl of 1x 10^6 lymphocytes in lymphocyte growth medium with 20U/ml IL-2 was added into the 96-well plate with 100μl of 1x10^4 B16-OVA(257-264aa) treated with STINGΔTM variants with or without cGAMP 48 hours ahead. On days 3, 100μl of lymphocytes were gently collected for flow cytometry analysis. 100μl fresh lymphocyte growth medium with 20U/ml IL-2 was added to each well for leftover lymphocyte growth. On day 5, after lymphocytes were collected, B16-OVA(257-264aa) attached wells were washed with PBS twice for subsequent MTT assay.

Immunizations, tumor inoculation and treatment in mice

Analysis of immunizations for adjuvant potential performed in C56BL/6 mice with B16-OVA (257-264aa) was conducted as previously described(44). For treatment study, one million Yummer1.7 cells in 100μl Opti-MEM were subcutaneously injected into the flank of mice. At 6-9 days later, when tumors reached 150 mm^3 in volume, animals were injected intratumorally with ~25ul vehicle control, 2.5 μg cGAMP only or 100 μg STINGΔTM variants and 2.5 μg cGAMP complex in Opti-MEM.

Statistical analysis

Statistical significance was evaluated using one-way ANOVA followed by Tukey *post hoc* test. P values less than 0.05 were considered significant. Statistical significance is indicated in all figures according to the following scale: *P<0.05, **P<0.01, ***P<0.001,

and ****P<0.0001. All graphs are expressed as the means ± SEM. In one-way ANOVA followed by *post hoc* tests, we marked asterisks only in pairs of our interest.

ACKNOWLEDGEMENTS

This work was supported by the Northeastern University Faculty start-up funding (JL), Northeastern University-Dana Farber Cancer Institute Cancer Drug Development (JL and DAB), and Peer Reviewed Medical Research Program from the Department of Defense's Congressionally Directed Medical Research Programs (JL). We are grateful to Dr. Yingzhong Li at the Koch Institute of Integrative Cancer Research at MIT for scientific advice. We would like to express our gratitude to Professor Sara Rouhanifard at Northeastern University's Department of Bioengineering for generously sharing her lab's fluorescent microscope; Professor Ke Zhang at Northeastern University's Department of Chemistry for sharing his lab's equipment.

Conflict of Interest: No conflict of interest is declared.

Figures and Figure legends

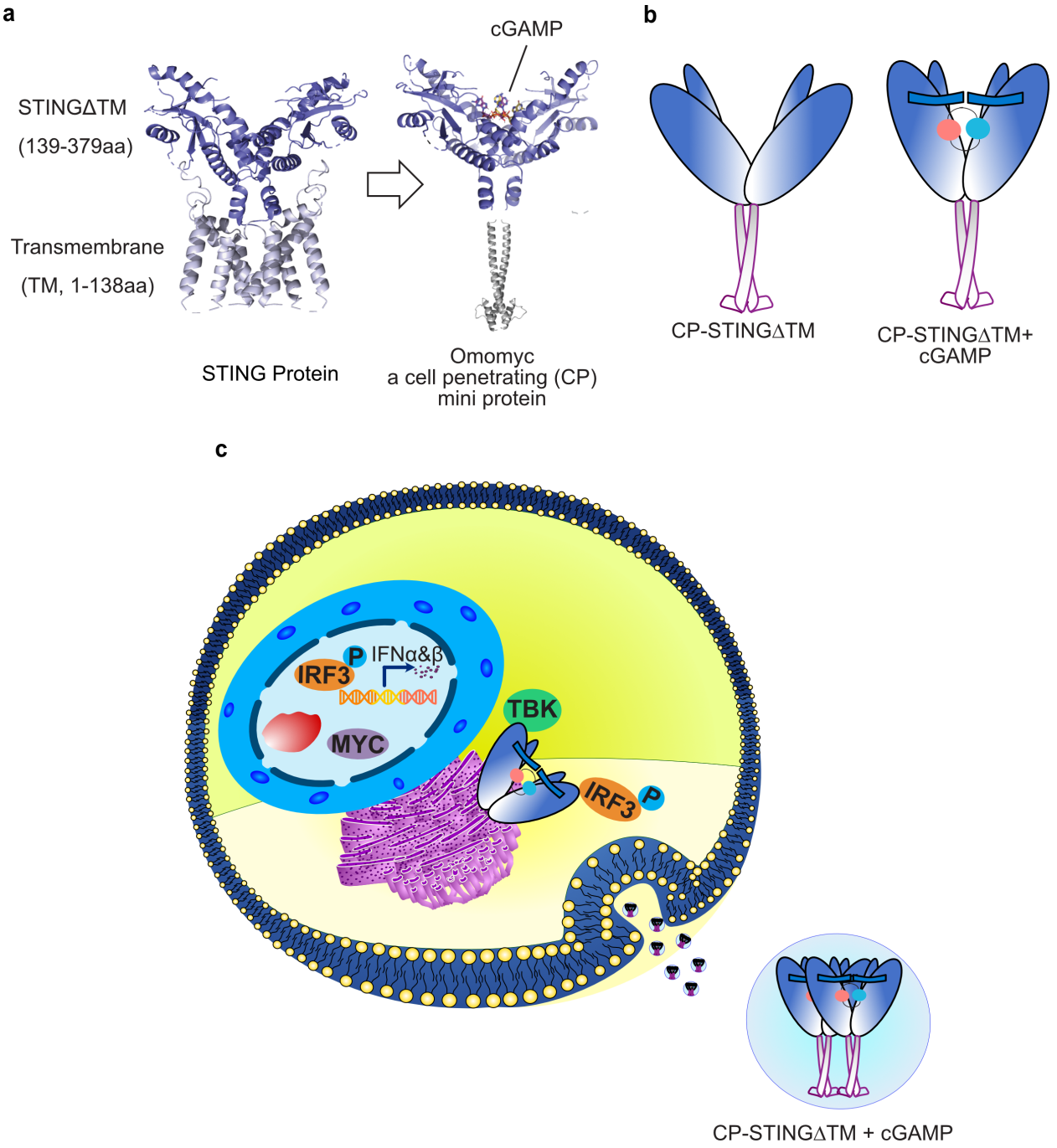


Figure 1. **Schematic of using recombinant cell-penetrating (CP)-STINGΔTM as a biologically functional platform for cGAMP delivery**. **(a)** To bypass the need for synthetic vehicles, we designed and engineered a CP-STINGΔTM by replacing the transmembrane (TM) of the full-length STING with Omomyc, a cell-penetrating mini protein. **(b)** A cartoon model illustrating how CP-STINGΔTM binds cGAMP. (**c**) By fusing

with the cell-penetrating domain, the CP-STINGΔTM is capable of penetrating cells, delivering cGAMP, and engaging with downstream proteins such as TBK1 and IRF3, which result in the production of type I IFNs.

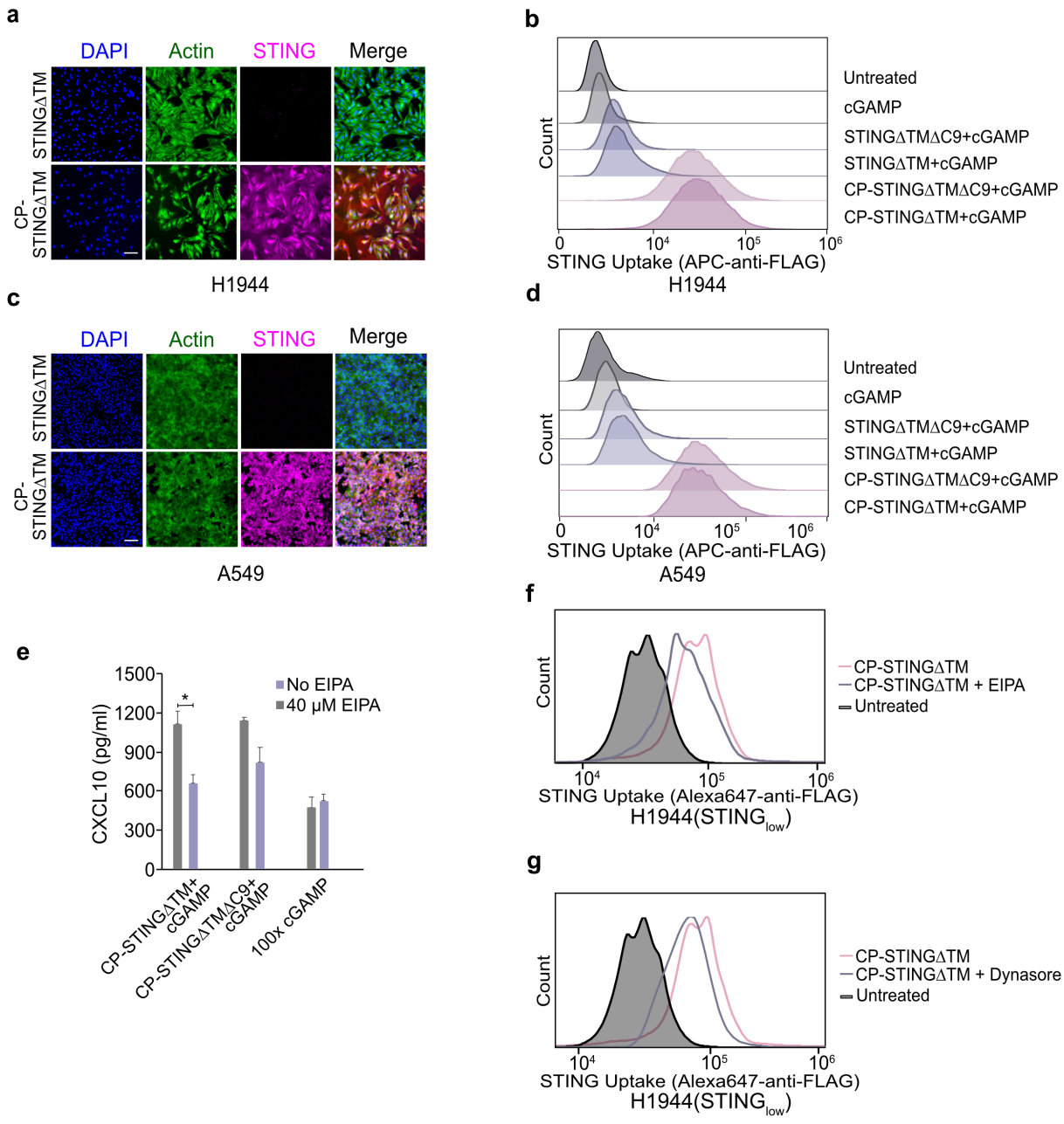


Figure 2. **CP-STINGΔTM spontaneously internalizes cancer cells**. Fluorescence microscopy imaging of internalized CP-STINGΔTM in H1944 ($STING_{low}$) with downregulated STING expression **(a)** and A549 ($STING_{absent}$) without any STING expression **(c)** (scale bar = 100 μm). Flow cytometry of internalized CP-STINGΔTM in H1944 ($STING_{low}$) with downregulated STING expression **(b)** and A549 ($STING_{absent}$)

without any STING expression **(d)**. Cells were treated with “40 μg/ml CP-STINGΔTM” + 1 μg/ml cGAMP” or “40 μg/ml STINGΔTM + 1 μg/ml cGAMP” for 24 hours before staining with APC-anti-FLAG. (**e**) H1944($STING_{low}$) were preincubated with 40μM EIPA for 2 hours and treated with “40 μg/ml CP-STINGΔTM + 1 μg/ml cGAMP” or “40 μg/ml STINGΔTM + 1 μg/ml cGAMP” or 100 μg/ml cGAMP, CXCL10 production was inhibited by macropinocytosis inhibitor EIPA. Representative flow cytometry analysis of CP-STINGΔTM uptake in H1944 pretreated with indicated inhibitors targeting macropinocytosis (f) and endocytosis (g), respectively.

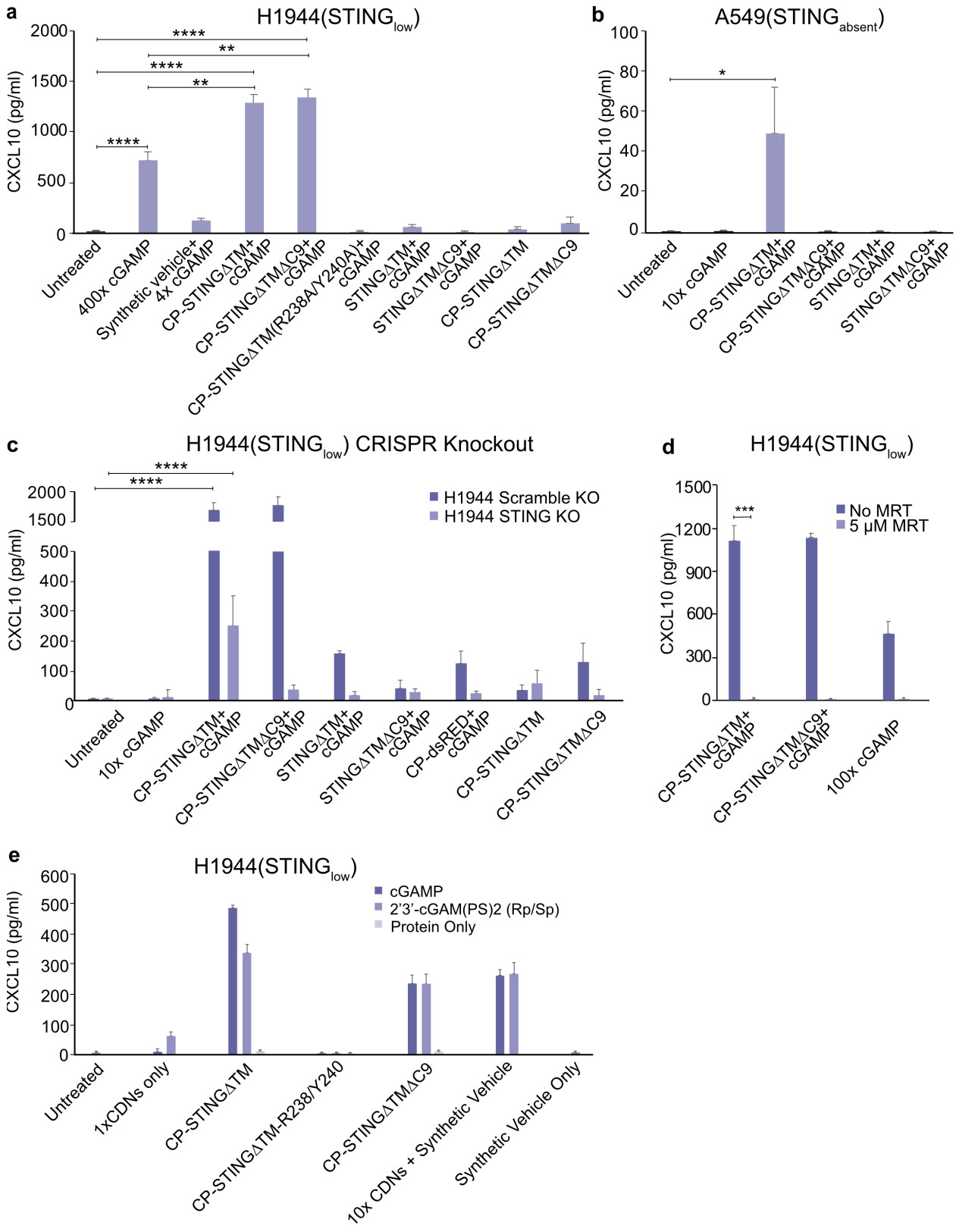


Figure 3. **CP-STINGΔTM markedly enhances cGAMP delivery and STING activation in cancer cell lines with impaired STING expression.** (**a**) CP-STINGΔTM plays a

chaperon role in H1994 ($STING_{low}$) that have down-regulated STING expression. Specifically, CXCL10 was remarkably enhanced by “10 μg/ml CP-STINGΔTM + 0.25 μg/ml cGAMP” or “10 μg/ml CP-STINGΔTMΔC9 (catalytically inactive mutant) + 0.25 μg/ml cGAMP” compared to 100-400 fold higher concentration of free cGAMP and 40 fold higher concentration of cGAMP delivered by Lipofectamine 2000. (**b**) “CP-STINGΔTM + cGAMP” forms a functional complex in A549 ($STING_{absent}$), which does not express endogenous STING. Only “40 μg/ml CP-STINGΔTM +1 μg/ml cGAMP” could induce CXCL10. (**c**) After knocking out endogenous STING in H1944 by CRISPR, CXCL10 expression was only induced by “40 μg/ml CP-STINGΔTM + 1 μg/ml cGAMP” but not by the catalytic inactive “40 μg/ml CP-STINGΔTMΔC9 + 1 μg/ml cGAMP” or free cGAMP. (**d**) The CXCL10 production was inhibited by the TBK1 inhibitor – MRT, which indicates that the enhanced STING signaling by CP-STINGΔTM or CP-STINGΔTMΔC9 was dependent on the TBK1, a key component in the STING pathway. (**e**) Codelivery of CP-STINGΔTM and a synthetic, non-degradable cGAMP analog, $cGAMP(PS)_2(Rp/Sp)$, also enhances CXCL10 production in comparison to free $cGAMP(PS)_2(Rp/Sp)$ or 10x $cGAMP(PS)_2(Rp/Sp)$ transfected by Lipofectamine 2000, which suggests that CP-STINGΔTM promotes the cGAMP delivery instead of protecting cGAMP from enzymatic degradation. *P<0.05, **P<0.01, ***P<0.001, ****P<0.0001. Values = mean ± SEM, n=4.

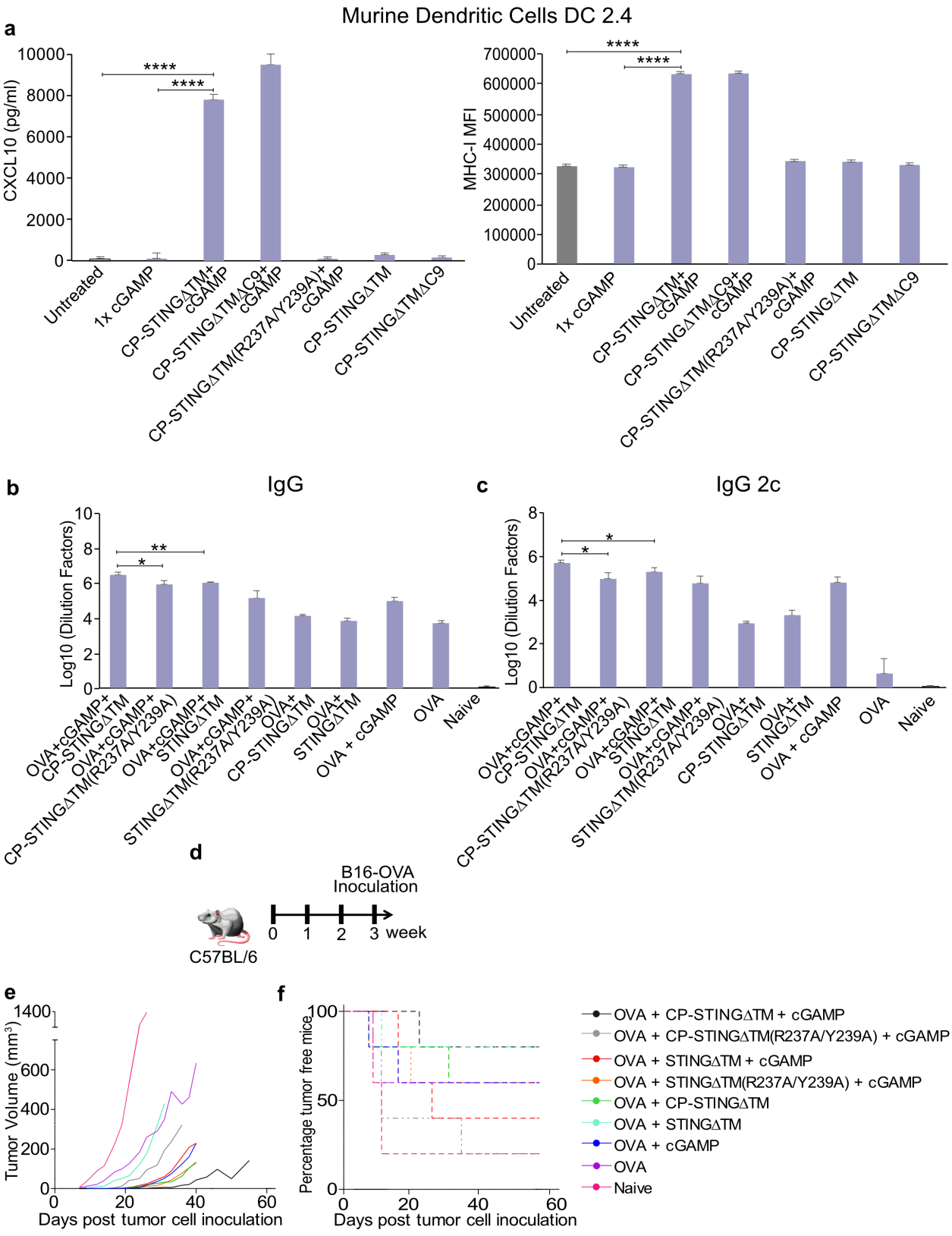


Figure 4. **CP-STINGΔTM enhances the efficacy of cGAMP as an adjuvant**. (**a**) In murine dendritic cells DC 2.4, "40 μg/ml CP-STINGΔTM + 1 μg/ml cGAMP" markedly

induced CXCL10 expression as evidenced by ELISA as well as upregulated surface expression of MHC-I measured by flow cytometry. Levels of OVA-specific total IgG (**b**) and the type I IFN-associated subtype IgG2c (**c**) in groups of C57BL/6 mice (n=5). Mice were immunized with OVA alone, or OVA mixed with 1 μg/ml free cGAMP or combinations of 40 μg/ml STINGΔTM variants with or without 1 μg/ml cGAMP on days 0 and 14 via tail-based injection. On days 21, sera from different vaccination combinations were collected for OVA-specific total IgG and IgG2c quantification. On day 21, the same cohort of mice were challenged with 1 million B16-OVA (257-264aa) subcutaneously. Data of overall tumor growth (**d**), with survival rate (**e**) at the end of the study were denoted. Values are reported as mean ± SEM. Statistical analysis was performed by one-way ANOVA according to the scales of *P<0.05, **P<0.01, ***P<0.001, and ****P<0.0001.

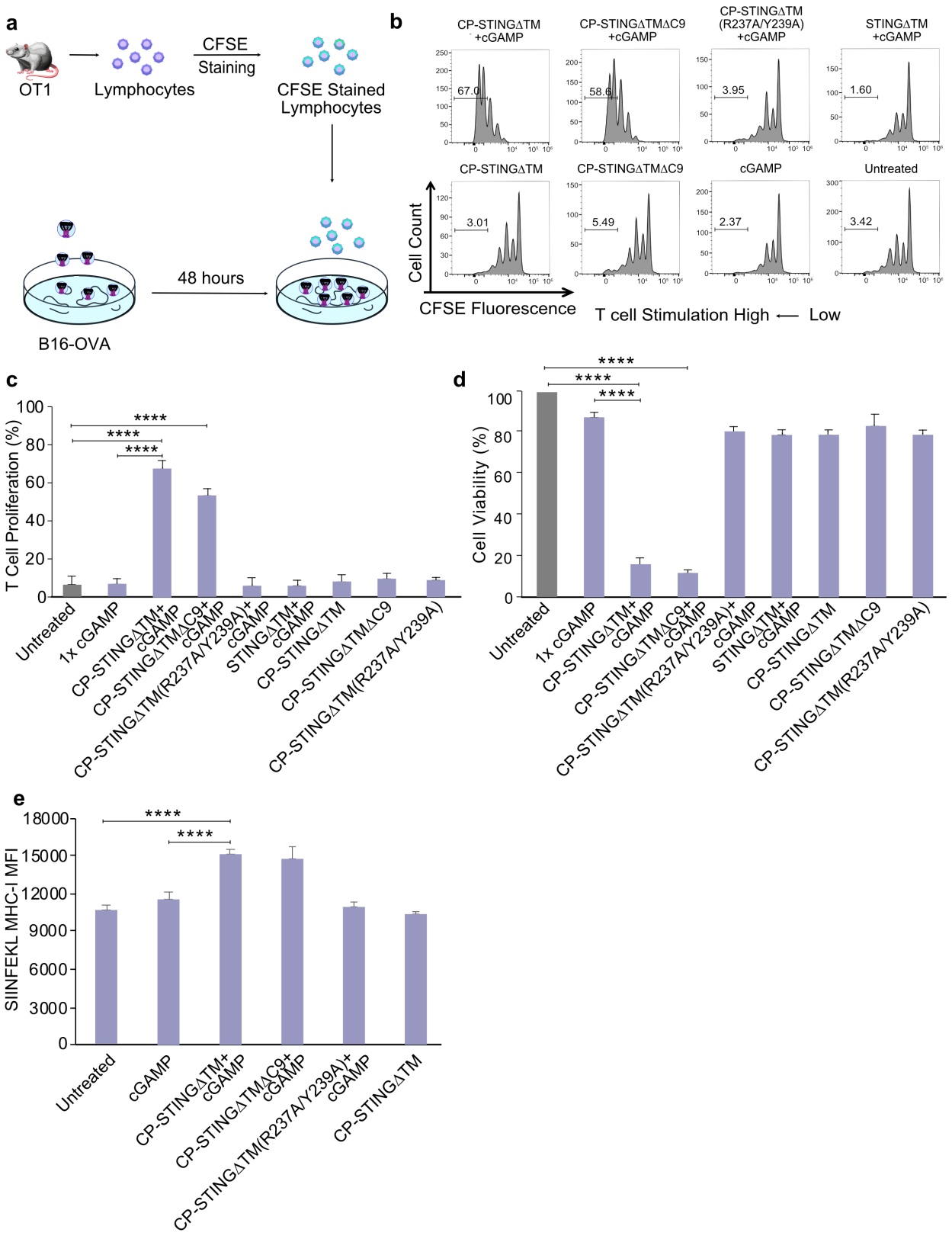


Figure 5. ***Ex vivo*** **T cell-mediated cancer cell killing after activating the STING pathway in tumor cells**. **(a)** CFSE-labeled OT1 cells were added into B16-OVA (257-

264aa) cells that were pretreated with cGAMP plus indicated STINGΔTM variants for 48 hours (~10:1 ratio of effector T cell to tumor cells). Proliferated T cells were assayed five days later. **(b)** Representative CFSE flow cytometry data from one of four independent experiments are displayed. **(c)** Quantification of T cell proliferation by CFSE staining. While the pretreatment groups “40 μg/ml CP-STINGΔTM + 1 μg/ml cGAMP” and “40 μg/ml CP-STINGΔTMΔC9 + 1 μg/ml cGAMP” promoted T cell proliferation, the variants with deficiency in cGAMP binding or cell penetration did not. **(d)** OT1-mediated cancer cell killing. B16-OVA (257-264aa) that had been pretreated with indicated STING variants plus cGAMP for 48 hours, were cocultured with OT1 cells. After five days, nonadherence T cells were removed by washing, and the viability of adherent tumor cells was assessed by the MTT assay. Experiments were repeated three times. **(e)** Upregulation of SIINFEKL-restricted MHC-I on the surface of B16-OVA (257-264aa). After treating tumor cells with 1 μg/ml cGAMP and 40 μg/ml STING variants for 48 hours, only “40 μg/ml CP-STINGΔTM + 1 μg/ml" cGAMP and “40 μg/ml CP-STINGΔTMΔC9 + 1μg/ml cGAMP” upregulated the expression of SIINFEKL-restricted MHC-I. Graphs are expressed as mean ± SEM (n=4) and statistical analysis by one-way ANOVA according to the following scale: *P<0.05, **P<0.01, ***P<0.001, and ****P<0.0001.

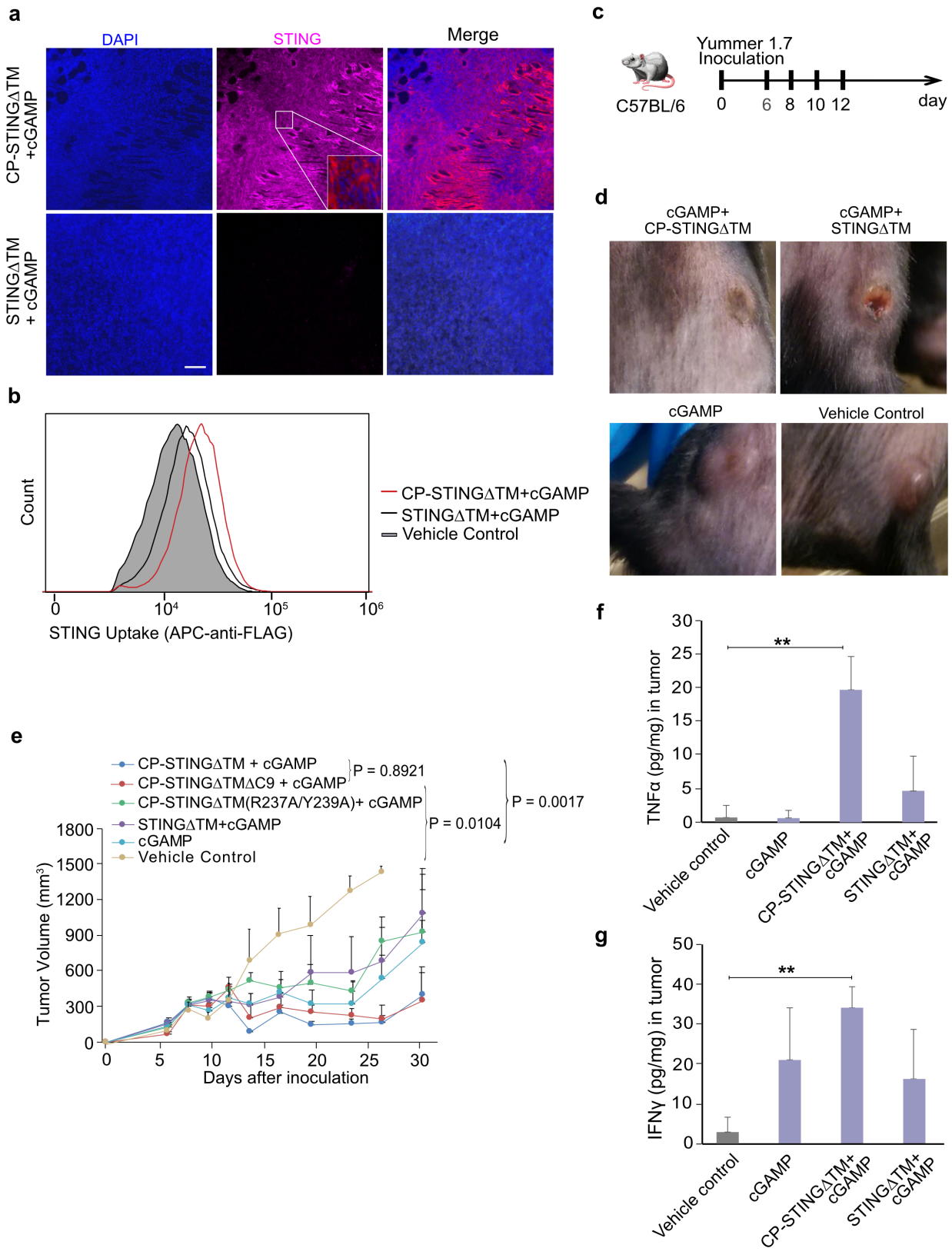

a
DAPI
STING
Merge
CP-STINGΔTM +cGAMP
STINGΔTM + cGAMP
b
Count
CP-STINGΔTM+cGAMP
STINGΔTM+cGAMP
Vehicle Control
STING Uptake (APC-anti-FLAG)
c
Yummer 1.7
Inoculation
C57BL/6
0 6 8 10 12
day
d
cGAMP+ CP-STINGΔTM
cGAMP+ STINGΔTM
cGAMP
Vehicle Control
e
CP-STINGΔTM + cGAMP
CP-STINGΔTMΔC9 + cGAMP
CP-STINGΔTM(R237A/Y239A)+ cGAMP
STINGΔTM+cGAMP
cGAMP
Vehicle Control
P = 0.8921
P = 0.0104
P = 0.0017
Tumor Volume (mm3)
Days after inoculation
f
TNFα (pg/mg) in tumor
**
Vehicle control
cGAMP
CP-STINGΔTM+ cGAMP
STINGΔTM+ cGAMP
g
IFNγ (pg/mg) in tumor
**
Vehicle control
cGAMP
CP-STINGΔTM+ cGAMP
STINGΔTM+ cGAMP

Figure 6. **Combining CP-STINGΔTM/cGAMP and anti-PD-1 in a syngeneic mouse melanoma model**. Groups of C57BL/6 mice were inoculated with 1 million YUMMER1.7 melanoma cells in the flank and when tumors reached ~150 mm^3, mice were treated with intraperitoneal injection of anti-PD-1 (200 μg per mouse) and concurrently with intratumoral injection of "100 μg/ml CP-STINGΔTM + 2.5 μg/ml cGAMP" (n = 5), "100 μg/ml CP-STINGΔTMΔC9 + 2.5 μg/ml cGAMP" (n=5), "100 μg/ml CP-STINGΔTM(R237A/Y239A) +cGAMP" (n=5), "2.5 μg/ml cGAMP only" (n=5), and vehicle control (n= 4) (**c**). Cellular uptake of CP-STINGΔTM (n=2) was evaluated with (**a**) microscopic imaging and (**b**) flow cytometry. (**d**) Photos for acute responses for the treatment were taken 72 hours after treatment. (**e**) Overall tumor growth curves were measured using clipper, and tumor volume was calculated using formulations V = (L x W x W)/2, where V is tumor volume, L is tumor length, and W is tumor width. Expression of TNF-alpha (**f**) and IFN-gamma (**g**) induced by various treatment groups (n=3) was quantified by ELISA. Statistical analysis was performed by one-way ANOVA: *P<0.05, **P<0.01.

REFERENCES

1. Ahn J, Barber GN. STING signaling and host defense against microbial infection. Exp Mol Med 2019;**51**:1-10.

2. Pollock AJ, Zaver SA, Woodward JJ. A STING-based biosensor affords broad cyclic dinucleotide detection within single living eukaryotic cells. Nature Communications 2020;**11**:3533.

3. Kwon J, Bakhoum SF. The cytosolic DNA-sensing cGAS-STING pathway in cancer. Cancer Discov 2020;**10**:26–39.

4. Ramanjulu JM, Pesiridis GS, Yang J, Concha N, Singhaus R, Zhang S-Y, et al. Design of amidobenzimidazole STING receptor agonists with systemic activity. Nature 2018;**564**:439–43.

5. Corrales L, Glickman LH, McWhirter SM, Kanne DB, Sivick KE, Katibah GE, et al. Direct Activation of STING in the Tumor Microenvironment Leads to Potent and Systemic Tumor Regression and Immunity. Cell Reports 2015;**11**:1018–30.

6. Hanson MC, Crespo MP, Abraham W, Moynihan KD, Szeto GL, Chen SH, et al. Nanoparticulate STING agonists are potent lymph node-targeted vaccine adjuvants. J Clin Invest 2015;**125**:2532–46.

7. Shae D, Becker KW, Christov P, Yun DS, Lytton-Jean AKR, Sevimli S, et al. Endosomolytic polymersomes increase the activity of cyclic dinucleotide STING agonists to enhance cancer immunotherapy. Nat Nanotechnol 2019;**14**:269–78.

8. Li L, Yin Q, Kuss P, Maliga Z, Millán JL, Wu H, et al. Hydrolysis of 2'3'-cGAMP by ENPP1 and design of nonhydrolyzable analogs. Nat Chem Biol 2014;**10**:1043–8.

9. Lu X, Miao L, Gao W, Chen Z, McHugh KJ, Sun Y, et al. Engineered PLGA microparticles for long-term, pulsatile release of STING agonist for cancer immunotherapy. Science Translational Medicine 2020;**12**:eaaz6606

10. Park KS, Xu C, Sun X, Louttit C, Moon JJ. Improving STING Agonist Delivery for Cancer Immunotherapy Using Biodegradable Mesoporous Silica Nanoparticles. Advanced Therapeutics 2020;**3**:2000130.

11. Wehbe M, Wang-Bishop L, Becker KW, Shae D, Baljon JJ, He X, et al. Nanoparticle delivery improves the pharmacokinetic properties of cyclic dinucleotide STING agonists to open a therapeutic window for intravenous administration. J Control Release 2020;**330**:1118-29

12. He Y, Hong C, Yan EZ, Fletcher SJ, Zhu G, Yang M, et al. Self-assembled cGAMP-STINGΔTM signaling complex as a bioinspired platform for cGAMP delivery. Science Advances 2020;**6**:eaba7589.

13. Beaulieu M-E, Jauset T, Massó-Vallés D, Martínez-Martín S, Rahl P, Maltais L, et al. Intrinsic cell-penetrating activity propels Omomyc from proof of concept to viable anti-MYC therapy. Science Translational Medicine. 2019; **11**:eaar5012

14. Junkins RD, Gallovic MD, Johnson BM, Collier MA, Watkins-Schulz R, Cheng N, et al. A robust microparticle platform for a STING-targeted adjuvant that enhances both humoral and cellular immunity during vaccination. J Control Release. 2018;**270**:1–13.

15. Wang-Bishop L, Wehbe M, Shae D, James J, Hacker BC, Garland K, et al. Potent STING activation stimulates immunogenic cell death to enhance antitumor immunity in neuroblastoma. J Immunother Cancer 2020;**8**:e000282.

16. Patel SA, Minn AJ. Combination Cancer Therapy with Immune Checkpoint Blockade: Mechanisms and Strategies. Immunity. 2018;**48**:417–33.

17. Ergun SL, Fernandez D, Weiss TM, Li L. STING Polymer Structure Reveals Mechanisms for Activation, Hyperactivation, and Inhibition. Cell. 2019;**178**:290-301.e10.

18. Ergun SL, Li L. Structural Insights into STING Signaling. Trends in Cell Biology. 2020;**30**:399–407.

19. Tanaka Y, Chen ZJ. STING Specifies IRF3 Phosphorylation by TBK1 in the Cytosolic DNA Signaling Pathway. Sci Sig. 2012;**5**:ra20–ra20.

20. Zhao B, Du F, Xu P, Shu C, Sankaran B, Bell SL, et al. A Conserved PLPLRT/SD Motif of STING Mediates the Recruitment and Activation of TBK1. Nature 2019;**569**:718–22.

21. Zhang C, Shang G, Gui X, Zhang X, Bai X, Chen ZJ. Structural basis of STING binding with and phosphorylation by TBK1. Nature 2019;**567**:394–8.

22. Zhang X, Shi H, Wu J, Zhang X, Sun L, Chen C, et al. Cyclic GMP-AMP Containing Mixed Phosphodiester Linkages Is An Endogenous High-Affinity Ligand for STING. Molecular Cell 2013;**51**:226–35.

23. Shang G, Zhang C, Chen ZJ, Bai X, Zhang X. Cryo-EM structures of STING reveal its mechanism of activation by cyclic GMP–AMP. Nature 2019;**567**:389–93.

24. Kitajima S, Ivanova E, Guo S, Yoshida R, Campisi M, Sundararaman SK, et al. Suppression of STING Associated with LKB1 Loss in KRAS-Driven Lung Cancer. Cancer Discov 2019;**9**:34–45.

25. Preta G, Cronin JG, Sheldon IM. Dynasore - not just a dynamin inhibitor. Cell Communication and Signaling. 2015;**13**:24.

26. Xia T, Konno H, Ahn J, Barber GN. Deregulation of STING Signaling in Colorectal Carcinoma Constrains DNA Damage Responses and Correlates With Tumorigenesis. Cell Rep 2016;**14**:282–97.

27. Sistigu A, Yamazaki T, Vacchelli E, Chaba K, Enot DP, Adam J, et al. Cancer cell-autonomous contribution of type I interferon signaling to the efficacy of chemotherapy. Nat Med 2014;**20**:1301–9.

28. Galluzzi L, Buqué A, Kepp O, Zitvogel L, Kroemer G. Immunogenic cell death in cancer and infectious disease. Nature Reviews Immunology 2017;**17**:97–111.

29. Falahat R, Perez-Villarroel P, Mailloux AW, Zhu G, Pilon-Thomas S, Barber GN, et al. STING Signaling in Melanoma Cells Shapes Antigenicity and Can Promote Antitumor T-cell Activity. Cancer Immunol Res 2019;**7**:1837–48.

30. Xia T, Konno H, Barber GN. Recurrent Loss of STING Signaling in Melanoma Correlates with Susceptibility to Viral Oncolysis. Cancer Res 2016;**76**:6747–59.

31. Li T, Chen ZJ. The cGAS–cGAMP–STING pathway connects DNA damage to inflammation, senescence, and cancer. J Exp Med 2018;**215**:1287–99.

32. Wang J, Li P, wu MX. Natural STING agonist as an “ideal” adjuvant for cutaneous vaccination. J Invest Dermatol 2016;**136**:2183–91.

33. Volckmar J, Knop L, Stegemann-Koniszewski S, Schulze K, Ebensen T, Guzmán CA, et al. The STING activator c-di-AMP exerts superior adjuvant properties than the formulation poly(I:C)/CpG after subcutaneous vaccination with soluble protein antigen or DEC-205-mediated antigen targeting to dendritic cells. Vaccine 2019;**37**:4963–74.

34. Budhu S, Schaer DA, Li Y, Toledo-Crow R, Panageas K, Yang X, et al. Blockade of surface-bound TGF-b on regulatory T cells abrogates suppression of effector T cell function in the tumor microenvironment. Sci Sig. 2017;**10:**eaak9702.

35. Wang J, Perry CJ, Meeth K, Thakral D, Damsky W, Micevic G, et al. UV-induced somatic mutations elicit a functional T cell response in the YUMMER1.7 mouse melanoma model. Pigment Cell Melanoma Res 2017;**30**:428–35.

36. Jin Q, Zhu W, Zhu J, Zhu J, Shen J, Liu Z, et al. Nanoparticle-Mediated Delivery of Inhaled Immunotherapeutics for Treating Lung Metastasis. Advanced Materials 2021;**33**:2007557.

37. Duan Q, Zhang H, Zheng J, Zhang L. Turning Cold into Hot: Firing up the Tumor Microenvironment. Trends in Cancer 2020;**6**:605–18.

38. Li Y, Su Z, Zhao W, Zhang X, Momin N, Zhang C, et al. Multifunctional oncolytic nanoparticles deliver self-replicating IL-12 RNA to eliminate established tumors and prime systemic immunity. Nature Cancer 2020;**1**:882–93.

39. Barber GN. STING: infection, inflammation and cancer. Nat Rev Immunol 2015;**15**:760–70.

40. Song S, Peng P, Tang Z, Zhao J, Wu W, Li H, et al. Decreased expression of STING predicts poor prognosis in patients with gastric cancer. Sci Rep 2017;**7**:39858

41. Ritter JL, Zhu Z, Thai TC, Mahadevan NR, Mertins P, Knelson EH, et al. Phosphorylation of RAB7 by TBK1/IKKε Regulates Innate Immune Signaling in Triple-Negative Breast Cancer. Cancer Res 2020;**80**:44–56.

42. Pantelidou C, Sonzogni O, Taveira MDO, Mehta AK, Kothari A, Wang D, et al. PARP Inhibitor Efficacy Depends on CD8+ T-cell Recruitment via Intratumoral STING Pathway Activation in BRCA-Deficient Models of Triple-Negative Breast Cancer. Cancer Discov 2019;**9**:722–37.

43. Xie YJ, Dougan M, Jailkhani N, Ingram J, Fang T, Kummer L, et al. Nanobody-based CAR T cells that target the tumor microenvironment inhibit the growth of solid tumors in immunocompetent mice. Proc Natl Acad Sci U S A 2019;**116**:7624–31.

DELIVERY STRATEGIES FOR STING AGONISTS

Xin Sun[1], Ian Hay[1], Peter Doran[1], Shreya Basireddy[1], Myria Scott[1], Yuqianxun Wu[1], Amal A Al-Dossary[2], Jiahe Li[*]

[1]Department of Bioengineering, Northeastern University, Boston, MA, 02115, United States.

[2]Department of Basic Sciences, Imam Abdulrahman Bin Faisal University, Dammam 34212, Saudi Arabi

[*]Correspondence:

Department of Bioengineering, Northeastern University, Boston, MA, 02115, United States. Email: jiah.li@northeastern.edu. Phone: 1-617-373-3233

1.The fundamentals of STING biology

1.1 Structure biology of STING

1.2 STING signaling in innate and adaptive immunities

1.2.1 Type I IFN pathway

1.2.2 NF-κB signal pathway

1.2.3 Autophagy pathway

1.3 The STING signaling in tumor biology

1.3.1 Colorectal cancer

1.3.2 Breast cancer

1.3.3 NSCLC

1.3.4 Melanoma

2. STING-activation in cancer immunotherapy and vaccine adjuvant

2.1. STING agonists and their transporter

2.1.1 STING agonists

2.1.2 cGAMP transporter

2.2. Delivery strategies of STING agonists for cancer immunotherapy

2.2.1. Direct intratumoral injection of free cGAMP

2.2.2 Delivery platform based on cGAMP charges for enhanced cancer immunotherapy

2.2.4 STING Agonists delivered by liposome to enhance immune cancer therapy

2.2.5 A bioinspired cGAMP delivery strategy based on cGAMP-STINGΔTM complex

2.2.6 Silica microspheres coated by lipid as STING agonists and T cells codelivery platform

2.3. STING agonists as vaccine adjuvants

2.3.1. STING Agonist as an adjuvant for cutaneous vaccination

2.3.2. Encapsulated STING agonists as robust lymph node-targeting vaccine adjuvants

2.3.3. Microparticle-encapsulated cGAMP as an adjuvant formulation

Abstract

Activation of the stimulator of interferon genes (STING) pathway through cyclic dinucleotides (CDNs) has been explored extensively as potent vaccine adjuvants against infectious diseases as well as to increase tumor immunogenicity towards cancer immunotherapy in tumors. Despite the promise of CDNs as immune adjuvants, they suffer from several limitations: **(1)** CDNs exhibit fast clearance from the injection site, which may induce systemic toxicity, **(2)** naturally derived CDNs are susceptible to enzymatic degradation, which can lower the efficacy of adjuvanticity potential, and **(3)** CDNs have inefficient intracellular transport properties due to limited endosomal escape or reliance on the expression of a specific transporter protein. To address these challenges, over the last decade, a myriad of synthetic vehicles, including liposomes, polymers, and other nanoparticle platforms, have been developed to improve the bioavailability and therapeutic efficacy of STING agonists in preclinical mouse models. In this review, we will first summarize recent progress in the fundamental biology of the STING pathway in cancer and immunology, and then review advances in developing new STING agonist compounds and delivery strategies to overcome many challenges in the field.

1.The fundamentals of STING biology

1.1 Structure biology of STING

STING (stimulator of interferon genes, encoded by TMEM173, also known as MITA, ERIS, MPYS) is a protein located in the endoplasmic reticulum (ER) widely expressed in immune and non-immune cells[1]. As a signaling protein, STING plays a pivotal role in microbial infections, cancer, and autoimmune diseases[2]. Human STING is composed of a N-terminal transmembrane with four putative motifs (1-154 amino acids), which anchor the STING to ER; a central globular domain (155-341 amino acids) for CDN binding, and a cytoplasmic C-terminal tail (CTT, 324-379 amino acids) required for IFN regulatory factor 3 (IRF3) activation[3, 4]. The CDN-binding domain (CBD) in STING features an α + β fold as a butterfly shape dimer when no ligands are bound (also known as "apo")[5, 6]. In the ligand-bound state, however, the central crevice of the hydrophobic STING dimer interface symmetrically sandwiches a CDN, and a sheet-like lid consisting of four antiparallel β-strands caps the CBD[7]. Therefore, the binding of CDN to STING triggers an open-to-closed conformational change at the STING CBD region[8].

Although STING orthologues in most species are generally similar, the structures and mechanisms of STING across species are not identical[10]. For example, the structures of apo mouse and human orthologues proteins (i.e., mSTING and hSTING) share a 68% sequence identity and an 81% amino acid similarity[3], the apo hSTING is in an 'open' dimer conformation and 'closed' upon binding with cGAMP while apo mSTING is in a 'closed' shape. Additional STING differences across species can be observed in the case of the molecule 5,6-dimethylxanthenone-4-acetic acid (DMXAA). In xenografted mouse models, DMXAA enabled immune modulatory activities by inducing cytokines and disrupting tumor vascularization[11]. However, DMXAA ultimately failed as a drug candidate in human phase III trials against non-small-cell lung cancer (NSCLC) despite showing promising results when combined with paclitaxel and carboplatin in a clinical phase II trial. This failure is attributed to differences between mSTING and hSTING—mSTING can recognize DMXAA but hSTING fails to do so[12]. Similarly, porcine STING has its distinct mechanism including its ligand binding preference. For example, porcine STING possesses slightly asymmetric binding pockets, which prefer recognizing asymmetric CDNs such as cGAMP, and this mechanism explains why porcine STING has a higher binding affinity for cGAMP than cyclic di-GMP[12]. In crystalized cGAMP- and c-di-AMP-bound structures, hSTING can form a polymeric structure characterized by elongated rows of packed STING dimers[4]. Likewise, cryogenic electron microscopy (cryo-EM) reveals higher-order multimers of the full-length chicken STING, which can

undergo a conformational change upon ligand binding[6]. The connecting region between the soluble C-terminal domain (CTD) and the N-terminal transmembrane domain is crossed when the ligand is not bound to hSTING[13], while a twisting reorientation is speculated to facilitate STING polymerization upon ligand binding. Mechanistically, in the ligand bound state, the uncrossing of the connecting region allows the 148th cysteine (C148) from neighboring dimers to form disulfide bonds and therefore stabilize the STING polymer[4].

Single and multiple amino acid mutations of STING have been shown to affect its dimerization capability, ligand binding capacity, and post-translational modifications through regulatory proteins[14-16]. For example, the R231H mutant of mSTING (corresponding to R232A or R232H in hSTING) responded poorly to cyclic di-GMP with open conformation upon crystallization, indicating the importance of this amino for responding to CDNs in m- and hSTING[10]. The other substitution, G230A, located in the linker region, is also required to restore the responsiveness to CDNs with residue R232[5]. Intriguingly, wild-type STING also binds c-di-AMP in closed conformation, which suggests that adenosine assists the closing of the STING dimer. Since c-di-GMP enables hSTING activation, closing of the hSTING dimer is essential for STING activation. Certain mutations in STING can inactivate its ability to bind with c-di-GMP. For instance, R238A mutation in hSTING (corresponding to R237A in mSTING) influences the connection between the c-di-GMP phosphate group and the side chain of R238 that abolishes the hydrophobic interplay between the side chain of the Y240 and c-di-GMP guanine base groups. Moreover, Y240A (Y239A in mSTING) induces an identical effect. Although D210A (D209A in mSTING) mutation does not affect the c-di-GMP binding site, it impacts the configuration of the lid region, as the side chain of D210 forms a hydrogen bond with the main chain amino group of A233 from the lid region if c-di-GMP is bound. Mutations of Q266A (Q265A in mSTING) and R232A (R231A in mSTING) affect the hydrogen bond formation between the Q266 side chain and R232 from the lid region[17]. While dimerization-deficient mutation of G158L partially hinders STING's role in IFN induction, point mutation of V155R, W161A, and Y164A fully exterminate STING's ability in IFN induction, which demonstrates the importance of STING dimerization[13]. Notably, three gain-of-function point mutations in the linker region around C148 of STING cause severe autoimmune syndromes, constitutive activation of STING, and hypersensitivity to ligand stimulation[18]. Thus, the uncrossing of the STING linker regions and

STING polymer stabilization via the formation of disulfide bridges may serve as models for understanding intracellular hyperactivity. hSTING is post-translationally modified by palmitoylation at the thiol groups of C88 and C91, especially after undergoing ligand binding. Inhibition in palmitoylation at C88/91 in both m- and hSTING abolishes STING signaling, which could present a promising treatment strategy for cytosolic DNA-triggered autoinflammatory diseases[19, 20]. While it is not fully understood how palmitoylation assists STING signaling, it is possible that it helps STING polymerization as STING palmitoylation inhibitors also inhibit polymerization.

1.2 STING signaling in innate and adaptive immunities

Innate immunity is essential for defense against microbial infection. Hosts with intact innate immunities can recognize microbial pathogen-associated molecular patterns (PAMPs) through pattern recognition receptors (PRRs) in immune cells and subsequently generate and secrete IFNs and cytokines to stimulate and activate the adaptive immune response[21]. STING represents one type of PRR located in the cytosol that can sense bacterial or aberrant host DNA in the cytoplasm, and trigger the Type I IFN production[22]. It is an essential step in activating innate and adaptive immune responses and is also a critical component of the anticancer immune response[2]. In contrast to STING, Toll-like receptors (TLRs) are another type of PRRs[23], and there are several members in the TLR family, each of which is responsible for recognizing different PAMPs. For example, TLR3, TLR7, and TLR9 recognize double-strand RNA (dsRNA), single-strand RNA (ssRNA) and CpG DNA, while TLR1, TLR2, TLR4, and TLR5 recognize bacterial lipopeptides, peptidoglycan, lipopolysaccharide (LPS), and flagellin. In addition to STING and TLRs, NOD-like receptors (NLRs) are responsible for recognizing bacterial cell-wall lipids and products from damaged host cells while the RIG-like receptors (RLR) are responsible for recognizing viral RNA[24].

1.2.1 Type I IFN pathway

The activation of STING triggers the production of Type I IFNs via STING-TANK-binding kinase 1(TBK1)-IRF3 signaling axis. There are 16 subgroups of type I IFN including 12 IFN-α subtypes, IFN-β, IFN-ε, IFN-κ, and IFN-ω. All type I IFNs are involved in antiviral immunity[25]. Type I IFNs promote the

activation and functional maturation of dendritic cells (DCs)—thereby facilitating antigen presentation to $CD4^+$ T cells, and antigen cross-presentation to $CD8^+$ T cells[26]. While the mechanism that controls these processes is not fully understood, it is plausible that DCs engulf necrotic tumor cells that allow the tumor cell-derived DNA to trigger STING signaling in DCs[27]. The resultant type I IFNs, via paracrine or autocrine, could trigger the production of additional cytokines in DCs to facilitate antigen presentation to $CD4^+$ T cells and antigen cross-presentation to $CD8^+$ T cells to bolster antitumor T cell responses[2829]. The STING signaling pathway is essential for antitumor T cell responses and radiation-induced antitumor T cell responses[30]. In contrast, STING-deficient mice fail to exhibit antitumor T cell immunity, and these mice are highly susceptible to tumor growth. Furthermore, the STING pathway augment the therapeutic efficacy of the immune checkpoint inhibitors (ICIs) against cancer, while STING-deficient mice responded poorly to ICIs[31].

1.2.2 NF-κB signal pathway

In addition to the STING-TBK1-IRF3 signaling axis, STING can also operate via the NF-κB pathway. Specifically, upon STING activation, NF-κB can be activated by the IκB kinase (IKK) complex, which is composed of kinase IKKα and IKKβ and the regulatory subunit IKKγ (also known as NEMO for NF-κB essential modulator). IKKβ is essential for cytokine production via NF-κB activation, and IKKα is involved in TLR7/9-induced type I IFN production via IRF1/3 activation. Activated IKKβ is required for NF-κB and TBK1-IRF3 activation[32]. Ultimately, these events lead to phosphorylation NF-κB, which can translocate to the nucleus and forms a positive-feedback loop for robust cytokine production during cGAS-STING activation [33].

1.2.3 Autophagy pathway

Autophagy and the signaling proteins associated with autophagy correlate with inflammatory disorders, cancer, and autoimmune diseases such as sclerosis and systemic lupus erythematosus (SLE)[34]. Defective autophagy can also result in protein accumulation, which can cause neurological disorders like Parkinson's diseases[35]. While most research on the cGAS-STING pathway has focused on the type I IFN induction, less attention has been paid to STING in autophagy and cell-death[36]. Specifically, the STING-mediated autophagy facilitates the elimination of intracellular microorganisms, subcellular

organelles, misfolded proteins, and the ER that loads the STING signalosome. The STING-mediated autophagy also plays a critical role in removing cytosolic DNA and inflammatory signaling factors, which are responsible for controlling the inflammatory responses. For example, the pathway plays a critical role in inducing autophagy during *M. tuberculosis infection*. Mechanistically, STING can translocate from the ER to the Golgi by an autophagy-like process that depends on Autophagy-related protein 9 (ATG9)[37]. ATG9 and lipidation of light chain3 (LC3) are responsible for autophagosome genesis and elongation[38]. However, excessive signaling of the autophagy cascade can cause irreversible apoptosis termed “autophagic cell death” [39]. Specifically, autophagy can function as a negative feedback loop that promotes a transient cGAS-STING signaling while preventing constant over-reaction of the pathway[40]. Thus, the impairment of autophagy can cause destructive inflammatory diseases[41].

1.3 The STING signaling in tumor biology

While the STING signaling pathway was initially identified to protect the host from antibacterial and antiviral infections [42, 43], recent evidence has shown a crucial role of STING in generating a spontaneous antitumor T cell response in the tumor microenvironment (TME) [44]. Activation of the STING pathway in the TME can augment dendritic cell maturation and the production of type I interferons (IFNs) and other cytokines, which elicit robust antitumor T cell responses and overcome resistance against immunosuppressive signals (**Figure 1**). These studies have motivated the development of STING agonists as a new class of therapeutic to make “cold” tumors “hot” [44-47]. Mechanistically, exogenously administered STING agonists such as CDNs activate innate immune cells to produce IFNs, and more recently, tumor vasculature endothelial cells were identified as another source of IFNs upon CDN delivery, as these cell types naturally express the CDN receptor STING [48-51]. However, tumor cells can often evade the host's immune recognition through elaborate mechanisms involving tumor cell-intrinsic events. One mechanism that impedes efficacious anti-tumor immune responses is silencing of the expression of stimulator of interferon genes (STING) in tumor cells[52]. Here, we discuss a few cancers in which the STING signaling is suppressed to promote immune surveillance.

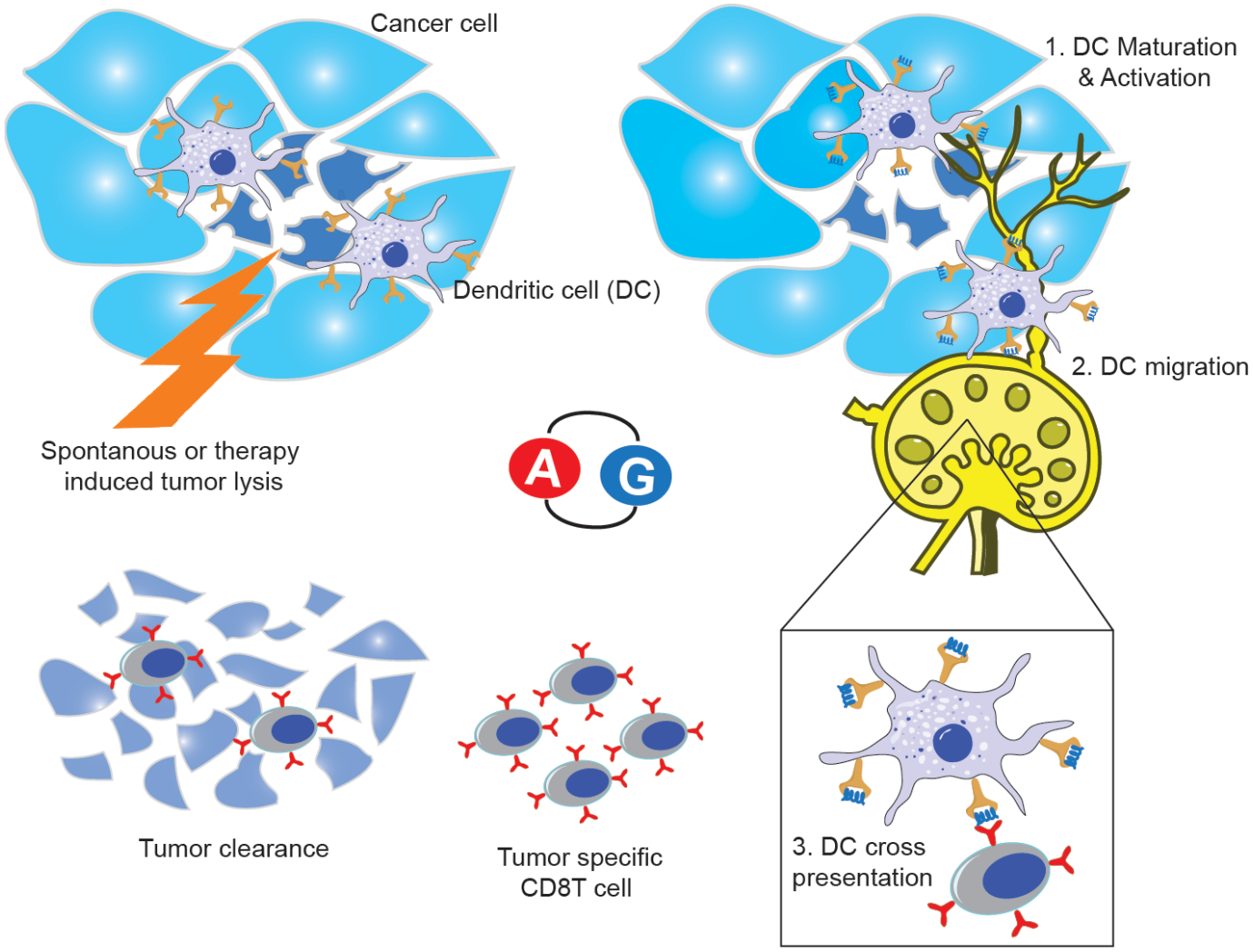


Figure 1. The cGAS-STING signaling pathway is profound at sensing neoplastic progression by promoting type I IFN production and initiating cytotoxic T cell-mediated anti-tumor immune response. Upon detecting cytosolic DNA from tumor cells, the intracellular nucleic acid sensor cGAS catalyzes the productions of cGAMP, which functions as a second messenger to bind the adaptor protein STING to initiate Type I IFN production and boost DC maturation and T cell infiltration.

1.3.1 Colorectal cancer

Colorectal cancer (CRC) is the second leading cause of cancer death in the United States in 2020. Even though death rates of CRC have declined in patients aged above 65 years annually since 2008, the 5-year survival rate remains 14% after stage IV[53]. Despite the impressive progress made on CRC treatment strategies, the genetic heterogeneity of CRC among patients still causes therapeutic discrepancies. Considering that the barely-immunogenic tumor cells and the immunosuppressive TME

significantly reduce the CRC immunotherapeutic efficacy, a deeper understanding of the immunologic characteristics of CRC and identification of novel immune targets are necessary to overcome the obstacles and elicit optimal immunity against CRC[54]. Through the immunohistochemical staining and RNA analysis of paraffin-embedded samples from colon adenocarcinoma patients, a significant loss of the STING expression was observed in later stages of diseases starting from stage II with a more profound reduction of STING expression in the most advanced lesions. By examining 11 human colorectal adenocarcinoma cell lines, Xia *et al*. found that dsDNA treatment led to lower levels of IFN-beta production in cancer cells than those in normal colon epithelial cells[55]. Despite none of the cell lines had major mutations in STING or cGAS encoding genes, only four cell lines exhibited STING trafficking or phosphorylation after incubation with dsDNA[52]. CRC patients with high STING expression in their tumors were also found to have favorable prognosis and longer survival rates than those with low STING expression[54]. Considering that $CD8^+$ TILs are highly accumulated in STING-upregulated CRCs, and that STING is vital for T-cell priming and activation, intratumoral STING expression could be a useful immune biomarker identifying T-cell-inflamed cancers.

1.3.2 Breast cancer

The cGAS/STING pathway can be activated to promote proinflammatory cytokine production in triple-negative breast cancer (TNBC) deficient for the DNA damage response. For example, STING-dependent signaling in TNBC is activated via poly ADP ribose polymerase (PARP) inhibition, which promotes the recruitment of $CD8^+$ T cells in a *BRCA1*- and *p53*-deficient genetically engineered mouse model (GEMM) of TNBC. The antitumor immune response, however, is reduced in $CD8^+$ T-cell depletion models[56]. Meanwhile, in a study of topoisomerase I (TOP1) inhibitor treatment using the E0771 breast cancer cell line, cGAMP was secreted to induce DC maturation and cytokine production, while these effects were abrogated in mice lacking STING expression[57]. Additionally, endothelial STING expression is relevant to enhanced T cell infiltration in breast cancer, from which distinct STING expressions in tumor endothelial cells were found[58]. Combined with Vascular endothelial growth factor receptor 2 (VEGFR2) and programmed cell death protein-1 (PD-1) inhibition, the administration of the STING agonist can effectively inhibit tumor progression and metastasis through vascular normalization.

1.3.3 NSCLC

Recent clinical trial data from NSCLC report unprecedented improvements in overall survival and progression-free survival when ICIs, anti-PD-1 or anti–programmed death ligand 1 (anti-PD-L1), are used in neoadjuvant or first-line therapy[59]. Since STING activation is correlated with elevated levels of intrinsic DNA damage, targetable immune checkpoints, and chemokines in immedicable and relapsed lung adenocarcinoma, STING pathway activation is hypothesized to correlate with antitumor immunity in NSCLC[60]. STING activation can be downregulated by genetic mutations and/or direct epigenetic silencing of either STING or cGAS. For instance, the Kirsten rat sarcoma gene (KRAS)- and Liver Kinase B1 (LKB1)-mutated NSCLC subtype epigenetically silenced STING and cGAS expression. As a result, loss of STING-cGAS signaling in cancer cells fail to induce robust antitumor immune responses[61]. On the contrary, STING activation has been observed to promote the proliferation and chemo-resistance of brain metastatic cells in NSCLC cells. Particularly, astrocyte gap-junctional networks, responsible for translocating cGAMP to astrocytes, are found in brain metastatic cancer cells, resulting in STING activation in astrocytes and inflammatory cytokines[62]. The inflammatory cytokines elicit the signal transducer and activator of transcription 1 (STAT1) and NF-κB pathways in brain metastatic cells, which induces tumor proliferation and chemoresistance. Furthermore, immune dysfunction is induced through extended IFN-I signaling. Overall, the double-sword function of STING activation may influence the balance between antitumor immune responses and the immune surveillance escape of cancer.

1.3.4 Melanoma

STING silencing has been observed in 23.2% of early-stage melanoma samples and 41.7% of the advanced metastatic disease[52]. Due to the occurrence of spontaneous $CD8^+$ T-cell responses that result in tumor regressions and the identification of $CD8^+$ T cells that recognize melanoma antigens, melanoma is recognized as a prototypical immunogenic tumor. Despite immunotherapeutic strategies that target T-cell-inhibitory pathways mediated by cytotoxic T-lymphocyte-associated protein 4 (CTLA4) and PD-1 have yielded encouraging clinical results, poor clinical efficacies are still observed[63]. On the other hand, Type I IFNs (IFN-α and IFN-β) which also play a role in expressing type I IFN-related genes in primary melanoma, are associated with spontaneous tumor regressions and correlated to the tumor

infiltration by specific $CD8^+$ T cells. Conversely, the lack of type I IFN signaling or IFN-β expression inhibits the generation of tumor-specific $CD8^+$ T cells and accelerated tumor growth in a murine melanoma model[64]. Loss of STING and/or cGAS expression are frequently found in melanoma, predominantly through epigenetic hypermethylation silencing[55]. While suppression of STING signaling is recognized as a crucial part of tumor development, conflicting findings have been shown in mouse melanoma cancer models. Specifically, STING knockout in tumor cells did not affect the proliferation of the B16F10 melanoma cell line in mice[52].

2. STING-activation in cancer immunotherapy and vaccine adjuvant

2.1. STING agonists and their transporter

2.1.1 STING agonists

CDNs were originally recognized as the critical secondary messengers in prokaryotic cells, and more recently they have been identified as activators of the innate immune response in mammalian cells[65,66,67], including c-di-GMP, c-di-AMP, and cGAMP (**Figure 2**). The most commonly used CDNs for cancer treatment are 3'3'-cGAMP and 2'3'-cGAMP. For example, intratumoral injection of 2'3'-cGAMP can induce the transient accumulation of $CD8^+$ T cells and macrophages inside the tumor site and remodel the tumor immune microenvironment for several cancers, including 4T1 murine breast cancer, CT26 murine colon cancer, and B16F10 murine melanoma[68]. In another study, it was shown that intraperitoneally-injected 3'3'-cGAMP could also induce the activation of the STING pathway and apoptosis of malignant B cells[69].

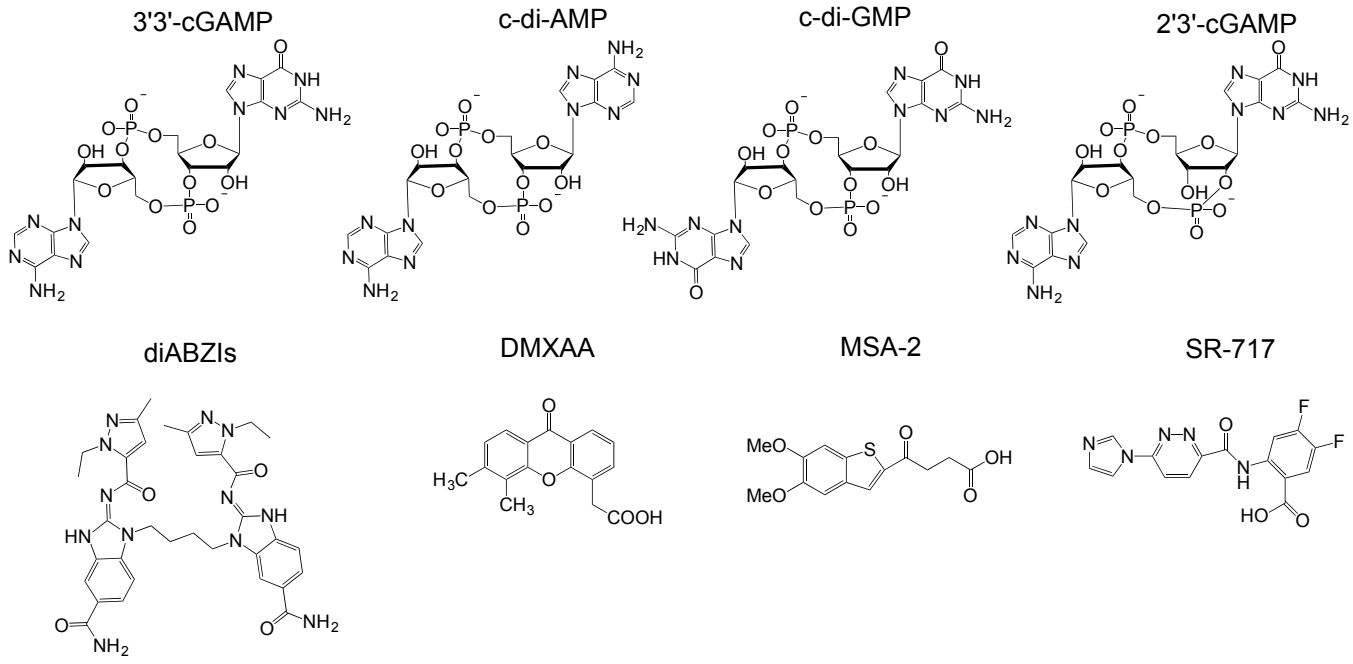


Figure 2. The molecular structures of nucleotide and non-nucleotide STING agonists

In addition to nucleotide STING agonists, non-nucleotide STING agonists, which can function as STING immune-stimulatory signals or adjuvants, have long been studied for the treatment of cancer[70]. DMXAA was primarily investigated as a STING activator and anticancer immunomodulator[71]. However, DMXAA can only activate the STING pathway in mice, but not human, due to its specific binding to murine

STING. Nevertheless, DMXAA has shed lights on the diversity of the STING agonist and highlighted the difference between human and murine STING agonists.

It wasn't until recently, however, that synthetic STING agonists that are efficacious in systemic administration were reported[45]. Ramanjulu et al. reported the discovery of a small molecule STING agonist that is not a CDN and is systemically efficacious for treating cancer in mice. Such STING agonist was designed by linking two symmetric amidobenzimidazole (ABZI)-based compounds to create linked ABZIs (diABZIs) with enhanced binding to STING. In immunocompetent mice with established syngeneic colon carcinoma, complete regression of tumors was induced after an intravenous administration of a diABZIs STING agonist. In addition, Pan et al. also reported a novel compound and non-CDN STING agonists (MSA-2) that are suitable for oral administration and advantageously target tumors[72]. Due to a weak acid property, both simulations and experimental analyses show the enhanced cellular penetration of MSA-2 in the acidified tumor microenvironment (TME) than that of normal. Meanwhile[73], Chin et al. also discovered a novel and non-CDN STING agonist through STING pathway cell-based. The identified small molecule, termed SR-717 (**Figure 2**), can mimic the functions of cGAMP by inducing the same conformational closing of STING protein, which was confirmed by the cocrystal complex of SR-717 and STING protein. SR-717 is capable of activating $CD8^+$ T and DCs tumor tissues, facilitating antigen cross-priming as well as stimulating antitumor activities. Additionally, SR-717 also induced the expression of PD-L1 in a STING pathway-dependent manner. The discovery of non-nucleotide and orally available STING agonists broadens the STING pathway's application in cancer immunotherapy.

2.1.2 cGAMP transporter

To activate the STING pathway, 2',3'-cGAMP must penetrate a target cell's membrane to stimulate its STING complex[74]. How these negatively charged CDNs pass through the cell membrane remained mysterious since its hydrophobic lipid bilayer is impermeable to ions. Using a genome-wide CRISPR-interference screen, Luteijn et al. recently reported that the folate carrier SLC19A1, a folate-organic phosphate antiporter, could be the major transporter of CDNs[75]. They found that CDNs' uptake and

functional responses could be blocked by depleting SLC19A1 and stimulated by overexpressing SLC19A1 in human cells. They also found that in human cell lines and primary cells ex vivo, CDNs' uptake can be inhibited by folates and the drugs: sulfasalazine and antifolate methotrexate, both of which have been approved for the treatment of inflammatory disorders. Meanwhile, Ritchie *et al.* also found that SLC19A1 is the immuno-transmitter importer for cGAMP[76]. Identifying SLC19A1 as the major transporter of CDNs into cells foresees the possibility of the immuno-therapeutic treatment of cancer, host responsiveness to CDN-producing pathogenic microorganisms and-potentially-for some inflammatory disorders. More recently, in addition to SLC19A1, Zhou et al. reported that LRRC8, a subunit of volume-regulated anion channels (VRACs), may play an important role in mediating the transmission of cGAMP during a host's immune response[77]. To find out whether anion channels contribute to cGAMP translocation and anti-viral defense, they performed a candidate screen across different membrane transporter proteins and demonstrated that the blockage of VRACs could increase the proliferation of the DNA virus, HSV-1, but not the RNA virus, VSV. Moreover, that IFNs response to HSV-1 could be inhibited after LRRC8A/SWELL1, a VRAC subunit, was subject to chemical inhibition or genetic ablation. Conversely, increasing VRAC activity by hypotonic cell swelling, cisplatin, GTPgS, cytokines TNF or IL-1 increased the STING-dependent IFN response to extracellular pathogens. In addition, LRRC8 knockout mice showed impaired Type I IFN responses and compromised immunity to HSV-1. They also reported that the function of LRRC8/VRAC-mediated in the transmission of cGAMP is likely through informing distant bystander cells to boost an effective IFN response to viruses. Their work collectively indicates that the cell-to-cell transmission and influx of cGAMP modulated by LRRC8/VRAC channels, is essential for anti-viral immunity in host defense against DNA virus.

2.2. Delivery strategies of STING agonists for cancer immunotherapy

Due to their ability to elicit potent innate and adaptive immune responses, STING agonists have versatile applications in tumor immunotherapy[78]. The intratumoral administration with STING agonists CDNs can boost both innate immunity and tumor antigen-specific $CD8^+$ T cell responses. CDNs induce $CD8^+$ T cells infiltration, increase the therapeutic efficacy of anti-CTLA-4, anti-PD-1, and anti-4-1BB, and remodel suppressive tumor-associated macrophages to the proinflammatory M1 phenotype[79].

Moreover, the antigen-enforced immune tolerance for tumor suppression can be overcome when STING agonists are co-administrated with PD-L1 inhibitors.

Despite the promise of CDNs such as cGAMP as immune adjuvants, they suffer from several limitations [80, 81]: **(1)** CDNs exhibit fast clearance from the injection site, which may induce systemic toxicity, **(2)** naturally derived CDNs are susceptible to enzymatic degradation, which can lower the efficacy of adjuvanticity potential, and **(3)** CDNs have inefficient intracellular transport properties due to limited endosomal escape or reliance on the expression of a specific transporter protein. To address these challenges, existing efforts are largely focused on the generation of novel biomaterial-based delivery systems to improve the *in vivo* delivery of CDNs to activate innate immune cells[81]. Here we summarize different biomaterials-based delivery strategies towards the noted challenges (**Table 1**).

2.2.1. Direct intratumoral injection of free cGAMP

Tumor-derived DNAs can trigger STING activation, and induce type I IFNs in the tumor-bearing host. The intratumoral administration of STING agonists such as c-di-GMP and cGAMP have *in vivo* anti-tumor effects via the induction of type I IFNs and the activation of innate and adaptive immunity[30]. Ohkuri et al. reported that upon intratumoral administration of 2'3'-cGAMP, a subset of cells characterized by $CD45^+$ $CD11b^{mid}$ $Ly6C^+$ transiently accumulated in the mouse tumor microenvironment of 4T1 breast cancer, squamous cell carcinomas, CT26 colon cancer, and B16F10 melanoma tissue[68]. The accumulated cells displayed a macrophage phenotype, while the same intratumoral cGAMP treatment did not induce macrophage accumulation in STING-deficient mice. Additionally, the anti-tumor activity of cGAMP treatment was dependent on $CD8^+$ T cells, as the therapeutic efficacy of cGAMP could be inhibited by anti-CD8 monoclonal antibodies. These results indicate that tumor-migrating macrophages induced by STING activation participates in $CD8^+$ T-mediated anti-tumor activities.

Table 1. STING-agonist delivery platforms for cancer immunotherapy

Carrier materials	Payload CDNs	Administration routes	Tumor models
PEG-containing lipids	2'3'-cGAMP	Intratumoral	Melanoma[81]
A pH-sensitive cationic lipid (YSK05)	c-di-GMP	Intravenous	Lung metastatic melanoma[82]

A pH-sensitive cationic lipid (YSK05)	c-di-GMP	Subcutaneous	T cell lymphoma[83]
PEGylated lipid	c-di-GMP	Subcutaneous	Lymphoma; Melanoma [47]
Soy-PC-DOTAP liposome	3'3'-cGAMP	Intravenous	Basal-like triple-negative breast cancers; Melanoma[84]
Phosphatidylserine coated liposome	2'3'-cGAMP	Inhalation	Lung metastases[85]
Poly (beta-amino ester) (PBAE)	ML-RR-CDA RR-CDG	Intratumoral	Melanoma[86]
In situ crosslinked PEG- DBP polymersomes	2'3'-cGAMP	Intratumoral; Intravenous	Melanoma[87]
	3'3'-cGAMP	Intraperitoneal;	Melanoma[88 89 90]
Acetalated dextran (Ace-DEX) microparticles		intramuscular; intravenous; intratumoral	
	--	Subcutaneous	Melanoma[91 92]
Ultra-pH-sensitive copolymers			
Cationic silica nanoparticles (CSiNPs)	c-di-GMP	Intratumoral	Melanoma [93]
Irradiated GM-CSF-secreting whole-cell vaccine	CDN derivative	Subcutaneous Implants	Melanoma[94] Pancreatic[95]
Lipid-coated silica microsphere	c-di-GMP	Intratumoral	--[96]
LPEI/HA hydrogels	cGAMP	Intratumoral	Oral cancer cell[97]
Peptide STINGel	ML RR-S2 CDA	Intratumoral	Breast cancers; Brain cancer; Melanoma[98] Melanoma[99]
Negatively charge nanotube hydrogel	c-di-AMP	Intratumoral	Melanoma; Brest cancer[100]
TM-deficient STING protein		Intratumoral	
Polylactic-co-glycolic acid (PLGA) microparticles	2'3'-cGAMP 3′3′-cGAMP		

2.2.2 Delivery platform based on cGAMP charges for enhanced cancer immunotherapy

Although the *in situ* immunotherapy approach is appealing, there are several disadvantages associated with the intratumoral injection of immunostimulants[85]. This approach is generally limited to accessible tumors, and becomes even more challenging with repeated injections. Structurally, cGAMP contains phosphodiester bonds that are susceptible to the degradation by extracellular phosphodiesterase. The two phosphodiester bonds in cGAMP restrict its penetration through the plasma membrane. As a result, a relatively high amount of cGAMP is commonly used to achieve adequate biological functioning. However, an excess of cGAMP's concentration in the tumor's microenvironment may induce the overexpression of PD-L1 on the surface of tumor cells and increase tumor-infiltrating regulatory T cells, which can have a negative impact on antitumor activity. Importantly, while the intratumoral

administration of immunostimulants could induce a local immune response at the injected site, the immune responses at distant untreated tumor sites have a limited effect, which indicates that either the local injection approach is insufficient to stimulate systemic immunity or the induced systemic response is inefficient when encountering the immunosuppressive TME at distant tumor sites.

Since activation of the STING pathway in the TME can induce DC maturation, T cell activation, and overcome resistance against immunosuppressive cells, extensive delivery strategies of cGAMP for cancer immunotherapy have been explored. The key challenge in the transfer of cGAMP to cytosolic STING is its negatively charged property and instability. To address the challenge of the anionic properties of STING agonists and their poorly membrane permeability, Wilson et al. utilized biodegradable and slightly positive surface charge poly(beta-amino ester) (PBAE) nanoparticles to deliver CDNs ML-RR-CDA and RR-CDG (a modified version of c-di-AMP and c-di-GMP for increased stability) to the cytosol, leading to strong immune response at less than one-hundredth (<0.01) of the extracellular CDN concentrations *in vitro*[86]. This nanoparticle-mediated cytosolic delivery platform for STING agonists can synergize with checkpoint inhibitors and provide a promising method to inhibit B16 melanoma tumors in vivo when combined with PD-1 blocking antibodies in comparison to native CDN. Moreover, Leach et al. reported an efficient method, based on positively charged Multi-domain peptides (MDP) to deliver a promising candidate CDN in clinical trials, Cyclic Dinucleotide dithio-(RP,RP)-[cyclic[A(2',5')pA(3',5')p]] (ML RR-S2 CDA), to prolong the duration and activity of STING agonists. Such a platform provides a sustained release profile of CDNs, demonstrating an 8-fold slower release rate than a regular collagen hydrogel[97]. The positively charged MDP can self-assemble to form a nanofibrous matrix and can be readily injected with a syringe. The local immune response in a subcutaneous model was highly stimulated after the CDNs were delivered from such nanostructured biomaterials, and the overall survival rate of tumor-bearing mice was dramatically improved in a murine model of head and neck cancer when compared to free CDN or CDN formulated into a collagen hydrogel.

Wang *et al.* reported a drug-bearing supramolecular hydrogel system to intratumorally deliver CDNs against malignant tumors to achieve cancer chemoimmunotherapy, and utilize the localized

chemotherapeutic drug to boost immune activation in a manner that is synergistic with CDNs therapy [98] . Their strategy was to chemically conjugate the hydrophilic peptide moiety iRGD (a tumor-penetrating peptide that can bind to neuropilin-1 (NRP-1) and trigger tumor tissue penetration)[36] to the hydrophobic anticancer drug camptothecin (CPT) for forming a self-assembling and self-formulating peptide–drug conjugate (diCPT–iRGD). In an aqueous solution, the designed drug amphiphile spontaneously assembled into supramolecular nanotubes (NTs) such that the negatively charged STING agonist (c-di-AMP) can condense on the surface of these positively charged NTs through electrostatic complexations. Once the injection into the tumor site, the CDA–NT solution can immediately form a hydrogel, functioning as a local reservoir for extended localized release of CDA and CPT to activate the innate and adaptive immune systems. In multiple mouse models of murine tumors, a single low dose of the STING agonist led to a successful antitumor therapy and increased animal survival, and induced long-term immunological memory and systemic immune surveillance, which protected the mice against tumor recurrence and metastases. Their results show that locally delivered STING agonists could help reduce tumor immunosuppression and enhance the efficacy of a wide range of cancer therapies.

2.2.3 Endosomolytic polymersomes increase the efficacy of CDN STING agonists for cancer immunotherapy

During the past years, polymersomes with tunable membrane and hollow properties have attracted broad attention as a class of versatile vesicles[101]. With the drug delivery technology, polymersomes have been used to construct sustained release systems to protect sensitive chemical drugs and biological therapeutics, including enzymes, proteins, and DNA or RNA fragments from adverse environment[101, 102]. Polymersomes are usually constructed from amphiphilic block copolymers to create a flexible membrane as well as an aqueous core. To optimize STING-NPs for cGAMP delivery, Shae et al. described STING-activating nanoparticles (STING-NPs) as rationally designed polymersomes for enhanced cytosolic delivery of the endogenous CDN ligand for STING [87]. To increase the loading efficiency of the hydrophilic 2’3’-cGAMP and mediate its intracellular release and endosomal escape, polymersomes were constructed by an aqueous core (PEG) and a pH-responsive and destabilizing

vesicle membrane, which were comprised of amphiphilic diblock copolymer chains. Cationic 2-(diethylamino) ethyl methacrylate (DEAEMA) was used as the pH-sensitive groups, and hydrophobic butyl methacrylate (BMA) moieties were incorporated to promote endosomal escape. Thiol-reactive pyridyl disulfide ethyl methacrylate (PDSMA) groups were integrated into the second block in order to in situ crosslink chains within the polymersome membrane. Owing to their nanoscale properties and immunostimulatory activity, STING-NPs offered several advantages: (1) the superior activation of the STING pathway; (2) the ability to enhance STING activation in both tumors and sentinel lymph nodes; (3) the therapeutic efficacy achieved through both intravenous and intratumoral administration routes; and (4) the enhanced synergy with ICB.

2.2.4 STING Agonists delivered by liposome to enhance immune cancer therapy

As the first nanomedicines approved by the FDA[103], liposomes have been extensively used to deliver nucleic acid inside cells. More recently, liposomes have been explored as a STING agonist delivery platform for the anticancer immunotherapy. The positive surface charge of cationic liposomes endows them with the potential to bind across the cell membrane and release their cargo into the cytosol. Motivated by these characteristics, Koshy et al. reported an efficient method for cytosolic 2'3'-cGAMP delivery, based on cationic liposomes with varying surface polyethylene glycol levels[81]. The cGAMP formulated into the liposome can significantly enhance the intracellular uptake of cGAMP and proinflammatory responses relative to free cGAMP in *in vitro* studies with APCs. Moreover, the liposomal formulation enabled cGAMP the capability to penetrate the melanoma tumors in the lung and play an antitumor role, whereas free cGAMP showed no antitumor activity at the same dose. The retention time of cGAMP at the tumor site was enhanced after the intratumoral injection of liposomal cGAMP into orthotopic melanoma tumors. Moreover, they found that Liposomal cGAMP inhibits the established tumor and induces an adaptive immune response that protects the mice from a second injection of the same tumor cells.

To increase the recognition and penetration of macrophages and DCs, Liu *et al.* reported a type of liposomal 2'3'-cGAMP assembled with phosphatidylserine (PS) on its surface, which can target the delivery of immunosignal agents to intratumoral APCs to enhance anticancer activity against lung

metastases[85]. As previously described, STING located on the ER membrane, that the intracellular delivery and subsequent release of cGAMPs from endosomes/lysosomes to the cytosol is critical. They showed that the acidic pH response cGAMP nanoparticles could successfully escape from the APCs lysosomes and initiate STING activation. Moreover, the inhalation of PS modified cGAMP liposomes can rapidly distribute cGAMP to the lung cells and increase the uptake by APCs in the mouse with lung metastases without causing side effects. Such NP-cGAMPs with the enhanced cytosolic release of cGAMP can activate STING signaling and APCs, leading to a pro-inflammatory response in the TME in multifocal lung metastases. Furthermore, they demonstrated that inhaled NP- cGAMP combined with fractionated radiation elicited systemic anticancer activities and confer enhanced survival rates in mice with lung metastases and repeated tumor challenges. In addition to lung cancer, Cheng et al. reported that liposomal nanoparticles incorporated with 3'3'-cGAMP can activate the STING pathway and enhance cGAMP antitumor activity in anti-PD-L1-resistant models of TNBC[84]. Collectively, these preclinical results demonstrate that the liposomes encapsulating cGAMP can provide a promising method to remodel the TME, therefore amplifying innate and adaptive antitumor immunity.

2.2.5 A bioinspired cGAMP delivery strategy based on cGAMP-STINGΔTM complex

Over the last decade, a myriad of synthetic vehicles, including liposomes, polymers, and other nanoparticle platforms, have been developed to improve the bioavailability and therapeutic efficacy of STING agonists in preclinical mouse models. However, synthetic materials may suffer from batch-to-batch variations due to complex formulations, in addition to side effects. In contrast, protein therapeutics such as recombinant cytokines and antibodies represent a unique therapeutic modality owing to their physical and biochemical homogeneity. To this end, He et al. uncovered an unnatural function of a recombinant STING protein that lacks the hydrophobic transmembrane (TM) domain (hereinafter referred to as STINGΔTM). Notably, following delivery via commercial transfection reagents, the cGAMP-STINGΔTM complexes can activate the STING signaling pathway even in cells without endogenous STING expression (**Figure 3**)[99]. They found that STINGΔTM can self-assemble a tetrameric structure induced by cGAMP under physiological conditions. Moreover, a ribonucleoprotein complex such as this, could effectively trigger a STING signaling pathway that is independent of the

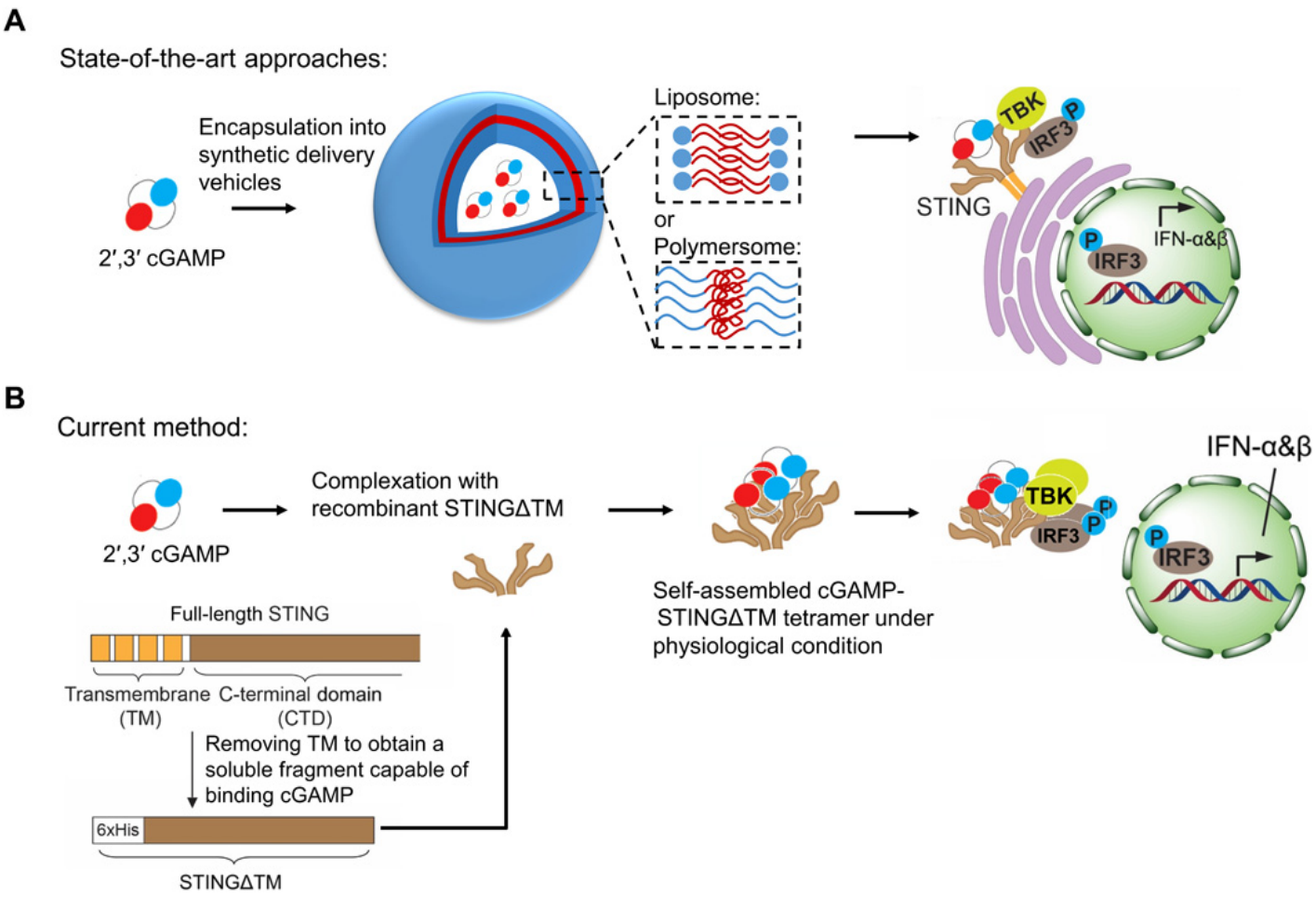


Figure 3. Overview of state-of-the-art approaches of cGAMP delivery and schematics of recombinant STINGΔTM structure and therapeutic strategy. (A) The State-of-the-art approach through directly encapsulating cGAMP into liposomes or polymersomes for cell transfection. (B) Delivery of cGAMP with a recombinant, transmembrane-deficient STING (STINGΔTM) as carrier in the form of a ribonucleoprotein complex.

status of endogenous STING. This finding is consistent with the previous studies that STINGΔTM is capable of activating IRF3 in cytosolic extracts[104]. To demonstrated the potential utility, they explored the cGAMP-STINGΔTM complex to *in vivo* applications. Vaccination studies demonstrated the enhancement of both innate and adaptive immune responses, including the augmentation of type I IFN's expression in vitro, both TNF-α and IFN-γ in vivo, robust antigen-specific T cell activation and antibody production. Furthermore, they observed a significant improvement in therapeutic efficacy in a prophylactic mouse model for melanoma and a treatment mouse model for colon cancer.

2.2.6 Silica microspheres coated by lipid as STING agonists and T cells codelivery platform

Chimeric antigen receptor (CAR) T cells therapies have been approved by the FDA and play an important role in the treatment of patients with hematologic malignancies[105]. However, CAR T cell treatments are less effective in solid tumors for several reasons, including inefficient infiltration of CAR T cells and immunosuppressive microenvironments that inactivates T cell responses. To solve the problems, Smith *et al.* established a porous alginate biopolymers scaffold that can co-deliver engineered CAR T cells and microparticles with the STING agonist c-di-GMP entrapped in the polymer core and stimulatory anti-CD3/CD28/CD137 antibodies tethered to their phospholipid membrane[95]. This porous alginate matrix was shown to convert the tumor into a "self" vaccine site, where eradicated cancer cells serve as antigens sources that can launch an antitumor immune response by the host [95]. Moreover, the implanted matrices comprised of c-di-GMP and programmed CAR T cells provided a synergistic activation of APCs, which increased the frequencies of activated DCs by 3.7 fold compared to free c-di-GMP. Mechanistically, the approach increased the expression of costimulatory molecules as well as MHC II on DCs. Moreover, tumor-specific host T cell activation was robustly primed when delivering the engineered CAR T cells and c-di-GMP in mouse cancer models bearing KPC pancreatic tumor cells or subcutaneously injected B16F10 melanoma cells. This work may provide a promising method to synergize engineered CAR T cells with the controlled delivery of STING agonists.

2.2.7 STING agonist delivery via PLGA microparticles for long-term cancer immunotherapy

Poly lactic-*co*-glycolic acid (PLGA) is a biodegradable, biocompatible, and FDA-approved polymer, which has caught considerable attention as a tunable platform for drug delivery and tissue engineering[106]. In light of the issue that the intratumoral injection of STING agonists has poor patient compliance, Lu et al. fabricated PLGA microparticles to enable a programmable pulse sequence such that encapsulated STING agonist (3'3'-cGAMP) can be systematically released at desired time slots for several weeks [100]. Unlike currently developed local delivery strategies, which only sustain drug release for a short time, these microfabricated PLGA-MPs can release individual doses of encapsulated STING agonist in pulses for up to several months with no leakage. They reported that the local and systemic antitumor immune responses can be triggered by a single intratumoral injection of such a multidose STING agonist delivery platform, which led to inhibition of tumor growth and prolonged

survival rates as effectively as multiple doses of free STING agonist in several mouse tumor models. Moreover, the encapsulated STING agonist can enhance the host response to ICI therapy and the cancer recurrence rate was reduced from 100 to 25% in mouse models of melanoma after surgical resection and continuing administration of the STING agonist-loaded microparticles. The discovery could directly improve the current STING agonist delivery and therapy efficacy with reduced injection times and lower metastasis risks.

2.3. STING agonists as vaccine adjuvants

2.3.1. STING Agonist as an adjuvant for cutaneous vaccination

Cutaneous vaccination, which can deliver vaccines into the skin, is an emerging and promising vaccination strategy[107]. Compared with muscle, the skin has a unique immunological property, for which a number of APCs reside in the epidermis and dermis characterized by the rich network of lymph vessels. Thus, cutaneous vaccination has shown a higher efficacy compared to the intramuscular injection for various vaccines, including Hepatitis B, Influenza, Rabies etc. To explore the utility of STING agonists in cutanenous vaccination, Wang et al. reported that the STING agonist cGAMP can enhance cellular and humoral immune responses induced by the H5N1 and 2009 H1N1 pandemic influenza vaccines following intradermal immunization with a single dose[108]. The slow diffusion of cGAMP in the skin was expected to stimulate robust immune responses without skin irritation and have sufficient time to activate dermal DCs. However, realistically, the cGAMP adjuvanticity potential was severely compromised in the setting of muscle immunization since APCs cannot be promptly recruited to the injection site before the clearance of the injected cGAMP. In addition to mouse models, the efficacy and safety of cGAMP as an adjuvant for cutaneous vaccination was further evaluated in a swine model, indicating that cGAMP can offer a promising adjuvant property for the cutaneous vaccination.

2.3.2. Encapsulated STING agonists as robust lymph node-targeting vaccine adjuvants

Following subcutaneous injection, the uptake of cyclic c-di-GMP by lymphatics/draining lymph nodes (dLNs) can suffer from fast diffusion into the blood circulation, which can also induce severe systemic

toxicity and side effects. To address this problem, Hanson et al. reported that the c-di-GMP can be redirected and accumulated in dLNs after being encapsulated within PEGylated lipid nanoparticles (NP-c-di-GMP). As a result, this strategy prevented the fast clearance of encapsulated CDNs, resulting in markedly enhanced dLN accumulation in murine models compared with free CDNs. They reported that a combination of a liposomal HIV gp41 peptide antigen and NP-c-di-GMP induced strong production of type I IFN, greater expansion of vaccine-specific $CD4^+$ T cells, and noticeably increased germinal center B cell differentiation in dLNs in mice, when compared with a combination of liposomal HIV gp41 and free c-di-GMP. Furthermore, the antibody titers induced by NP-c-di-GMPs were substantially higher than that of the well-studied TLR agonist monophosphoryl lipid A or a much larger dose of free c-di-GMPs. This method can be readily applied to other immunomodulating small molecules for vaccines.

2.3.3. Microparticle-encapsulated cGAMP as an adjuvant formulation

Most of the adjuvants used for infection only stimulates humoral, but not cellular immune responses [89]. Adjuvant candidates that can induce robust type I IFN have caught a broad interest due to the ability of type I IFN to promote balanced cellular and humoral immune responses in vaccination by promoting DC maturation and antigen presentation, and IgG class switching[109, 110]. To this end, the activation of the STING pathway by CDNs has been recognized as an appealing adjuvant candidate to induce cellular immunity. However, as previously described, the bioavailability of STING agonists is very low due to the requirement for cytosolic targeting of STING. Junkins *et al.* reported that 3′3′-cGAMP encapsulated within acid-sensitive acetylated dextran (Ace-DEX) polymeric microparticles (MPs) by electrospray provided an efficient and potentially scalable strategy for the induction of potent type I IFNs, as well as pro-inflammatory cytokine responses[89]. They demonstrated that these microparticles enhanced the production of type I IFNs nearly 1000-fold *in vitro* and 50-fold *in vivo*, which resulted in up to a 104 -fold boost in antibody titers, increased Th1-associated responses, and expanded germinal center B cells and memory T cells, compared to free cGAMP. Furthermore, the encapsulated cGAMP had no detectable side effects in animals and protected mice against a lethal influenza infection seven months post-immunization with CDN adjuvant doses up to 100-fold lower than that of previous reports. Together these results demonstrate that Ace-DEX MP-encapsulated cGAMP represents a promising strategy towards the balanced Th1/Th2-mediated humoral and the cellular immunity.

Acknowledgements

This work was supported by the Northeastern University Faculty start-up funding (JL) and Peer Reviewed Medical Research Program from the Department of Defense's Congressionally Directed Medical Research Programs (JL). We also acknowledge an international award from Research & Innovation, Ministry of Education Saudi Arabia (AA and JL).

References

1. Sun, L.; Wu, J.; Du, F.; Chen, X.; Chen, Z. J., Cyclic GMP-AMP synthase is a cytosolic DNA sensor that activates the type I interferon pathway. *Science* **2013,** *339* (6121), 786-791.

2. Barber, G. N., STING: infection, inflammation and cancer. *Nat Rev Immunol* **2015,** *15* (12), 760-70.

3. Gao, P.; Ascano, M.; Zillinger, T.; Wang, W.; Dai, P.; Serganov, A. A.; Gaffney, B. L.; Shuman, S.; Jones, R. A.; Deng, L.; Hartmann, G.; Barchet, W.; Tuschl, T.; Patel, D. J., Structure-function analysis of STING activation by c[G(2',5')pA(3',5')p] and targeting by antiviral DMXAA. *Cell* **2013,** *154* (4), 748-62.

4. Ergun, S. L.; Fernandez, D.; Weiss, T. M.; Li, L., STING Polymer Structure Reveals Mechanisms for Activation, Hyperactivation, and Inhibition. *Cell* **2019,** *178* (2), 290-301 e10.

5. Huang, Y. H.; Liu, X. Y.; Du, X. X.; Jiang, Z. F.; Su, X. D., The structural basis for the sensing and binding of cyclic di-GMP by STING. *Nat Struct Mol Biol* **2012,** *19* (7), 728-30.

6. Shang, G.; Zhu, D.; Li, N.; Zhang, J.; Zhu, C.; Lu, D.; Liu, C.; Yu, Q.; Zhao, Y.; Xu, S., Crystal structures of STING protein reveal basis for recognition of cyclic di-GMP. *Nature structural & molecular biology* **2012,** *19* (7), 725.

7. Kranzusch, P. J.; Wilson, S. C.; Lee, A. S.; Berger, J. M.; Doudna, J. A.; Vance, R. E., Ancient origin of cGAS-STING reveals mechanism of universal 2′, 3′ cGAMP signaling. *Molecular cell* **2015,** *59* (6), 891-903.

8. Gao, P.; Zillinger, T.; Wang, W.; Ascano, M.; Dai, P.; Hartmann, G.; Tuschl, T.; Deng, L.; Barchet, W.; Patel, D. J., Binding-pocket and lid-region substitutions render human STING sensitive to the species-specific drug DMXAA. *Cell Rep* **2014,** *8* (6), 1668-1676.

9. Zhang, X.; Shi, H.; Wu, J.; Zhang, X.; Sun, L.; Chen, C.; Chen, Z. J., Cyclic GMP-AMP containing mixed phosphodiester linkages is an endogenous high-affinity ligand for STING. *Mol Cell* **2013,** *51* (2), 226-35.

10. Diner, E. J.; Burdette, D. L.; Wilson, S. C.; Monroe, K. M.; Kellenberger, C. A.; Hyodo, M.; Hayakawa, Y.; Hammond, M. C.; Vance, R. E., The innate immune DNA sensor cGAS produces a noncanonical cyclic dinucleotide that activates human STING. *Cell Rep* **2013,** *3* (5), 1355-61.

11. Baguley, B. C.; Ching, L.-M., DMXAA: an antivascular agent with multiple host responses. *International Journal of Radiation Oncology* Biology* Physics* **2002,** *54* (5), 1503-1511.

12. Shih, A. Y.; Damm-Ganamet, K. L.; Mirzadegan, T., Dynamic Structural Differences between Human and Mouse STING Lead to Differing Sensitivity to DMXAA. *Biophys J* **2018,** *114* (1), 32-39.

13. Ouyang, S.; Song, X.; Wang, Y.; Ru, H.; Shaw, N.; Jiang, Y.; Niu, F.; Zhu, Y.; Qiu, W.; Parvatiyar, K.; Li, Y.; Zhang, R.; Cheng, G.; Liu, Z. J., Structural analysis of the STING adaptor protein reveals a hydrophobic dimer interface and mode of cyclic di-GMP binding. *Immunity* **2012,** *36* (6), 1073-86.

14. Tang, E. D.; Wang, C. Y., Single amino acid change in STING leads to constitutive active signaling. *PLoS One* **2015,** *10* (3), e0120090.

15. König, N.; Fiehn, C.; Wolf, C.; Schuster, M.; Costa, E. C.; Tüngler, V.; Alvarez, H. A.; Chara, O.; Engel, K.; Goldbach-Mansky, R., Familial chilblain lupus due to a gain-of-function mutation in STING. *Annals of the rheumatic diseases* **2017,** *76* (2), 468-472.

16. Konno, H.; Konno, K.; Barber, G. N., Cyclic dinucleotides trigger ULK1 (ATG1) phosphorylation of STING to prevent sustained innate immune signaling. *Cell* **2013,** *155* (3), 688-98.

17. Burdette, D. L.; Monroe, K. M.; Sotelo-Troha, K.; Iwig, J. S.; Eckert, B.; Hyodo, M.; Hayakawa, Y.; Vance, R. E., STING is a direct innate immune sensor of cyclic di-GMP. *Nature* **2011,** *478* (7370), 515-8.

18. Liu, Y.; Jesus, A. A.; Marrero, B.; Yang, D.; Ramsey, S. E.; Sanchez, G. A. M.; Tenbrock, K.; Wittkowski, H.; Jones, O. Y.; Kuehn, H. S.; Lee, C. R.; DiMattia, M. A.; Cowen, E. W.; Gonzalez, B.; Palmer, I.; DiGiovanna, J. J.; Biancotto, A.; Kim, H.; Tsai, W. L.; Trier, A. M.; Huang, Y.; Stone, D. L.; Hill, S.; Kim, H. J.; St Hilaire, C.; Gurprasad, S.; Plass, N.; Chapelle, D.; Horkayne-Szakaly, I.; Foell, D.; Barysenka, A.; Candotti, F.; Holland, S. M.; Hughes, J. D.; Mehmet, H.; Issekutz, A. C.; Raffeld, M.; McElwee, J.; Fontana, J. R.; Minniti, C. P.; Moir, S.; Kastner, D. L.; Gadina, M.; Steven, A. C.; Wingfield, P. T.; Brooks, S. R.; Rosenzweig, S. D.; Fleisher, T. A.; Deng, Z.; Boehm, M.; Paller, A. S.; Goldbach-Mansky, R., Activated STING in a vascular and pulmonary syndrome. *N Engl J Med* **2014,** *371* (6), 507-518.

19. Hansen, A. L.; Mukai, K.; Schopfer, F. J.; Taguchi, T.; Holm, C. K., STING palmitoylation as a

therapeutic target. *Cell Mol Immunol* **2019,** *16* (3), 236-241.

20. Mukai, K.; Konno, H.; Akiba, T.; Uemura, T.; Waguri, S.; Kobayashi, T.; Barber, G. N.; Arai, H.; Taguchi, T., Activation of STING requires palmitoylation at the Golgi. *Nature communications* **2016,** *7*, 11932.

21. Ahn, J.; Barber, G. N., STING signaling and host defense against microbial infection. *Exp Mol Med* **2019,** *51* (12), 1-10.

22. Li, T.; Chen, Z. J., The cGAS-cGAMP-STING pathway connects DNA damage to inflammation, senescence, and cancer. *J Exp Med* **2018,** *215* (5), 1287-1299.

23. Kawai, T.; Akira, S., Toll-like receptors and their crosstalk with other innate receptors in infection and immunity. *Immunity* **2011,** *34* (5), 637-50.

24. Osorio, F.; e Sousa, C. R., Myeloid C-type lectin receptors in pathogen recognition and host defense. *Immunity* **2011,** *34* (5), 651-664.

25. Lee, A. J.; Ashkar, A. A., The Dual Nature of Type I and Type II Interferons. *Front Immunol* **2018,** *9*, 2061.

26. Kallies, A.; Good-Jacobson, K. L., Transcription factor T-bet orchestrates lineage development and function in the immune system. *Trends in immunology* **2017,** *38* (4), 287-297.

27. Rivera Vargas, T.; Benoit-Lizon, I.; Apetoh, L., Rationale for stimulator of interferon genes-targeted cancer immunotherapy. *Eur J Cancer* **2017,** *75*, 86-97.

28. Ng, D.; Gommerman, J. L., The Regulation of Immune Responses by DC Derived Type I IFN. *Front Immunol* **2013,** *4*, 94.

29. Vatner, R. E.; Janssen, E. M., STING, DCs and the link between innate and adaptive tumor immunity. *Mol Immunol* **2019,** *110*, 13-23.

30. Deng, L.; Liang, H.; Xu, M.; Yang, X.; Burnette, B.; Arina, A.; Li, X. D.; Mauceri, H.; Beckett, M.; Darga, T.; Huang, X.; Gajewski, T. F.; Chen, Z. J.; Fu, Y. X.; Weichselbaum, R. R., STING-Dependent Cytosolic DNA Sensing Promotes Radiation-Induced Type I Interferon-Dependent Antitumor Immunity in Immunogenic Tumors. *Immunity* **2014,** *41* (5), 843-52.

31. Wang, H.; Hu, S.; Chen, X.; Shi, H.; Chen, C.; Sun, L.; Chen, Z. J., cGAS is essential for the antitumor effect of immune checkpoint blockade. *Proc Natl Acad Sci U S A* **2017,** *114* (7), 1637-1642.

32. Solt, L. A.; May, M. J., The IkappaB kinase complex: master regulator of NF-kappaB signaling. *Immunol Res* **2008,** *42* (1-3), 3-18.

33. Pourcelot, M.; Zemirli, N.; Silva Da Costa, L.; Loyant, R.; Garcin, D.; Vitour, D.; Munitic, I.;

Vazquez, A.; Arnoult, D., The Golgi apparatus acts as a platform for TBK1 activation after viral RNA sensing. *BMC Biol* **2016,** *14*, 69.

34. He, C.; Klionsky, D. J., Regulation mechanisms and signaling pathways of autophagy. *Annu Rev Genet* **2009,** *43*, 67-93.

35. Hou, X.; Watzlawik, J. O.; Fiesel, F. C.; Springer, W., Autophagy in Parkinson's Disease. *J Mol Biol* **2020,** *432* (8), 2651-2672.

36. Sharma, M.; Rajendrarao, S.; Shahani, N.; Ramirez-Jarquin, U. N.; Subramaniam, S., Cyclic GMP-AMP synthase promotes the inflammatory and autophagy responses in Huntington disease. *Proc Natl Acad Sci U S A* **2020,** *117* (27), 15989-15999.

37. Saitoh, T.; Fujita, N.; Hayashi, T.; Takahara, K.; Satoh, T.; Lee, H.; Matsunaga, K.; Kageyama, S.; Omori, H.; Noda, T.; Yamamoto, N.; Kawai, T.; Ishii, K.; Takeuchi, O.; Yoshimori, T.; Akira, S., Atg9a controls dsDNA-driven dynamic translocation of STING and the innate immune response. *Proc Natl Acad Sci U S A* **2009,** *106* (49), 20842-6.

38. Wu, M. Y.; Lu, J. H., Autophagy and Macrophage Functions: Inflammatory Response and Phagocytosis. *Cells* **2019,** *9* (1).

39. Kroemer, G.; Marino, G.; Levine, B., Autophagy and the integrated stress response. *Mol Cell* **2010,** *40* (2), 280-93.

40. Liu, D.; Wu, H.; Wang, C.; Li, Y.; Tian, H.; Siraj, S.; Sehgal, S. A.; Wang, X.; Wang, J.; Shang, Y.; Jiang, Z.; Liu, L.; Chen, Q., STING directly activates autophagy to tune the innate immune response. *Cell Death Differ* **2019,** *26* (9), 1735-1749.

41. Li, Y.; Wilson, H. L.; Kiss-Toth, E., Regulating STING in health and disease. *J Inflamm (Lond)* **2017,** *14*, 11.

42. Ding, Q.; Gaska, J. M.; Douam, F.; Wei, L.; Kim, D.; Balev, M.; Heller, B.; Ploss, A., Species-specific disruption of STING-dependent antiviral cellular defenses by the Zika virus NS2B3 protease. *Proc Natl Acad Sci U S A* **2018,** *115* (27), E6310-E6318.

43. Hansen, A. L.; Buchan, G. J.; Ruhl, M.; Mukai, K.; Salvatore, S. R.; Ogawa, E.; Andersen, S. D.; Iversen, M. B.; Thielke, A. L.; Gunderstofte, C.; Motwani, M.; Moller, C. T.; Jakobsen, A. S.; Fitzgerald, K. A.; Roos, J.; Lin, R. T.; Maier, T. J.; Goldbach-Mansky, R.; Miner, C. A.; Qian, W.; Miner, J. J.; Rigby, R. E.; Rehwinkel, J.; Jakobsen, M. R.; Arai, H.; Taguchi, T.; Schopfer, F. J.; Olagnier, D.; Holm, C. K., Nitro-fatty acids are formed in response to virus infection and are potent inhibitors of STING palmitoylation

and signaling. *P Natl Acad Sci USA* **2018,** *115* (33), E7768-E7775.

44. Corrales, L.; Glickman, L. H.; McWhirter, S. M.; Kanne, D. B.; Sivick, K. E.; Katibah, G. E.; Woo, S. R.; Lemmens, E.; Banda, T.; Leong, J. J.; Metchette, K.; Dubensky, T. W., Jr.; Gajewski, T. F., Direct Activation of STING in the Tumor Microenvironment Leads to Potent and Systemic Tumor Regression and Immunity. *Cell Rep* **2015,** *11* (7), 1018-30.

45. Ramanjulu, J. M.; Pesiridis, G. S.; Yang, J.; Concha, N.; Singhaus, R.; Zhang, S. Y.; Tran, J. L.; Moore, P.; Lehmann, S.; Eberl, H. C.; Muelbaier, M.; Schneck, J. L.; Clemens, J.; Adam, M.; Mehlmann, J.; Romano, J.; Morales, A.; Kang, J.; Leister, L.; Graybill, T. L.; Charnley, A. K.; Ye, G.; Nevins, N.; Behnia, K.; Wolf, A. I.; Kasparcova, V.; Nurse, K.; Wang, L.; Puhl, A. C.; Li, Y.; Klein, M.; Hopson, C. B.; Guss, J.; Bantscheff, M.; Bergamini, G.; Reilly, M. A.; Lian, Y.; Duffy, K. J.; Adams, J.; Foley, K. P.; Gough, P. J.; Marquis, R. W.; Smothers, J.; Hoos, A.; Bertin, J., Design of amidobenzimidazole STING receptor agonists with systemic activity. *Nature* **2018,** *564* (7736), 439-443.

46. Ager, C. R.; Reilley, M. J.; Nicholas, C.; Bartkowiak, T.; Jaiswal, A. R.; Curran, M. A., Intratumoral STING Activation with T-cell Checkpoint Modulation Generates Systemic Antitumor Immunity. *Cancer Immunol Res* **2017,** *5* (8), 676-684.

47. Hanson, M. C.; Crespo, M. P.; Abraham, W.; Moynihan, K. D.; Szeto, G. L.; Chen, S. H.; Melo, M. B.; Mueller, S.; Irvine, D. J., Nanoparticulate STING agonists are potent lymph node-targeted vaccine adjuvants. *J Clin Invest* **2015,** *125* (6), 2532-46.

48. Surpris, G.; Chan, J.; Thompson, M.; Ilyukha, V.; Liu, B. C.; Atianand, M.; Sharma, S.; Volkova, T.; Smirnova, I.; Fitzgerald, K. A.; Poltorak, A., Cutting Edge: Novel Tmem173 Allele Reveals Importance of STING N Terminus in Trafficking and Type I IFN Production. *J Immunol* **2016,** *196* (2), 547-552.

49. Borriello, F.; Pietrasanta, C.; Lai, J. C. Y.; Walsh, L. M.; Sharma, P.; O'Driscoll, D. N.; Ramirez, J.; Brightman, S.; Pugni, L.; Mosca, F.; Burkhart, D. J.; Dowling, D. J.; Levy, O., Identification and Characterization of Stimulator of Interferon Genes As a Robust Adjuvant Target for Early Life Immunization. *Front Immunol* **2017,** *8*.

50. Shae, D.; Becker, K. W.; Christov, P.; Yun, D. S.; Lytton-Jean, A. K. R.; Sevimli, S.; Ascano, M.; Kelley, M.; Johnson, D. B.; Balko, J. M.; Wilson, J. T., Endosomolytic polymersomes increase the activity of cyclic dinucleotide STING agonists to enhance cancer immunotherapy. *Nature Nanotechnology* **2019,** *14* (3), 269-+.

51. Demaria, O.; De Gassart, A.; Coso, S.; Gestermann, N.; Di Domizio, J.; Flatz, L.; Gaide, O.; Michielin, O.; Hwu, P.; Petrova, T. V.; Martinon, F.; Modlin, R. L.; Speiser, D. E.; Gilliet, M., STING activation of tumor endothelial cells initiates spontaneous and therapeutic antitumor immunity. *Proc Natl Acad Sci U S A* **2015,** *112* (50), 15408-13.

52. Sokolowska, O.; Nowis, D., STING Signaling in Cancer Cells: Important or Not? *Arch Immunol Ther Exp (Warsz)* **2018,** *66* (2), 125-132.

53. Rittmeyer, A.; Barlesi, F.; Waterkamp, D.; Park, K.; Ciardiello, F.; von Pawel, J.; Gadgeel, S. M.; Hida, T.; Kowalski, D. M.; Dols, M. C.; Cortinovis, D. L.; Leach, J.; Polikoff, J.; Barrios, C.; Kabbinavar, F.; Frontera, O. A.; De Marinis, F.; Turna, H.; Lee, J.-S.; Ballinger, M.; Kowanetz, M.; He, P.; Chen, D. S.; Sandler, A.; Gandara, D. R., Atezolizumab versus docetaxel in patients with previously treated non-small-cell lung cancer (OAK): a phase 3, open-label, multicentre randomised controlled trial. *The Lancet* **2017,** *389* (10066), 255-265.

54. Havel, J. J.; Chowell, D.; Chan, T. A., The evolving landscape of biomarkers for checkpoint inhibitor immunotherapy. *Nat Rev Cancer* **2019,** *19* (3), 133-150.

55. Della Corte, C. M.; Sen, T.; Gay, C. M.; Ramkumar, K.; Diao, L.; Cardnell, R. J.; Rodriguez, B. L.; Stewart, C. A.; Papadimitrakopoulou, V. A.; Gibson, L., STING Pathway Expression Identifies NSCLC With an Immune-Responsive Phenotype. *Journal of Thoracic Oncology* **2020**.

56. Kitajima, S.; Ivanova, E.; Guo, S.; Yoshida, R.; Campisi, M.; Sundararaman, S. K.; Tange, S.; Mitsuishi, Y.; Thai, T. C.; Masuda, S.; Piel, B. P.; Sholl, L. M.; Kirschmeier, P. T.; Paweletz, C. P.; Watanabe, H.; Yajima, M.; Barbie, D. A., Suppression of STING Associated with LKB1 Loss in KRAS-Driven Lung Cancer. *Cancer Discov* **2019,** *9* (1), 34-45.

57. Chen, Q.; Boire, A.; Jin, X.; Valiente, M.; Er, E. E.; Lopez-Soto, A.; Jacob, L.; Patwa, R.; Shah, H.; Xu, K.; Cross, J. R.; Massague, J., Carcinoma-astrocyte gap junctions promote brain metastasis by cGAMP transfer. *Nature* **2016,** *533* (7604), 493-498.

58. Fuertes, M. B.; Kacha, A. K.; Kline, J.; Woo, S. R.; Kranz, D. M.; Murphy, K. M.; Gajewski, T. F., Host type I IFN signals are required for antitumor CD8+ T cell responses through CD8{alpha}+ dendritic cells. *J Exp Med* **2011,** *208* (10), 2005-16.

59. Kitai, Y.; Kawasaki, T.; Sueyoshi, T.; Kobiyama, K.; Ishii, K. J.; Zou, J.; Akira, S.; Matsuda, T.; Kawai, T., DNA-Containing Exosomes Derived from Cancer Cells Treated with Topotecan Activate a STING-

Dependent Pathway and Reinforce Antitumor Immunity. *J Immunol* **2017,** *198* (4), 1649-1659.

60. Yang, H.; Lee, W. S.; Kong, S. J.; Kim, C. G.; Kim, J. H.; Chang, S. K.; Kim, S.; Kim, G.; Chon, H. J.; Kim, C., STING activation reprograms tumor vasculatures and synergizes with VEGFR2 blockade. *J Clin Invest* **2019,** *129* (10), 4350-4364.

61. Gaston, J.; Cheradame, L.; Yvonnet, V.; Deas, O.; Poupon, M.-F.; Judde, J.-G.; Cairo, S.; Goffin, V., Intracellular STING inactivation sensitizes breast cancer cells to genotoxic agents. *Oncotarget* **2016,** *7* (47), 77205.

62. Bray, F.; Ferlay, J.; Soerjomataram, I.; Siegel, R. L.; Torre, L. A.; Jemal, A., Global cancer statistics 2018: GLOBOCAN estimates of incidence and mortality worldwide for 36 cancers in 185 countries. *CA Cancer J Clin* **2018,** *68* (6), 394-424.

63. Song, S.; Peng, P.; Tang, Z.; Zhao, J.; Wu, W.; Li, H.; Shao, M.; Li, L.; Yang, C.; Duan, F.; Zhang, M.; Zhang, J.; Wu, H.; Li, C.; Wang, X.; Wang, H.; Ruan, Y.; Gu, J., Decreased expression of STING predicts poor prognosis in patients with gastric cancer. *Sci Rep* **2017,** *7*, 39858.

64. Lamb, A.; Chen, L. F., Role of the Helicobacter pylori-induced inflammatory response in the development of gastric cancer. *J Cell Biochem* **2013,** *114* (3), 491-7.

65. Sharma, M.; Rajendrarao, S.; Shahani, N.; Ramírez-Jarquín, U. N.; Subramaniam, S., Cyclic GMP-AMP synthase promotes the inflammatory and autophagy responses in Huntington disease. *PNAS* **2020,** *117* (27), 15989-15999.

66. Karaolis, D. K. R.; Cheng, K.; Lipsky, M.; Elnabawi, A.; Catalano, J.; Hyodo, M.; Hayakawa, Y.; Raufman, J.-P., 3′,5′-Cyclic diguanylic acid (c-di-GMP) inhibits basal and growth factor-stimulated human colon cancer cell proliferation. *Biochemical and Biophysical Research Communications* **2005,** *329* (1), 40-45.

67. Su, T.; Zhang, Y.; Valerie, K.; Wang, X. Y.; Lin, S.; Zhu, G., STING activation in cancer immunotherapy. *Theranostics* **2019,** *9* (25), 7759-7771.

68. Ohkuri, T.; Kosaka, A.; Ishibashi, K.; Kumai, T.; Hirata, Y.; Ohara, K.; Nagato, T.; Oikawa, K.; Aoki, N.; Harabuchi, Y.; Celis, E.; Kobayashi, H., Intratumoral administration of cGAMP transiently accumulates potent macrophages for anti-tumor immunity at a mouse tumor site. *Cancer Immunol Immunother* **2017,** *66* (6), 705-716.

69. Tang, C.-H. A.; Zundell, J. A.; Ranatunga, S.; Lin, C.; Nefedova, Y.; Del Valle, J. R.; Hu, C.-C. A., Agonist-Mediated Activation of STING Induces Apoptosis in Malignant B Cells. *Cancer Research* **2016,** *76* (8),

2137-2152.

70. Flood, B. A.; Higgs, E. F.; Li, S.; Luke, J. J.; Gajewski, T. F., STING pathway agonism as a cancer therapeutic. *Immunol Rev* **2019,** *290* (1), 24-38.

71. Baguley, B. C.; Ching, L. M., DMXAA: an antivascular agent with multiple host responses. *Int. J. Radiat. Oncol. Biol. Phys.* **2002,** *54* (5), 1503-1511.

72. Pan, B. S.; Perera, S. A.; Piesvaux, J. A.; Presland, J. P.; Schroeder, G. K.; Cumming, J. N.; Trotter, B. W.; Altman, M. D.; Buevich, A. V.; Cash, B.; Cemerski, S.; Chang, W.; Chen, Y.; Dandliker, P. J.; Feng, G.; Haidle, A.; Henderson, T.; Jewell, J.; Kariv, I.; Knemeyer, I.; Kopinja, J.; Lacey, B. M.; Laskey, J.; Lesburg, C. A.; Liang, R.; Long, B. J.; Lu, M.; Ma, Y.; Minnihan, E. C.; O'Donnell, G.; Otte, R.; Price, L.; Rakhilina, L.; Sauvagnat, B.; Sharma, S.; Tyagarajan, S.; Woo, H.; Wyss, D. F.; Xu, S.; Bennett, D. J.; Addona, G. H., An orally available non-nucleotide STING agonist with antitumor activity. *Science* **2020,** *369* (6506).

73. Chin, E. N.; Yu, C.; Vartabedian, V. F.; Jia, Y.; Kumar, M.; Gamo, A. M.; Vernier, W.; Ali, S. H.; Kissai, M.; Lazar, D. C.; Nguyen, N.; Pereira, L. E.; Benish, B.; Woods, A. K.; Joseph, S. B.; Chu, A.; Johnson, K. A.; Sander, P. N.; Martínez-Peña, F.; Hampton, E. N.; Young, T. S.; Wolan, D. W.; Chatterjee, A. K.; Schultz, P. G.; Petrassi, H. M.; Teijaro, J. R.; Lairson, L. L., Antitumor activity of a systemic STING-activating non-nucleotide cGAMP mimetic. *Science* **2020,** *369* (6506), 993-999.

74. Motwani, M.; Pesiridis, S.; Fitzgerald, K. A., DNA sensing by the cGAS-STING pathway in health and disease. *Nat Rev Genet* **2019,** *20* (11), 657-674.

75. Luteijn, R. D.; Zaver, S. A.; Gowen, B. G.; Wyman, S. K.; Garelis, N. E.; Onia, L.; McWhirter, S. M.; Katibah, G. E.; Corn, J. E.; Woodward, J. J.; Raulet, D. H., SLC19A1 transports immunoreactive cyclic dinucleotides. *Nature* **2019,** *573* (7774), 434-438.

76. Ritchie, C.; Cordova, A. F.; Hess, G. T.; Bassik, M. C.; Li, L., SLC19A1 Is an Importer of the Immunotransmitter cGAMP. *Mol Cell* **2019,** *75* (2), 372-381 e5.

77. Zhou, C.; Chen, X.; Planells-Cases, R.; Chu, J.; Wang, L.; Cao, L.; Li, Z.; Lopez-Cayuqueo, K. I.; Xie, Y.; Ye, S.; Wang, X.; Ullrich, F.; Ma, S.; Fang, Y.; Zhang, X.; Qian, Z.; Liang, X.; Cai, S. Q.; Jiang, Z.; Zhou, D.; Leng, Q.; Xiao, T. S.; Lan, K.; Yang, J.; Li, H.; Peng, C.; Qiu, Z.; Jentsch, T. J.; Xiao, H., Transfer of cGAMP into Bystander Cells via LRRC8 Volume-Regulated Anion Channels Augments STING-Mediated Interferon Responses and Anti-viral Immunity. *Immunity* **2020,** *52* (5), 767-781 e6.

78. Libanova, R.; Becker, P. D.; Guzman, C. A., Cyclic di-nucleotides: new era for small molecules as adjuvants. *Microb Biotechnol* **2012,** *5* (2), 168-76.

79. Barber, G. N., STING: infection, inflammation and cancer. *Nature Reviews. Immunology* **2015,** *15* (12), 760-770.

80. Li, L.; Yin, Q.; Kuss, P.; Maliga, Z.; Millan, J. L.; Wu, H.; Mitchison, T. J., Hydrolysis of 2'3'-cGAMP by ENPP1 and design of nonhydrolyzable analogs. *Nat Chem Biol* **2014,** *10* (12), 1043-8.

81. Koshy, S. T.; Cheung, A. S.; Gu, L.; Graveline, A. R.; Mooney, D. J., Liposomal Delivery Enhances Immune Activation by STING Agonists for Cancer Immunotherapy. *Adv Biosyst* **2017,** *1* (1-2).

82. Nakamura, T.; Miyabe, H.; Hyodo, M.; Sato, Y.; Hayakawa, Y.; Harashima, H., Liposomes loaded with a STING pathway ligand, cyclic di-GMP, enhance cancer immunotherapy against metastatic melanoma. *J Control Release* **2015,** *216*, 149-57.

83. Miyabe, H.; Hyodo, M.; Nakamura, T.; Sato, Y.; Hayakawa, Y.; Harashima, H., A new adjuvant delivery system 'cyclic di-GMP/YSK05 liposome' for cancer immunotherapy. *J Control Release* **2014,** *184*, 20-7.

84. Cheng, N.; Watkins-Schulz, R.; Junkins, R. D.; David, C. N.; Johnson, B. M.; Montgomery, S. A.; Peine, K. J.; Darr, D. B.; Yuan, H.; McKinnon, K. P.; Liu, Q.; Miao, L.; Huang, L.; Bachelder, E. M.; Ainslie, K. M.; Ting, J. P., A nanoparticle-incorporated STING activator enhances antitumor immunity in PD-L1-insensitive models of triple-negative breast cancer. *JCI Insight* **2018,** *3* (22).

85. Liu, Y.; Crowe, W. N.; Wang, L.; Lu, Y.; Petty, W. J.; Habib, A. A.; Zhao, D., An inhalable nanoparticulate STING agonist synergizes with radiotherapy to confer long-term control of lung metastases. *Nat Commun* **2019,** *10* (1), 5108.

86. Wilson, D. R.; Sen, R.; Sunshine, J. C.; Pardoll, D. M.; Green, J. J.; Kim, Y. J., Biodegradable STING agonist nanoparticles for enhanced cancer immunotherapy. *Nanomedicine* **2018,** *14* (2), 237-246.

87. Shae, D.; Becker, K. W.; Christov, P.; Yun, D. S.; Lytton-Jean, A. K. R.; Sevimli, S.; Ascano, M.; Kelley, M.; Johnson, D. B.; Balko, J. M.; Wilson, J. T., Endosomolytic polymersomes increase the activity of cyclic dinucleotide STING agonists to enhance cancer immunotherapy. *Nat Nanotechnol* **2019,** *14* (3), 269-278.

88. Watkins-Schulz, R.; Tiet, P.; Gallovic, M. D.; Junkins, R. D.; Batty, C.; Bachelder, E. M.; Ainslie, K. M.; Ting, J. P. Y., A microparticle platform for STING-targeted immunotherapy enhances natural killer cell- and CD8(+) T cell-mediated anti-tumor immunity. *Biomaterials* **2019,** *205*, 94-105.

89. Junkins, R. D.; Gallovic, M. D.; Johnson, B. M.; Collier, M. A.; Watkins-Schulz, R.; Cheng, N.;

David, C. N.; McGee, C. E.; Sempowski, G. D.; Shterev, I.; McKinnon, K.; Bachelder, E. M.; Ainslie, K. M.; Ting, J. P., A robust microparticle platform for a STING-targeted adjuvant that enhances both humoral and cellular immunity during vaccination. *J Control Release* **2018,** *270*, 1-13.

90. Collier, M. A.; Junkins, R. D.; Gallovic, M. D.; Johnson, B. M.; Johnson, M. M.; Macintyre, A. N.; Sempowski, G. D.; Bachelder, E. M.; Ting, J. P.; Ainslie, K. M., Acetalated Dextran Microparticles for Codelivery of STING and TLR7/8 Agonists. *Mol Pharm* **2018,** *15* (11), 4933-4946.

91. Luo, M.; Wang, H.; Wang, Z.; Cai, H.; Lu, Z.; Li, Y.; Du, M.; Huang, G.; Wang, C.; Chen, X.; Porembka, M. R.; Lea, J.; Frankel, A. E.; Fu, Y. X.; Chen, Z. J.; Gao, J., A STING-activating nanovaccine for cancer immunotherapy. *Nat Nanotechnol* **2017,** *12* (7), 648-654.

92. Luo, M.; Liu, Z.; Zhang, X.; Han, C.; Samandi, L. Z.; Dong, C.; Sumer, B. D.; Lea, J.; Fu, Y. X.; Gao, J., Synergistic STING activation by PC7A nanovaccine and ionizing radiation improves cancer immunotherapy. *J Control Release* **2019,** *300*, 154-160.

93. An, M.; Yu, C.; Xi, J.; Reyes, J.; Mao, G.; Wei, W. Z.; Liu, H., Induction of necrotic cell death and activation of STING in the tumor microenvironment via cationic silica nanoparticles leading to enhanced antitumor immunity. *Nanoscale* **2018,** *10* (19), 9311-9319.

94. Fu, J.; Kanne, D. B.; Leong, M.; Glickman, L. H.; McWhirter, S. M.; Lemmens, E.; Mechette, K.; Leong, J. J.; Lauer, P.; Liu, W.; Sivick, K. E.; Zeng, Q.; Soares, K. C.; Zheng, L.; Portnoy, D. A.; Woodward, J. J.; Pardoll, D. M.; Dubensky, T. W., Jr.; Kim, Y., STING agonist formulated cancer vaccines can cure established tumors resistant to PD-1 blockade. *Sci Transl Med* **2015,** *7* (283), 283ra52.

95. Smith, T. T.; Moffett, H. F.; Stephan, S. B.; Opel, C. F.; Dumigan, A. G.; Jiang, X.; Pillarisetty, V. G.; Pillai, S. P. S.; Wittrup, K. D.; Stephan, M. T., Biopolymers codelivering engineered T cells and STING agonists can eliminate heterogeneous tumors. *J Clin Invest* **2017,** *127* (6), 2176-2191.

96. Lee, E.; Jang, H. E.; Kang, Y. Y.; Kim, J.; Ahn, J. H.; Mok, H., Submicron-sized hydrogels incorporating cyclic dinucleotides for selective delivery and elevated cytokine release in macrophages. *Acta Biomater* **2016,** *29*, 271-281.

97. Leach, D. G.; Dharmaraj, N.; Piotrowski, S. L.; Lopez-Silva, T. L.; Lei, Y. L.; Sikora, A. G.; Young, S.; Hartgerink, J. D., STINGel: Controlled release of a cyclic dinucleotide for enhanced cancer immunotherapy. *Biomaterials* **2018,** *163*, 67-75.

98. Wang, F.; Su, H.; Xu, D.; Dai, W.; Zhang, W.; Wang, Z.; Anderson, C. F.; Zheng, M.; Oh, R.;

Wan, F.; Cui, H., Tumour sensitization via the extended intratumoural release of a STING agonist and camptothecin from a self-assembled hydrogel. *Nat Biomed Eng* **2020**.

99. He, Y.; Hong, C.; Yan, E. Z.; Fletcher, S. J.; Zhu, G.; Yang, M.; Li, Y.; Sun, X.; Irvine, D. J.; Li, J.; Hammond, P. T., Self-assembled cGAMP-STINGΔTM signaling complex as a bioinspired platform for cGAMP delivery. *Science Advances* **2020,** *6* (24), eaba7589.

100. Lu, X.; Miao, L.; Gao, W.; Chen, Z.; McHugh, K. J.; Sun, Y.; Tochka, Z.; Tomasic, S.; Sadtler, K.; Hyacinthe, A.; Huang, Y.; Graf, T.; Hu, Q.; Sarmadi, M.; Langer, R.; Anderson, D. G.; Jaklenec, A., Engineered PLGA microparticles for long-term, pulsatile release of STING agonist for cancer immunotherapy. *Science Translational Medicine* **2020,** *12* (556), eaaz6606.

101. Lee, J. S.; Feijen, J., Polymersomes for drug delivery: Design, formation and characterization. *Journal of Controlled Release* **2012,** *161* (2), 473-483.

102. Lomas, H.; Canton, I.; MacNeil, S.; Du, J.; Armes, S. P.; Ryan, A. J.; Lewis, A. L.; Battaglia, G., Biomimetic pH Sensitive Polymersomes for Efficient DNA Encapsulation and Delivery. *Advanced Materials* **2007,** *19* (23), 4238-4243.

103. Shi, J.; Kantoff, P. W.; Wooster, R.; Farokhzad, O. C., Cancer nanomedicine: progress, challenges and opportunities. *Nat Rev Cancer* **2017,** *17* (1), 20-37.

104. Tanaka, Y.; Chen, Z. J., STING Specifies IRF3 Phosphorylation by TBK1 in the Cytosolic DNA Signaling Pathway. *Science Signaling* **2012,** *5* (214), ra20-ra20.

105. O'Rourke, D. M.; Nasrallah, M. P.; Desai, A.; Melenhorst, J. J.; Mansfield, K.; Morrissette, J. J. D.; Martinez-Lage, M.; Brem, S.; Maloney, E.; Shen, A.; Isaacs, R.; Mohan, S.; Plesa, G.; Lacey, S. F.; Navenot, J.-M.; Zheng, Z.; Levine, B. L.; Okada, H.; June, C. H.; Brogdon, J. L.; Maus, M. V., A single dose of peripherally infused EGFRvIII-directed CAR T cells mediates antigen loss and induces adaptive resistance in patients with recurrent glioblastoma. *Science Translational Medicine* **2017,** *9* (399), eaaa0984.

106. Makadia, H. K.; Siegel, S. J., Poly Lactic-co-Glycolic Acid (PLGA) as Biodegradable Controlled Drug Delivery Carrier. *Polymers (Basel)* **2011,** *3* (3), 1377-1397.

107. Wang, J., Fractional Delivery: Toward a Painless, Safe and Effective Cutaneous Vaccination. *Journal of Vaccines & Vaccination* **2017,** *08* (01).

108. Wang, J.; Li, P.; Wu, M. X., Natural STING Agonist as an "Ideal" Adjuvant for Cutaneous Vaccination. *J Invest Dermatol* **2016,** *136* (11), 2183-2191.

109. Diamond, M. S.; Kinder, M.; Matsushita, H.; Mashayekhi, M.; Dunn, G. P.; Archambault, J. M.; Lee, H.; Arthur, C. D.; White, J. M.; Kalinke, U.; Murphy, K. M.; Schreiber, R. D., Type I interferon is selectively required by dendritic cells for immune rejection of tumors. *J Exp Med* **2011,** *208* (10), 1989-2003.

110. Alsharifi, M.; Lobigs, M.; Regner, M.; Lee, E.; Koskinen, A.; Mullbacher, A., Type I interferons trigger systemic, partial lymphocyte activation in response to viral infection. *J Immunol* **2005,** *175* (7), 4635-40.